INVESTIGATIONS ON ALKALINE EARTH SULPHIDE PHOSPHORS ACTIVATED BY COPPER FOR FLUORO-OPTIC TEMPERATURE SENSING

THESIS

Submitted in partial fulfillment
of the requirements for the degree of

DOCTOR OF PHILOSOPHY

By

RAJESH PUROHIT

Under the supervision

of

PROF. R.P. KHARE

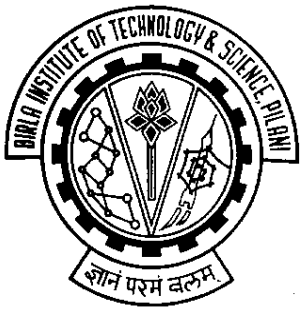

BIRLA INSTITUTE OF TECHNOLOGY AND SCIENCE
PILANI (RAJASTHAN), INDIA
2013

Dedicated

to

My Parents

Late Shri Ram Niranjanji Purohit

&

Smt. Triveni Devi

BIRLA INSTITUTE OF TECHNOLOGY AND SCIENCE
PILANI (RAJASTHAN), INDIA
2013

BIRLA INSTITUTE OF TECHNOLOGY AND SCIENCE
PILANI (RAJASTHAN)

CERTIFICATE

This is to certify that the thesis entitled **"Investigations on Alkaline Earth Sulphide Phosphors Activated by Copper for Fluoro-optic Temperature Sensing"** and submitted by **Rajesh Purohit** ID No. **1997PHXF004** for award of Ph.D. Degree of the Institute embodies the original work done by him under my supervision.

Signature in full of the Supervisor _____

Name in capital block letters **R.P. KHARE**

Date:

Designation Visiting Professor
Electrical & Electronics Engineering
B.I.T.S., Pilani-333031

ACKNOWLEDGEMENTS

I would like to express my deepest gratitude to my Param Pujya Gurudev "Pandit Shri Shriram Sharma Acharya" and Param Vandaniya Mataji Bhagwati Devi Sharma.

My acknowledgements are due to the imaginative, creative, and learned scientists of many nations who, over the past several decades, have shaped and reshaped the ideas of fluorescence thermometry as we now know them.

For an experimental research work of this stature demanding modern infrastructure and supportive intervention, the academic nurturing bestowed by Dr. R.P. Khare is highly praiseworthy and it was his expertise and knowledge that led me to move boldly towards this goal. I take this opportunity to extend my sincere gratitude to him for his patience and constructive support. His patience and support helped me overcome many crisis situations and finish this thesis. I hope that one day I would become as good an advisor to my students as Prof. Khare has been to me.

My sincere thanks are due to Late Prof. S. Venkateswaran, Prof. L.K. Maheshwari, presently Advisor, BITS Pilani, Prof. K.E. Raman, BITS Pilani, Goa Campus, for providing me an opportunity to work in such an important and interesting field of fluoro-optic temperature measurement.

In addition, I am indebted to Prof. S. Gurunarayanan, Dean WILP Division, and Prof. Anu Gupta for their constructive and cheerful support.

Much appreciation is expressed to Prof. Prof Surekha Bhanot and Prof. V. K. Chaubey who are the members of Doctoral Advisory Committee (DAC), for their kind suggestions, moral support and assistance.

My special gratitude is due to Prof. B.N. Jain, Vice Chancellor, BITS, Pilani and Prof. G. Raghurama, Director, BITS, Pilani, Pilani campus for providing me facility to carry out this work in BITS, Pilani.

I am also thankful to Prof. S.K. Verma, Dean, Research and Consultancy Division, BITS, Pilani and Prof. Ravi Prakash, for their cooperation and encouragement, during various stages of this work.

I am thankful to all the office, library and technical staff of the Department of EEE and E & I for their help and cooperation.

The successful completion of this manuscript was made possible through the invaluable contribution of a number of people. To say “thank you” to all of you is not even enough to express my gratitude. You are all angels sent to me by Our Heavenly Father. I feel highly blessed by the Almighty in making my dream come true.

Lastly, no words of mine can adequately express my debt to my Late father "Shri Ram Niranjanji Purohit" who always wanted me to do a research work, and my kids, Swapna, Deepshikha and Shubham, who have been a constant source of encouragement for me and who showed me a great patience which enabled me to complete this thesis smoothly.

RAJESH PUROHIT

Abstract

Temperature measurement is crucial for many industrial processes and monitoring tasks. Most of these measurement tasks can be carried out using conventional electric temperature sensors, but with limitations. Particularly under harsh conditions, fiber optic temperature sensors show their advantages over conventional instrumentation. There are several other benefits of using such sensing techniques; e.g. immunity from electrical, magnetic and electromagnetic interference, small sensor size, safety, capability of remote measurements, simplicity of calibration.

One thermometric technique that is adaptable to the needs of a wide variety of situations is based on fluorescing materials, many of them phosphors. The temperature sensitive fluoro-optic behaviour of a phosphor can provide a viable means of monitoring the temperature profiles of surfaces and also measuring the temperature in a variety of situations. The thermographic phosphors and related techniques of measurement have been developed by many researchers; but the numbers of such phosphors which satisfy the requirements of linearity of response, stability, ease of synthesis, phosphors/binder (adhesive) compatibility, etc. are indeed very few.

Therefore, there is a need to investigate more materials for this kind of application. In this context, copper-activated alkaline earth sulphides seem to be promising candidates as they can be easily synthesized, they are quite stable over long period of time, if protected from moisture and their fluorescence / phosphorescence is sensitive to temperature.

Although these phosphors have been known for a very long time, almost no effort has been made to study the temperature sensitive behaviour of these phosphors for this kind of application. Therefore, the present work aims at investigating the thermographic / thermometric properties of CaS:Cu, BaS:Cu and SrS:Cu phosphors.

The objectives of the present investigation are:

(i) To synthesize alkaline earth sulphide phosphors activated by copper with and without flux.

(ii) To investigate the temperature dependence of fluorescence intensity

(iii) To investigate the temperature dependence of phosphorescent lifetime of these phosphors; and

(iv) To develop a fiber-optic temperature probe for measuring the temperature of hot surfaces and to assess the suitability of these materials for other thermographic applications.

Consistent with these objectives, six series of alkaline earth sulphide phosphors have been synthesized by solid state fusion reaction. They are CaS:Cu (without flux), CaS:Cu (with Na_2SO_4 as flux), BaS:Cu (without flux), BaS:Cu (with flux) and SrS:Cu (without flux) and SrS:Cu (with flux). The crystalline structure of these materials has been confirmed by X-ray diffraction studies. The following investigations have been carried out on all the six series of phosphors.

(i) Recording of excitation spectra at RT

(ii) Recording of fluorescence spectra at RT

(iii) Study of the variation of fluorescence intensity at λ_{max} (wavelength of maximum emission) with temperature

(iv) Recording of phosphorescent lifetime at λ_{max} at RT and its variation with temperature

The excitation and emission (fluorescence) spectra recorded at room temperature both show single bands in the case of CaS:Cu, peaking around 310 nm and 480 nm respectively. Addition of flux gives rise to two excitation peaks, one at 310 nm and second, at 345 nm. But the emission peak remains same at 480 nm. The intensity, of course, changes with the concentration of Cu or flux.

In the case of BaS:Cu phosphors, two peaks around 340 nm and 410 nm are observed in the excitation spectra in all the samples. The emission spectra of all the samples consist of a single peak with a maximum around 560 nm.

In copper doped strontium sulphide phosphors, excitation spectra shows two prominent peaks around 310 and 345 nm and the emission peak is observed around 500 nm.

The study of variation of fluorescence intensity at λ_{max} (the wavelength of maximum intensity at RT) of all the series of phosphors shows that it decreases with increase in temperature; in most cases almost linearly. The lifetime of phosphorescence also decreases with temperature.

In the present thesis, these two properties have been utilized for designing a fiber-optic probe for measurement of temperature of hot surfaces. The potential applications of these phosphors in a variety of other temperature monitoring cases have also been discussed at the end.

Table of Contents

List of Tables

List of Figures

List of Abbreviations / Symbols

AR	Analytical reagent
CB	Conduction band
CRT	Cathode-ray tube
Co	Cobalt
Cu	Copper
DC	Direct current
F	Excited state
Fe	Iron
G	Ground state
gm	gram
I	Luminescence intensity
kV	kilo Volt
L_1	Occupied state of luminescence centre
L_2	Unoccupied state of luminescence centre
L_3	Ground state of luminescence centre
L_4	Excited state of luminescence centre
mV	millivolt
M	Metastable state
n	Order of diffraction
N	Number of photons
Ni	Nickel
ns	Nanosecond
PMT	Photomultiplier tube
P_{nr}	Non-radiative transitions
P_r	Radiative transitions
Q_E	Quantum efficiency
RF	Radio Frequency
RT	Room temperature
s	Frequency factor

T	Temperature
T_B	Breaking Point Temperature
T_H	Half-Value Temperature
T_Q	Quenching Temperature
UV	Ultraviolet
VB	Valence band
W	Thermal activation energy
XRD	X-ray diffraction
Δ E	Energy
^{0}C	Degree centigrade
Å	Angstrom
hkl	Miller indices
τ	Lifetime
k_r	Radiative rate constant
k_{nr}	Non-Radiative rate constant
μs	Microsecond
μA	Micro ampere
λ_{max}	Wavelength of maximum emission
λ	Wavelength
θ	Angle of diffraction
λ_{exc}	Wavelength of excitation
η	Fluorescence efficiency

Chapter 1

Introduction

1.1 Importance of Temperature Measurement

The subject of temperature measurement is one of the most important in the field of measurement science and process control. Innumerable industrial processes, biomedical monitoring systems and environmental regulatory systems, to name the few primary applications depend on accurate, reliable temperature information to function effectively. With the continuing technological developments in aerospace and automotive design, as well as newer medical instruments, the need to extend the range of measurement of temperatures has never been greater. In particular, the requirement to measure temperatures in otherwise inaccessible or difficult circumstances, such as those bathed in RF radiation, or other noisy electromagnetic environments, has been one of the imperatives in the development of optical sensors for this purpose.

The importance of temperature measurement can even be seen simplistically by consideration of the financial aspects of the sensors and devices used internationally. Estimates of the worldwide sales of temperature sensors run to several hundred million dollars per year, a figure that could be increased several times when the associated controllers, indicators and other aspects of the measurement system are added.

Industrial, biological, research and development spheres pose to be real difficult environments for the determination of temperature. The region to be measured may be extremely hostile, moving or in a position where access is extremely difficult, or where the physical contact of a sensing probe may even be impossible, or where the presence of interference from other forms of electromagnetic noise excludes the use of electronic thermometers. These situations are, for example, the measurement of the winding temperature of a rotating blade of a turbine engine, the monitoring of winding temperatures in electrical transformers, and temperature monitoring during clinical RF heat treatment. In order to seek alternative means of temperature sensing, one of the alternative research and development areas in thermometry based on the use of fiber optics.

1.2 Fiber Optic Sensors for Temperature Measurement

There are several optical properties of materials that vary with temperature and hence there are as many ways of making the temperature measurement. As the sensor can either be formed using the fiber itself as the sensing medium (termed 'intrinsic sensing') or from a material or structure attached to the end of the fiber (termed 'extrinsic sensing'), the number of possible fiber optic temperature sensor devices is quite large. Indeed, there has been something of an explosion of device proposals seen in the literature. Extensive reviews have been given by Udd and Spillman [1], Udd [2], Grattan [3] and Wickersheim [4], amongst others, on various proposed sensor schemes.

1.2.1 Advantages of fiber optic sensors:

The primary reason for interest in fiber optic sensors, in most cases, stems from the fundamental differences between optical fiber and metal wire for signal transmission. These differences give fiber optic sensors the following valuable characteristics:

(a) Electrical, magnetic and electromagnetic immunity

This is the dominant attribute of the fiber optic sensor. The materials in the probe are typically good electrical insulators. Since they do not conduct electricity, the probes cannot (in principle) introduce electrical shorting paths or cause electrical safety problems. Likewise, they do not absorb significant amounts of electromagnetic radiation or get heated by such fields with the resultant introduction of thermal artifacts into the readings. Last, but not the least, stray fields cannot induce electrical noise in fibers, so the probes exhibit a very high level of immunity to electromagnetic interferences (EMI) when used in electrically or magnetically hostile environments.

(b) Small sensor size

Since the typical sensor does not have to be any larger in diameter than the fiber itself, the sensor can, in principle, be extremely small. This allows its use in applications such as in medicine or in microelectronics where size is critical. Further, since small size means small thermal mass, the fiber optic sensors typically exhibit a commensurate very rapid thermal response.

(c) Safety

The safety issue may be the main reason for use of fiber optic sensors in some particular areas of application. Most fiber optic sensors require no electrical power at sensor end of the system. They generate their own optical signal or they are 'powered' remotely by radiation from a light source located within the instrument, therefore, introducing no danger of electrical sparking in hazardous environments. There is reason to believe that at normal levels of optical power coupled into an optical fiber, i.e., levels of upto several hundred milliwatts of optical power, there is almost no hazard with any accidental fracture of cable and the possible focusing of the optical radiation by the lensing effects of the broken end. Particularly in the chemical industry, where highly explosive gases or gas mixtures may be used, this is an important consideration, but on the whole in normal use, fiber optic sensing systems can be considered intrinsically safe.

(d) Capability of remote measurements

The small size of the fiber and its electrical, chemical and thermal inertness can allow for long-term location of the sensor deep inside complex equipment and thereby provide access to locations which are difficult to address, where monitoring the temperature may be of interest. Beyond this, however, certain of the optical techniques allow non-contact or remote sensing of temperature. For example, the sensor may be located some distance from the fiber tip. This is most easily accomplished with the use of fluorescence-based fiber optic techniques and with infrared radiometry. The point of interest may in fact be located on a moving or rotating part or behind a transparent window as in a pressure or vacuum chamber, and yet the radiation can be readily collected and analyzed to gain temperature information remotely.

(e) Other advantages

Beyond these generic advantages, certain of the optical techniques exhibit an unusually wide range of operation with precision good enough to meet reasonable requirements. At the same time these techniques provide simplicity of calibration (or, as in the case of the fluorescence lifetime techniques, the absence of the need for calibration for individual probes).

1.3 Fluoro-optic Temperature Sensing

One thermometric technique that is adaptable to the needs of a variety of situations is based on fluorescing materials, many of them phosphors. The thermal dependence of phosphor fluorescence may be exploited to provide for a non-contact, emissivity-independent, optical alternative to other more conventional techniques, e.g., those employing pyrometry, thermocouples, or thermistors. In fact, there are certain situations in which the advantages fluorescence-based thermometry has over other methods make it the only useful approach. Prior to discussing those properties of phosphors important to thermometry, some relevant terminology should be introduced.

Luminescence refers to the absorption of energy by a material, with the subsequent emission of light. This is a phenomenon distinct from blackbody radiation, incandescence, or other such effects that cause material to glow at high temperature. Fluorescence refers to the same process as luminescence, but with the qualification that the emission is usually in the visible band and has a duration of typically 10^{-9} to 10^{-3} s. Phosphorescence is a type of luminescence of greater duration, $\approx 10^{-3}$ to 10^{3} s. Emission, luminescence, phosphorescence, and fluorescence are closely related terms [5]. These terms have been explained in detail in Chapter 3.

A phosphor is a fine white, or slightly colored powder designed to fluoresce very efficiently. Color television and cathode-ray tube (CRT) displays employ phosphor screens that emit visible light when seen by the viewer. The source of energy that excites this fluorescence is a beam of electrons. Other examples of phosphor uses are in fluorescent spray paints, fluorescent lighting, photocopy lamps, scintillators and x-ray conversion screens. For the last, a beam of x-rays provides the excitation. Other excitation sources are gamma rays, ultraviolet (UV) light and, in some cases visible light. Many different phosphors are manufactured for these and other applications. The lighting and display industries have provided the impetus for the study of thousands of phosphor materials over the last several decades [6,7,8].

In terms of their composition, phosphors may be divided into two classes: organic and inorganic. It is the latter that have primarily but not exclusively found use in thermometry. Inorganic phosphors consist of two components: a host inorganic compound and an activator or doping agent, from which the light is emitted. Such

materials do not have to be in the powdered form to be useful. Some phosphors are fabricated into macroscopic pieces of crystal or glass.

1.4 **Factors influencing fluorescence process**

1.4.1 Dopant concentration

The parameters describing the luminescence characteristics of any given phosphor are dependent on the concentration of the activating impurity. Overall intensity, relative spectral distribution, decay time, rise time, and response to temperature are all affected to some degree. It is standard practice when characterizing the thermal response of a given phosphor to measure its brightness as a function of dopant concentration.

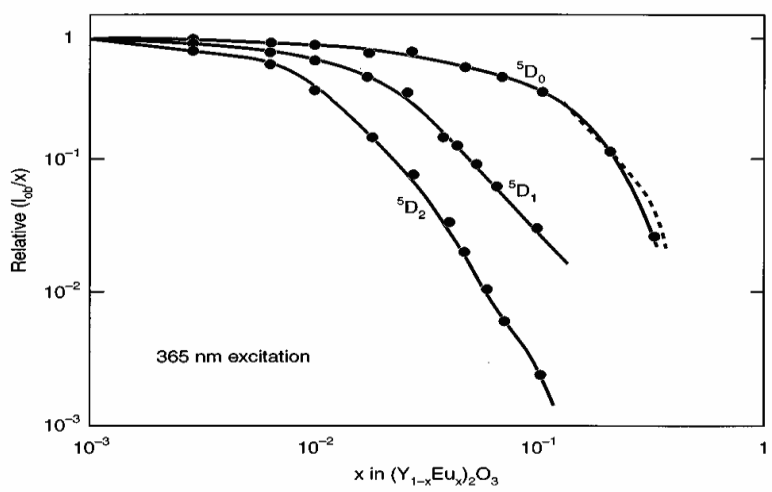

Fig. 1.1: *Fluorescence intensity vs dopant concentration for Eu in a host of* Y_2O_3 [12]

A representative case [9] is shown in Fig. 1.1. These data illustrate that a high dopant concentration of Eu in a host of Y_2O_3 results in most of the luminescence being concentrated into the $^5D_0$ emission line (at 611 nm) that is of importance to color televisions. They further illustrate that the more activator centers there are in a phosphor, the more it will fluoresce, up to a point. However, when the concentration levels reach a certain point, another nonradiative deexcitation pathway becomes important. As the activator density is increased, the probability that an excited activator will transfer energy nonradiatively to a neighboring dopant ion increases. The arrival at a cutoff in this process is usually referred to as concentration quenching. For other dopants, even when in the same host, the concentration that produces the maximum brightness will be different. For example, the optimum concentration of Sm or Dy in Y_2O_3 is 0.5% [7, 10].

Generally, one seeks to maximize the brightness of the phosphor. With respect to thermometry applications, however, there are other considerations that may warrant the use of different strategies. For instance, at high concentrations the fluorescence decay profile may not be that of simple single-exponential decay. This is important for decay time based approaches since multiexponential and nonexponential decay profiles are more difficult to model. (Multiexponential decay is not necessarily a problem if measurements based on continuous line intensities are being made though.) These more complex waveforms can make calibration and data analysis difficult but not intractable. An example of this phenomenon arises in the use of YAG:Tb, which is a good phosphor for high temperature thermometry. At low concentrations, about 5/6 of the excitation energy drives the $^5D_3$ states (blue bands between 350 and 450 nm) while the remainder excites the $^5D_4$ states (blue-green and green bands at 488 and 544 nm). At sufficiently high dopant levels, there is an energy transfer from the higher to the lower states. Whereas the latter states exhibit exponential decay at up to 3% dopant concentration, the former appear to follow the Förster model [11], the decay function for which is

$$\frac{x(t)}{x(0)} = \exp\left[\frac{-t}{\tau} - \frac{\frac{N}{N_0}}{\sqrt{\frac{\pi t}{\tau}}}\right] \qquad (1.1)$$

where $N_0 = 3/(4\,\pi R_0^3)$ with R_0 being the critical distance for energy transfer (≥ 1 nm), N is the dopant concentration in number of atoms per cm^3, and τ is the unquenched spontaneous lifetime. The spectral emission distribution can be a sensitive function of dopant concentration. At low Eu concentrations, the shorter wavelength lines are stronger than they are at higher concentrations. Kusama *et al* [12] noted that this is particularly important for intensity based thermometry. They indicate that the $^5D_2$ emission of Y_2O_2S:Eu is especially sensitive to Eu concentrations. In comparing temperature dependent ratios of this line to a $^5D_0$ emission line, a difference of 0.1 mol % between samples will vary the ratio by about 5% and lead to an estimated error.

1.4.2 Saturation Effects

Saturation effects on YAG:Tb, another phosphor of interest in thermometry, are discussed by de Leeuw and 't Hooft [13]. A survey of the study of saturation effects is given there.

High incident fluxes, whether from laser, particle beam, or any other excitation source, can lead to luminescence saturation effects. When this occurs, phosphor efficiency changes as a function of the incident flux. In typical applications, this would manifest itself as a spurious temperature change if the flux were to increase to the point of causing saturation. An illustrative example arises in the description of saturation of Y_2O_3S:Eu by Imanaga *et al.* [14] where the relative dopant concentrations were 0.1% and 4%. A nitrogen laser (337 nm) focused to a spot size of about 1 mm^2 was used for short duration (4 ns) photon excitation. For cathode ray excitation, a 10 kV electron beam of 5 μs duration was used and a number of effects were noted. With the latter form of excitation, the spectral distribution changed as a function of input fluence beginning at about 0.1 $\mu A/cm^2$. The effect was more pronounced at higher concentrations. Above a certain threshold value, overall intensity decreases, but for the lower concentration, this threshold value itself is lower and the rate of decrease is faster than at higher concentrations. Increasing the beam voltage, independently of beam current, will degrade the saturation of this phosphor according to Yamamoto and Kano [15]. Conversely, the situation may improve for some phosphors over a certain range, as observed in the case of ZnS and Zn_2SiO_4 by Dowling and Sewell [16]. For short-pulse excitation via nitrogen laser, the saturation effects are even more complex. Moreover, saturation is itself a temperature dependent phenomenon. Generally, for all concentrations, the saturation thresholds are lower at higher temperatures. Saturation is enhanced at higher concentrations, but the rates will be different from one emission line to another.

There is evidence for a decrease in fluorescence decay time with increasing laser fluence (energy over the area of the spot size of laser). Imanaga *et al.* [14] suggest several possible mechanisms that may cause luminescence saturation behavior in this case. Beam-induced temperature rise was ruled out as a possible cause since saturation was less pronounced for the most temperature-dependent emission lines, as well as for other reasons, although this might be the dominant mechanism at work in

other cases. Thermodynamic considerations, coupled with experimental studies, can help determine if beam-related effects will be a problem in a given situation. The results found by Imanaga *et al* may likely be due to the increased probability of having two excited dopant atoms in close proximity to each other. Evidently, when this occurs, an additional nonradiative deexcitation path is allowed. For instance, one of the excited atoms might transfer its energy to its neighbor, thus creating a doubly excited atom which nonetheless can emit only one fluorescence photon rather than two, thus decreasing the emission rate.

In most applications, one does not have the opportunity to deliver a surfeit of laser excitation due to the necessity for transporting beams long distances, usually over optical fibers which have limited fluence-handling capacity. Saturation becomes a relatively important problem during laboratory calibrations, however, when a more nearly ideal optical arrangement is employed, i.e., one having higher available laser power and finer focusing.

Finally, we note that Raue *et al.* [17] have studied saturation effects in Tb-doped phosphors excited by cathode ray beams. They have developed a model that is consistent with the results of excited state absorption experiments carried out on a variety of these materials.

1.4.3 Impurities

There are inevitably small amounts of undesired species in solid solution in the host material, and these change the atomic electronic environment experienced by the activators so as to either augment or hinder phosphor performance. For instance, at concentrations greater than 1 ppm, transition metal impurities will decrease phosphor brightness. This is because they absorb at wavelengths similar to those of the typical activators, thus effectively stealing excitation energy and decreasing the number of excited fluorescence centers. Moreover, nonradiative energy transfer from an excited activator to such impurities is efficient, thus increasing the decay rate and quenching the emission.

Even so, it is possible to mix powdered phosphors with a great variety of substances, from epoxies to inorganic binders, without affecting emission characteristics. In fact, ceramic binders can be flame sprayed, plasma sprayed, etc., as long as the result is a suspension of mixed materials. Properly chosen additives can also play a positive role.

For example, addition of small amounts of Dy and Tb or Pr to Y_2O_3:Eu has the effect of decreasing the lifetime by as much as a factor of 3 with little or no change in quantum efficiency [18]. Having a faster response can be important when using phosphor thermometry to interrogate, e.g., a high speed rotating shaft that has a ‘‘viewing time’’ that is limited [19,20].

1.4.4 Sensitizers

A sensitizer is a material that, when added to a phosphor, increases the fluorescence output. Weber [21], in a survey of rare-earth laser research, formulated a table of rare-earth ions that have been used as active laser media, and included in it the corresponding rare earths used as sensitizers for each. The sensitizing dopant will absorb energy and, rather than emitting fluorescence, it transfers its energy to the main dopant from which an optical transition occurs. For example, Khare [22,23] notes that cerium has been found to be a sensitizer for erbium, while gadolinium is a sensitizer for cerium. A prospective sensitizer must exhibit no absorption at the emission wavelength of interest. It must also have absorption bands that do not steal excitation energy from the activator. Finally, it must have energy levels that are above the fluorescing line which feed the activator but which do not quench it [24].

1.4.5 Quantum efficiency

Quantum efficiency, Q_E, is a parameter often used to help scale a phosphor’s ability to produce bright light. Knowledge of the approximate quantum efficiency of a phosphor can aid in determining expected signal levels. Numerically, the quantum efficiency is the ratio of the rate of photons absorbed by the phosphor to the rate that are absorbed. If $Q_E \geq 0.8$, a material is considered to be an efficient phosphor. Q_E is not as dominant a criterion for fluorescence thermometry as it is for lighting and display applications. Fig. 1.2. presents the emission intensities for a variety of activators in YVO_4. With Eu as an activator, the resulting phosphor is most efficient and useful in thermometry only above the quenching temperature of ≈ 500°C. On the other hand, a Dy activator in this host will produce decay times that make the phosphor useful in the range from 300 to 500°C. (The ratio of two emitting lines in this case can also be used to make measurements at somewhat lower temperatures.) It is interesting to note that YVO_4:Nd is being used as a laser medium despite its low efficiency. For YVO_4:Eu, QE = 68% at the optimum concentration of 0.05 mol % (253.7 nm excitation) whereas

QE = 88% for YVO_4:Dy at a concentration of 0.003 mol %. The latter is clearly a more efficient phosphor, except for the fact that the concentration dependence is more pronounced.

Efficiency is a wavelength-dependent phenomenon. Therefore, if, e.g., instrumentation availability prevents the use of mid-UV excitation with a phosphor that happens to be efficient in that band, then a substitute material better suited to the wavelength of the excitation source should be used instead.

Fig. 1.2: *The emission intensities for various rare-earth activators in YVO_4 p. 438, Ref.* [7]

1.5 Temperature sensitive luminescence parameters

Phosphors are thermographic if they exhibit luminescence properties that change with temperature. This gives the phosphors their temperature sensing characteristics. a number of schemes have been proposed based on these characteristics [25,26]. This section reviews all known temperature responses of phosphors. These are illustrated schematically in Fig.1.3.

1.5.1 Fluorescence intensity

Normally it has been observed that intensity of fluorescence varies with temperature. As an illustration of this fact, a comparison of the two spectra of La_2O_2S:Eu [7] presented in Fig. 1.4. shows that the relative intensities of the lines near 465 and 512 nm are temperature dependent.

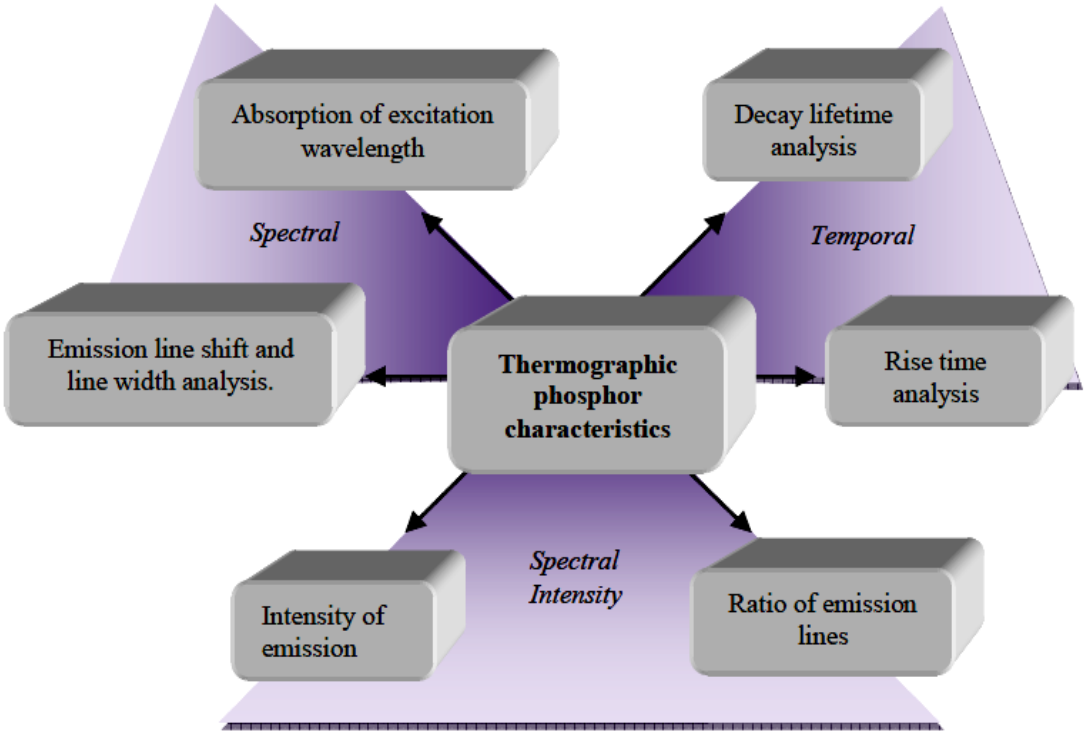

Fig 1.3: Different response modes for thermographic phosphors.

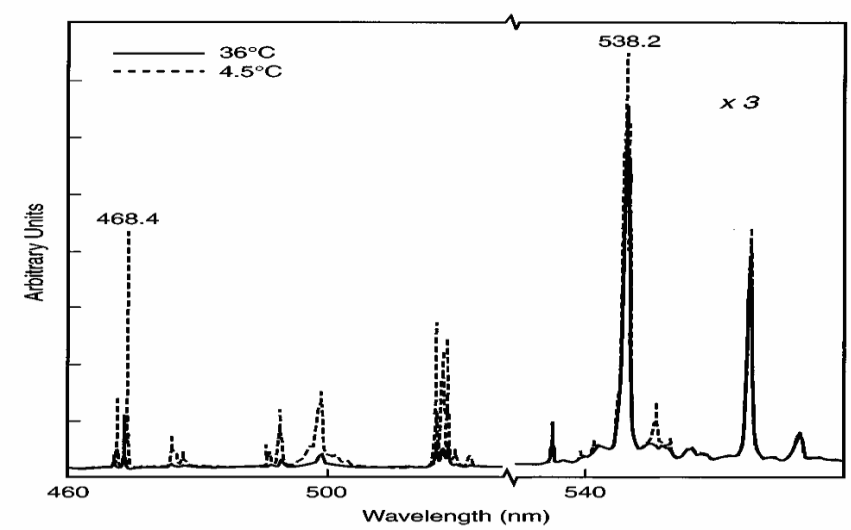

Fig. 1.4: *Temperature dependence of La_2O_2S:Eu spectra.[7]*

In fact, it is generally the case that certain of the lines in these phosphors get weaker, i.e., become less bright, as the temperature of the material is increased. A plot of intensity versus temperature is shown in Fig. 1.5 Clearly, for this material, there is a region where the selected emission line is no longer sensitive to temperature change. At a particular value, viz., the "quenching temperature" (as discussed above), the strength of the emission line falls off drastically. The quenching temperatures and the

slopes of the temperature dependencies usually differ for each type of phosphor and for each of the emission lines within the spectrum of a given phosphor. In some cases there may be an increase in intensity with temperature over a given range of temperatures, although the opposite is more typical.

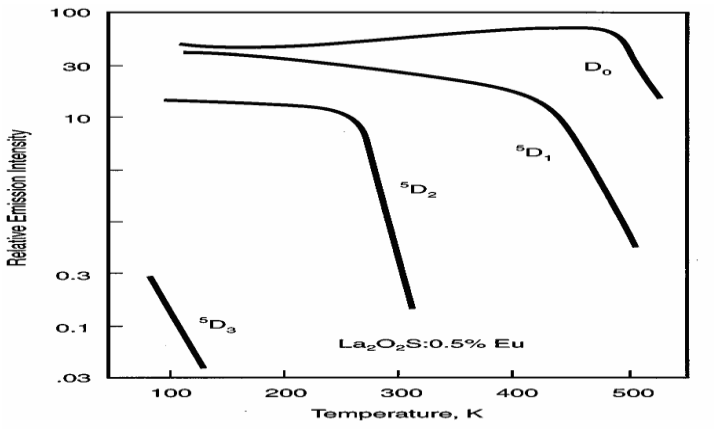

Fig. 1.5: *Emission intensity vs temperature for La_2O_2S:Eu* (*after Ref.* [27]).

1.5.2 Fluorescence lifetime

When a phosphor is excited by a pulsed source, the persistence of the resulting fluorescence can be observed providing that the length of the source pulse is much shorter than the persistence time of the phosphor's fluorescence. This is illustrated in Fig. 1.6 for the 514 nm line of La_2O_2S:Eu monitored at two different temperatures. The luminescence intensity decays exponentially in this case, according to the relation:

$$I = I_0 e^{-t/\tau} \qquad (1.2)$$

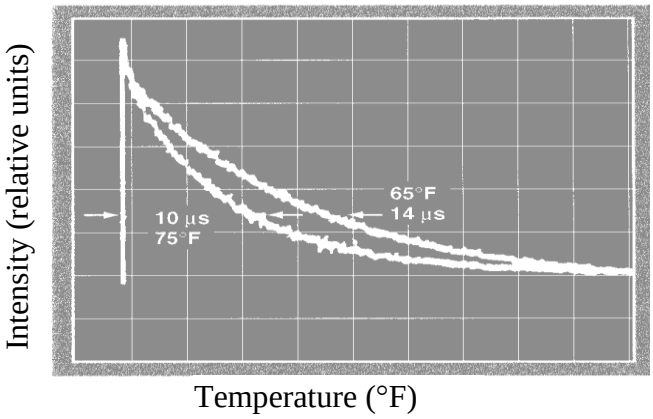

Fig. 1.6: *Phosphor decay characteristics at 65 and 75 F (La_2O_2S:Eu at 514 nm).*[27]

where τ (the lifetime or decay time) is the standard 1/*e* (≈ 37%) folding time for the fluorescence. The decay time is often a very sensitive function of temperature and, therefore, a determination of its value constitutes a very useful method of thermometry. A portion of a calibration curve for La_2O_2S:Eu is shown in Fig. 1.7 for three of its emission lines.

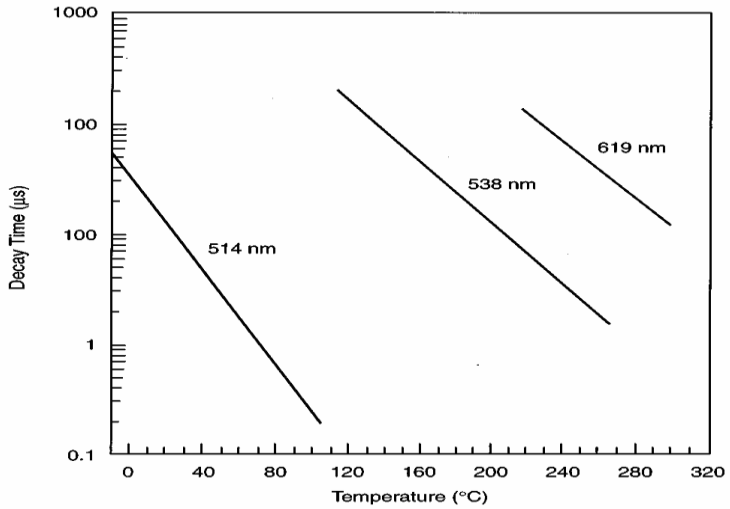

Fig. 1.7: *Fluorescence decay time vs temperature for La_2O_2S:Eu [27].*

1.5.3 Fluorescence line shift

Each emission line is characterized by a wavelength for which the intensity is maximum. Its value may change slightly with temperature, and this is termed a line shift. Also, an emission line has a finite width, called the line width, which is often designated by the spectral width at half the maximum line intensity. Line width and line shift changes as a function of temperature are generally small, and are not often used in fluorescence thermometry. However, as previously mentioned, Kusama *et al* [12] utilized this approach for cathode-ray-tube thermometry. As shown in Fig. 1.8, they observed a shift to the blue of about 0.2 nm in going from –15 to 72°C.

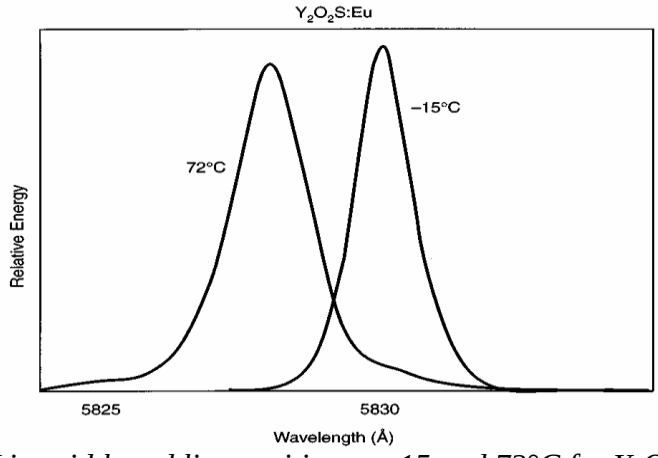

Fig. 1.8: *Linewidth and line position at –15 and 72°C for Y_2O_2S:Eu* [12].

The data they presented indicate that the line shift has an approximately quadratic dependence on frequency.

1.5.4 Temperature dependence of absorption band and excitation spectra

The absorption spectra of many phosphors consist of a relatively broad band at the blue or ultraviolet end of the spectrum, along with sharper absorption features in the visible and near-IR. The sharper features are often due to atomic transitions of the dopant atom and, as noted above, exhibit some temperature sensitivity. The broad absorption band, however, since it results from direct interaction with the host, may show more marked temperature dependence.

Bugos [28] studied the temperature-dependent excitation spectra of a number of thermographic phosphors. The results were very instructive, because an excitation spectrum provides an alternate means of determining the position and strength of absorption features in a material. Whereas absorption spectra are obtained by measuring the amount of light transmitted through a specimen as a function of wavelength, an excitation spectrum is determined by monitoring the intensity of an emission line while the excitation wavelength is varied. An example is shown in Fig.1.9 which presents the temperature-dependent excitation spectra [28] of Y_2O_3:Eu. Within the resolution of the Perkin-Elmer model 650-10S spectrometer (≈ 1 nm) used in that work, no discernible change was found in the atomic-transition bandwidths. Even so, the charge-transfer band is seen to move toward the red end of the spectrum by about 30 nm per 50°C (i.e., 0.6 nm/°C.) The peak of the absorption for this material increases up to about 400°C. (At this point, the heat generated by the oven placed inside the spectrometer could begin to affect the measurement.) We note that at room temperature this phosphor is not excited efficiently by standard sources such as a nitrogen laser (337 nm), a tripled YAG laser (355 nm), or a long-wavelength mercury vapor lamp (365 nm). Even so, these particular sources are efficiently absorbed at higher temperatures and are quite useful in that regime.

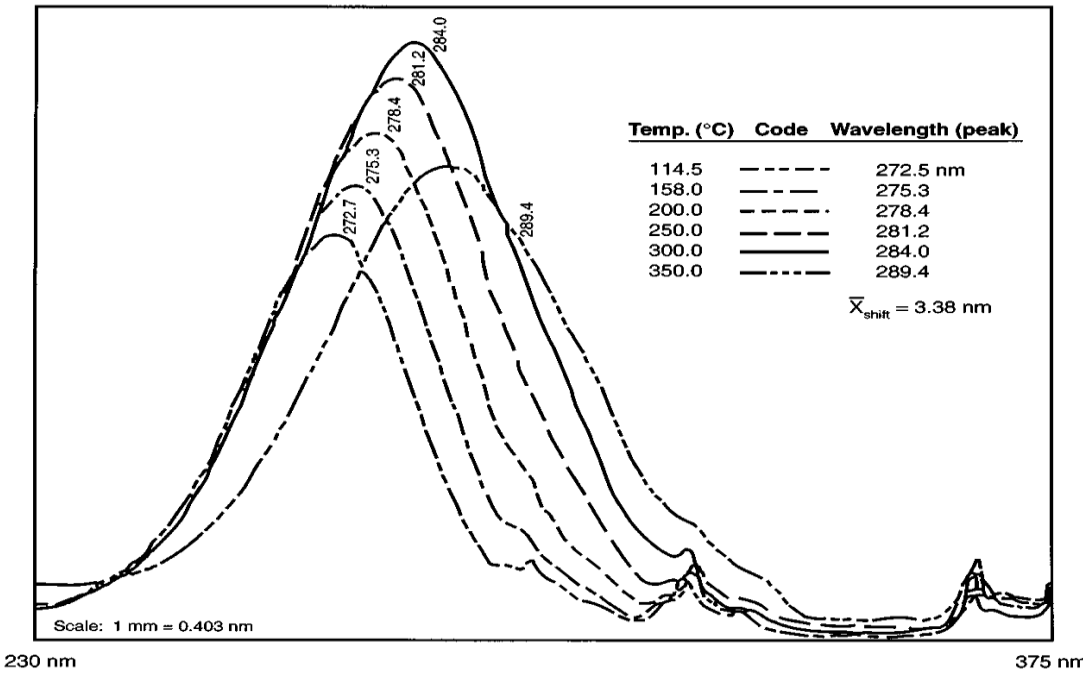

Fig. 1.9: *The temperature-dependent excitation spectra of Y_2O_3 :Eu, as measured with a Perkin-Elmer model 650-10S spectrometer with a resolution of approximately 1 nm. (after* [28]*)*

The temperature dependence of the absorption was exploited by Turley *et al.* [29] to infer the energy of a CO_2 laser by its heating of a phosphor sample. For this, constant excitation was applied to a YVO_4:Dy phosphor by a flash lamp that was filtered to illuminate at 365 nm. This wavelength is weakly absorbed by the phosphor at room temperature. When the 100 ns laser pulse heated the sample, the absorption and the resulting (detected) fluorescence increased in proportion to the incident laser energy. The associated temperature rise did not exceed the quenching temperature of the phosphor.

1.6 Statement of the problem

In the preceding section, we have discussed that the parameters of fluorescence like intensity, decay time, etc. vary as a function of temperature. These parameters of fluorescence of some specific phosphors have been used for remote as well as direct measurement of temperature of both static and moving objects. The state of art of these thermographic phosphors and related techniques of measurement have been recently reviewed by Brübach et al [30], Khalid and Kontis [31], McSherry M., Fitzpatrick C. and Lewis E. [32]. However, the number of such phosphors, which satisfy the requirement of linearity of response, spectral tunability, stability and ease of synthesis, are very few. Therefore, there is a need to investigate more materials for this application. In this context, copper activated alkaline earth sulphides seem to be

promising candidates as these phosphors can be easily synthesized, they are quite stable over long period of time (ten to fifteen years), if protected from moisture and their luminescence is sensitive to temperature. Although these phosphors have been known for a very long time [33] and their photoluminescence, cathodoluminescence and electroluminescence have been reported by many investigators in single sulphides [34-56] as well as mixed sulphides [57-60], no systematic efforts have been made to study the temperature dependence of luminescence of this system. A summary of the important results reported so far is given as follows.

First detailed and systematic investigation on CaS was reported by Lehmann and Ryan and Lehmann [34, 35]. They concluded that it is an excellent host material for efficient cathode-ray tube phosphors when activated with rare earths. Since then a number of reports have appeared describing spectroscopic properties of pure and activated sulphides and revealing applications of BaS, SrS and MgS in alloy semiconductiors [61], radiation dosimetry [62] and fast high resolution optically stimulated luminescence imaging [63].

Experimental band gap energies of sulphides determined from the optical reflection spectra by various workers [34, 64, 65] are listed in Table 1.2.

Table 1.1: Experimental band gap energies of alkaline earth sulphides

Band-gap(eV)	CaS	SrS	BaS
Polycrystalline, 300K(∗)	4.8	4.4	3.8
Single crystal, 77K(∃)	5.3	-	-
Single crystal, 2K(∂)	5.343	4.831	3.941
Lattice constant (Å)	5.6975(Î)	6.0190(Î)	6.3842(Î)

(∗) Lehmann and Ryan [35] (∂) Kaneko and Koda [64] (∃) Realo and Jaek [65]
(Î) Kaneko et al. [66]

The work so far reported on Cu-activated sulphides is limited to emission studies. The emission spectrum strongly depends on the presence of a co-activator in the lattice influencing the peak positions of the emission band [38]. However, no systematic trend in the peak-shift has been observed as either the host lattice or co-activators are varied [34].

The Cu emission also depends on the Cu-concentration in the lattice and shows concentration quenching at higher Cu concentrations. In mixed sulphides, SrS-BaS, a gradual shift of emission spectra to longer wavelengths with increasing BaS content

was observed as expected [67]. A similar shift has been reported by Yamashita et. al [59,68] in CaS-SrS mixed suphides. In spite of so much research work on these phosphors, the variation of fluorescence intensity and the mean lifetime of phosphorescence with temperature have not been investigated thoroughly. Such an investigation may lead to a better understanding of the mechanism of luminescence processes in this system as well as may lead to the development of materials for thermometry / thermography

Therefore, the present work aims at investigating the fluoro-optic behaviour of copper-activated alkaline earth sulphide phosphors at room temperature and as a function of temperature.

The objectives of the present investigations are:

(i) To synthesize alkaline earth sulphide phosphors activated by copper with and without flux (a compatible low melting salt)

(ii) To ascertain the crystalline structure of synthesized materials

(iii) To study the spectral behaviour of these phosphors at room temperature

(iv) To investigate the temperature dependence of fluorescence intensity and phosphorescent lifetime of these phosphors; and

(v) To assess the suitability of these materials for thermographic applications

Consistent with these objectives, six series of alkaline earth sulphide phosphors have been synthesized by solid state fusion reaction. They are CaS:Cu (without flux), CaS:Cu (with flux), BaS:Cu(without flux), BaS:Cu(with flux) and SrS:Cu(without flux) and SrS:Cu (with flux). The following investigations have been carried out on all the six series of phosphors.

(i) Recording of excitation spectra at RT

(ii) Recording of fluorescence spectra at RT

(iii) Study of the variation of fluorescence intensity at λ_{max} (wavelength of maximum emission) with temperature

(iv) Recording of phosphorescent lifetime at λ_{max} at RT.

(v) Study of the variation of phosphorescent lifetime at λ_{max} with temperature.

Finally the results of all the experiments have been correlated and suitability of these materials for thermograhphic applications has been discussed.

References

[1] Eric Udd and William B. Spillman, Jr (Eds), *Fiber Optic Sensors – An introduction for engineers and scientists* (Second Edition), Wiley, New York (2011)

[2] Eric Udd (Ed) *Fiber Optic Sensors and Applications -V,* Proc. of SPIE Vol. **6770**, (677002) 1-10 (2007).

[3] K.T.V. Grattan, Fiber optic techniques for temperature sensing, In: *Fiber Optic Chemical Sensors and Biosensors*, Vol. II, Ed. O.S. Wolfbeis (London: CRC Press): 151-192 (1991).

[4] K.A. Wickersheim, Fiberoptic thermometry: an overview. In: *Temperature-Its Measurement and Control in Science and Industry*, **6**, Part 2. New York: American Institute of Physics, pp 711-714 (1992).

[5] P. Pringsheim, *Fluorescence and Phosphorescence*, Interscience, New York, pp. 1-5 (1949).

[6] K.H. Butler, *Fluorescent Lamp Phosphors*, Pennsylvania State university Press, University Park, PA (1980).

[7] R.C. Ropp, Luminescence and the Solid State, *Studies in Inorganic Chemistry* Vol.12, Elsevier, Amsterdam (1991).

[8] R.C. Ropp, The Chemistry of Artificial Lighting Devices: Lamps, Phosphors and Cathode Ray Tubes, *Studies in Inorganic Chemistry*, **17**, Elsevier, Amsterdam, (1993).

[9] L. Ozawa and P. M. Jaffe, *J. Electrochem. Soc*. **118**, 1678 (1971).

[10] J. L. Sommerdijk and A. Bril, *J. Electrochem. Soc*. **122**, 952 (1975).

[11] W. F. van der Weg, T. J. A. Popma, and A. T. Vink, *J. Appl. Phys.* **57**, 5450 (1985).

[12] H. Kusama, O. J. Sovers, and T. Yoshioka, *Jpn. J. Appl. Phys.* **15**, 2349 (1976).

[13] D. M. de Leeuw and G. W. 't Hooft, *J. Lumin.* **28**, 275 (1983).

[14] S. Imanaga, S. Yokono, and T. Hoshima, *Jpn. J. Appl. Phys.* **19**, 41 (1980).

[15] H. Yamamoto and T. Kano, *J. Electrochem. Soc.* **126**, 305 (1979).

[16] P. H. Dowling and J. R. Sewell, *J. Electrochem. Soc.* **100**, 22 (1953).

[17] R. Raue, K. Nieuwesteeg, and W. Busselt, *J. Lumin*. **48 & 49**, 485 (1991).

[18] J. L. Ferri and J. E. Mathers, *US Patent No. 3*, 639, 932 (8 February 1972).

[19] S. S. Lutz, W. D. Turley, H. M. Borella, B. W. Noel, M. R. Cates, and M. R. Robert, Proceedings of the 34th International Instrumentation Symposium: Instrumentation for the Aerospace Industry, *Instrument Society of America*, Research Triangle Park, NC, pp. 217–229, (1988).

[20] S. W. Allison, M. R. Cates, B. W. Noel, and G. T. Gillies, *IEEE Trans. Instrum. Meas.* **37**, 637 (1988).

[21] M. J. Weber, in The *Handbook on the Physics and Chemistry of Rare Earths,* edited by K. A. Gschneidner, Jr. and L. Eyring, North-Holland, Amsterdam Chap. 35, pp. 275–315 (1979).

[22] R.P. Khare, J.D. Ranade, *J. Matter. Sc. (UK)*, **15**, 1868 (1980).

[23] R.P. Khare, J.D. Ranade, *Indian J. Pure Appl. Physics*, **13**, 664 (1975).

[24] Guo Chang-Xin, Zhang Wei-Ping, and Shi Chao-Shu, *J. Lumin.* **24–25**, 297 (1981).

[25] S.W. Allison and G.T. Gillies, *Rev. Sci. Instrumn.* **68**, 2615 (1997).

[26] K.T.V. Grattan and Z.Y. Zhang, "*Fiber Optic Fluorescence Thermometry*", Chapman & Hall, London (1995).

[27] W. H. Fonger and C. W. Struck, *J. Chem. Phys.* **52**, 6364 (1970).

[28] A. R. Bugos, S. W. Allison, D. L. Beshears, and M. R. Cates, in *Proceedings of the IEEE Southeastcon Conference*, IEEE, New York, pp. 228-233 (1988).

[29] W. D. Turley, C. E. Iverson, S. S. Lutz, R. L. Flurer, J. R. Schaub, S. W. Allison, J. S. Ladish, and S. E. Caldwell, *Proc. SPIE*, **1172**, 27 (1989).

[30] J. Brübach, C. Pflitsch, A. Dreizler, and B. Atakan: *Progress in Energy and Combustion Science* **39**, 37- 60 (2013).

[31] A. H. Khalid and K. Kontis: *Sensors*, **8**, 5673-5744, (2008).

[32] Mc Sherry M., Fitzpatrick C. and Lewis E., *Sensor Review*, **25**, 56–62, (2005).

[33] F. Urbach, D. Pearlman and H. Hemmendinger, *J. Opt. Soc. Am.*, **36**, 372 (1946).

[34] W. Lehman, *J Electrochem. Soc.* **117,** 1389 (1970).

[35] W. Lehmann and M. F. Ryan, *J. Electrochem. Soc.* **118**, 477 (1971).

[36] W. Lehman, *J Lumin.*, **5,** 87 (1972).

[37] N. Singh, G.L. Marwaha and V.K. Mathur, *Phys Status Solidi* (a) **66,** 761 (1981).

[38] R. Pandey and S. Sivaraman, *J Phys. Chem. Solids*, **52,** 211 (1991).

[39] N. Yamashita, *Jpn. J. Appl. Phys* **30,** 3335 (1991).

[40] W. M. Li, et al, *J Appl. Phys.* **86,** 5017 (1999).

[41] C. Barthou, J. Benoit, P. Benalloul, K. Polamo and E. Soininen, *J. Appl. Phys.* **88,** 1061, (2000).

[42] D. Jia, W. Jia, D. R. Evans, W. M. Dennis, H. Liu, J. Zhu and W. M. Yen, *J. Appl. Phys.*, **88,** 3402, (2000).

[43] C. J. Summers, B. K. Wagner, W. Tong, W. Park, M. Chaichimansour, Y. B. Xin, *J. Cryst. Growth*, **214**, 918 (2000).

[44] M. Peter, M. Murayama, S. Nishimura, K. Ohmi, S. Tanaka and H. Kobayashi, *J. Appl. Phys.*, **90**, 1992 (2001).

[45] D. C. Morton, E. W. Forsythe, S. S. Sun, M. C. Wood, M. H. Ervin and K. Kirchner, *Appl. Phys. Lett.*, **78**, 1400, (2001).

[46] H. Z. Yi, W. Y. Sheng, S. Li, X. X. Rong, *J. Phys: Condens. Matter.*, **13**, 3665 (2001).

[47] J. Wu, D. Newman, Ian V. F. Viney, *J. Phys. D: Appl. Phys.*, **35**, 968 (2002).

[48] V. G. Kravets, A. A. Kryuchin, V. A. Ataev, V. M. Shershukov, *Optic. Matter.*, **19**, 421, (2002).

[49] D. Wruck, R. Boyn, M. Wienecke, F. Henneberger, U. Troppenz, B. Huttl, W. Bohne, B. Reinhold, H. E. Mahnke, *J. Appl. Phys.*, **91,** 2847 (2002).

[50] P. F. Smet, J. V. Gheluwe, D. Poleman, R. L. V. Meirhaeghe, *J. Lumin.*, **104,** 145 (2003).

[51] J. M. Fitzgerald, J. G. Hoekstra, R. K. Bansal, J. D. Fowlkes, P. D. Rack, *Mat. Res. Soc. Symp. Proc.*, **780,** Y1.4.1, (2003).

[52] J. Ihanus, M. Ritala, M. Leskela, E. Soininen, W. Park, A. E. Kaloyeros, W. Harris, K. W. Barth, A. W. Topol, T. Sajavaara and J. Keinonen, *J. Appl. Phys.*, **94,** 3862 (2003).

[53] S. J. Yun, S. H. Ko Park, *Electrochem. Solid State Lett.*, **6,** C30 (2003).

[54] J. Wu, D. Newman and I. Viney, *J. Phys. D: Appl. Phys.*, **37,** 1371 (2004).

[55] Y. S. Kim, S. J. Yun, *J. Phys.: Condens. Matter.*, **16,** 569, (2004).

[56] P. F. Smet, D. Poelman and R. L. Meirhaeghe, *J. Appl. Phys.*, **95,** 184 (2004).

[57] A.M. Rastogi and S.L. Mor, *Phys. Status Solidi(b)*, **63**, 75 (1981).

[58] B.B.Laud and V. W. Ku1karni, *Phys. Status Solidi(a)*, **51,** 269 (1979).

[59] N. Yamashita, K. Ebisumori and K. Nakamura, *Jpn. J. Appl Phys.*, **32**, 3846 (1993).

[60] N. Yamashita, K. Ebisumori and K. Nakamura, *J. Lumin.*, **62,** 25 (1994).

[61] H. Hollway and G. Jesion, *Phys. Rev.*, **B26**, 5617, (1982).

[62] R. P. Rao and D. R. Rao, *Hlth. Phys.*, **45,** 1001, (1983).

[63] J. Gaslot, P. Braunlich and J.P. Fillard, *Appl. Phys. Lett.*, **40**, 376 (1982).

[64] Y. Kaneko and T. Koda , *J. Cryst. Growth*, **86,** 72, (1988).

[65] K. Realo and I. Jaek Eesti NSV Teaduste *Akad. Toimetised Fuus Mat.*, **27**, 79 (1978).

[66] Y. Kaneko., K. Morimoto and T. Koda, *J. Phys. Soc. Japan*, **51,** 2247 (1982).

[67] R.P. Khare, K.C. Sati and Abhinav Asati, *Int J. Appl Engg*, **2,** 144-147 (2012)

[68] K.C. Sati, Abhinav Asati and R.P. Khare, *Indian Journal of Physics* ,**85**, 629-635 (2011)

Chapter 2

Synthesis of Fluoro-optic Materials

2.1 Introduction:

An inorganic solid may be made to luminesce either by the 'built in' traces of beneficial impurity and / or by structural defects foreign to the general pattern of its composition. Impurity-activated phosphors, thus, essentially consist of a bulk material which has a normal crystal structure, and an activating impurity which is incorporated in the host lattice by heating an intimate mixture of phosphor components to high temperatures. In some cases, certain low melting salts, called fluxes, are mixed with the charge to obtain efficient phosphors. The characteristics of a phosphor are jointly determined by these three components which play different roles and have, therefore, different requirements.

Phosphors can be prepared in different forms according to the experimental needs or practical utility of the various forms such as single crystals [1], thin films [2,3], microcrystalline powder phosphors [4,5] and nano-phosphors [6]. The powder phosphors are the simplest and most commonly used.

2.2 Basic Ingredients

The basic ingredients of activated phosphors are, in general, as follows:

2.2.1 Host material

The pure insulating crystalline material forms the base or host, which primarily functions as a suspension for activator or imperfections and also as an energy transfer medium which surrounds the activator atoms [7]. It promotes luminescence by favourably altering the energy levels under the perturbing influence of the activator so that storage and radiative transitions are possible.

2.2.2 Activator

In general, the role of activator is to create a domain in the host lattice where electron and hole can recombine with the emission of radiation [8]. More specifically, activator may promote luminescence by:

(i) Intensifying the latent emission bands of the host crystal;

(ii) Originating a new line or band emission,

(iii) Sensitizing a luminescence emission attributable to another activator as in the case of Ce and Gd, which individually sensitize Tb and Ce in CaO under X-ray excitation [9]

(iv) Furthermore activator may introduce electron and hole trapping states and may act predominantly as poison: (a) when present in excess; and (b) when incorporated in small proportion in certain phosphors in which it is incompatible.

The site that an activator occupies within the host crystal depends upon the ionic radii of the activator and host crystal cation. Thus, if they are within 15% of each other, the activator atom occupies substitutional sites in place of regular host crystal atoms thereby forming s-centre, otherwise, it occupies interstitial sites between regular host crystal ions leading to an i-centre [10].

2.2.3 Flux

These are salts that readily fuse below the firing temperature. The commonly used fluxes are alkali or alkaline earth halides, borates and sulphates which are water-soluble and have low melting points. The precise function of fluxes is still a matter of conjecture. Prevalent views regarding their role in phosphor synthesis and the mechanism by which they affect luminescence characteristics are:

(i) They act as mineralizer and catalyst which allows lower firing temperature and shorter firing time by promoting low temperature recrystallization so rapidly that large grains with lattice imperfections are formed [10,11].

(ii) They act as an inhibiter of sublimation [10].

(iii) They promote even distribution and incorporation of activator in the host lattice [10,11].

(iv) Flux atoms arrange themselves around activator atoms.

(v) Flux provides charge compensating ions when ionic charge of the activator differs from that of the lattice ion it replaces and facilitates the entry of such activator, probably, because this way of charge compensation is less costly in energy than formation of vacancies and interstitials [12].

(vi) They promote the formation of defects of lattice distortions and thus affect the luminescence efficiency.

In many cases the anions and cations of the flux play an important role in the formation of luminescence centers [12]. The nature and quality of the fluxes have also been found to affect the characteristics of a phosphor.

2.3 Method of Synthesis

2.3.1 General considerations

The luminescent properties of phosphors are known to be affected by a number of preparative parameters, e.g. purity of ingredients [10], particle size of the ingredients, firing time, temperature and atmosphere during firing [13], rate of cooling [10,12], grinding and the grain size of the phosphor [14].

2.3.2 Present method of synthesis

Alkaline earth sulphide phosphors can be synthesized by several methods [15-20]. Theoretically it is possible to start with carbonates, nitrates or sulphates of alkaline earths and reduce them in the form of sulphides. It is also possible to start directly with the sulphides. When the starting materials are carbonates ($CaCO_3$, $SrCO_3$ or $BaCO_3$) or nitrates (e.g. Ca $(NO_3)_2$), they are heated at elevated temperature in the presence of H_2S gas to obtain respective sulphides; and when the starting materials are sulphates, carbon is used as a reducing agent. It is also possible to grow a single crystal of the sulphide or start directly with the poly-crystalline sulphides.

In the present investigation, the starting materials were extra pure grade $CaSO_4$, $SrSO_4$, and $BaSO_4$. They were reduced to respective sulphides by heating with the reducing agent, Carbon, (in the form of activated charcoal) as per the following reactions.

$$CaSO_4 + 2C \xrightarrow{900°C} CaS + 2CO_2 \uparrow$$

$$SrSO_4 + 2C \xrightarrow{900°C} SrS + 2CO_2 \uparrow$$

$$BaSO_4 + 2C \xrightarrow{900°C} BaS + 2CO_2 \uparrow$$

In order to investigate the role of flux, samples with Na_2SO_4 (as flux) were also investigated.

The charge consisting of constituent alkaline earth sulphides, reducing agent, carbon, and desired amount of activator compound/flux was thoroughly grinded and dried in the oven and then kept in fused silica crucibles with lids closed. The charge was then fired in the muffle furnace at 900°C ±10°C for one hour. The fired mass was cooled and crushed to the fine powdered form. Six series of samples have been prepared. The composition of the representative samples is given in the Tables 2.1 to 2.6.

Table 2.1: Composition of CaS:Cu phosphors (without flux)

S.No	Ingredients	Final composition
C1	$CaSO_4$: 10 gm, C: 1.8 gm 0.1 ml of stock solution of $CuSO_4$ (1M)	CaS : Cu (0.001M)
C2	$CaSO_4$: 10 gm, C: 1.8 gm 0.3 ml of stock solution of $CuSO_4$ (1M)	CaS : Cu (0.003M)
C3	$CaSO_4$: 10 gm, C: 1.8 gm 0.5 ml of stock solution of $CuSO_4$ (1M)	CaS : Cu (0.005M)
C4	$CaSO_4$: 10 gm, C: 1.8 gm 0.7 ml of stock solution of $CuSO_4$ (1M)	CaS : Cu (0.007M)
C5	$CaSO_4$: 10 gm, C: 1.8 gm 1.0 ml of stock solution of $CuSO_4$ (1M)	CaS : Cu (0.01M)

Table 2.2: Composition of CaS:Cu phosphors (with flux)

S.No	Ingredients	Final composition
C′1	$CaSO_4$: 10 gm, C: 1.8 gm Soln. - 0.3 ml of stock solution of $CuSO_4$ (1M), Flux - 104.3 mg	CaS : Cu (0.003M) Flux (0.01M)
C′2	$CaSO_4$: 10 gm, C: 1.8 gm 0.3 ml of stock solution of $CuSO_4$ (1M) Flux - 312.9 mg	CaS : Cu (0.003M) Flux (0.03M)
C′3	$CaSO_4$: 10 gm, C: 1.8 gm 0.3 ml of stock solution of $CuSO_4$ (1M) Flux - 521.5 mg	CaS : Cu (0.003M) Flux (0.05M)
C′4	$CaSO_4$: 10gm, C: 1.8 gm 0.3 ml of stock solution of $CuSO_4$ (1M) Flux - 1.043 gm	CaS : Cu (0.003M) Flux (0.1M)

C′5	$CaSO_4$: 10 gm, C: 1.8 gm 0.3 ml of stock solution of $CuSO_4$ (1M) Flux - 3.129 gm	CaS : Cu (0.003M) Flux (0.3M)

Table 2.3: Composition of BaS:Cu phosphors (without flux)

S.No	Ingredients	Final composition
B1	$BaSO_4$ -10 gm,C-1.0283 gm 0.1 ml of stock solution of $CuSO_4$ (1M)	BaS : Cu (0.001M)
B2	$BaSO_4$ –10 gm,C-1.0283 gm 0.3 ml of stock solution of $CuSO_4$ (1M)	BaS : Cu (0.003M)
B3	$BaSO_4$-10 gm, C-1.0283 gm 0.5 ml of stock solution of $CuSO_4$ (1M)	BaS : Cu (0.005M)
B4	$BaSO_4$ –10 gm, C-1.0283 gm 0.7 ml of stock solution of $CuSO_4$ (1M)	BaS : Cu (0.007M)
B5	$BaSO_4$ –10 gm, C-1.0283 gm 1.0 ml of stock solution of $CuSO_4$ (1M)	BaS : Cu (0.01M)

Table 2.4: Composition of BaS:Cu phosphors (with flux)

S.No	Composition mixture	Final composition
B′1	$BaSO_4$ -10gm, C-1.0283 gm 0.3 ml of stock solution of $CuSO_4$ (1M) Flux-60.86 mg	BaS : Cu (0.003M) Flux (0.01M)
B′2	$BaSO_4$ –10 gm, C-1.0283 gm 0.3 ml of stock solution of $CuSO_4$ (1M) Flux-182.57 mg	BaS : Cu (0.003M) Flux (0.03M)
B′3	$BaSO_4$ –10 gm, C-1.0283 gm 0.3 ml of stock solution of $CuSO_4$ (1M) Flux-304.3 mg	BaS : Cu (0.003M) Flux (0.05M)
B′4	$BaSO_4$-10 gm, C-1.0283 gm 0.3 ml of stock solution of $CuSO_4$ (1M) Flux - 608.6 mg	BaS:Cu (0.003M) Flux (0.1M)
B′5	$BaSO_4$-10 gm, C-1.0283 gm 0.3 ml of stock solution of $CuSO_4$ (1M) Flux-1.8258 gm	BaS : Cu (0.003M) Flux (0.3M)

Table 2.5: Composition of SrS:Cu phosphors (without flux)

Sl. no	Composition Mixture	Final Composition
S1	$SrSO_4$: 10 gm, C : 1.4 gm 0.1 ml of stock solution of $CuSO_4$ (1M)	SrS : Cu (0.001M)
S2	$SrSO_4$: 10 gm, C : 1.4 gm 0.3 ml of stock solution of $CuSO_4$ (1M)	SrS : Cu (0.003M)
S3	$SrSO_4$: 10 gm, C : 1.4 gm 0.5 ml of stock solution of $CuSO_4$ (1M)	SrS : Cu (0.005M)
S4	$SrSO_4$: 10 gm, C : 1.4 gm 0.7 ml of stock solution of $CuSO_4$ (1M)	SrS : Cu (0.007M)
S5	$SrSO_4$: 10 gm, C : 1.4 gm 1.0 ml of stock solution of $CuSO_4$ (1M)	SrS : Cu (0.01M)

Table 2.6: Composition of SrS:Cu phosphors (with flux)

S′1	$SrSO_4$: 10 gm, C:1.4 gm, 0.3 ml of stock solution of $CuSO_4$ (1M) Flux : 77.3 mg	SrS : Cu (0.003M) Flux (0.01M)
S′2	$SrSO_4$: 10 gm, C : 1.4 gm 0.3 ml of stock solution of $CuSO_4$ (1M) Flux : 231.99 mg	SrS : Cu (0.003M) Flux (0.03M)
S′3	$SrSO_4$: 10 gm, C : 1.4 gm 0.3 ml of stock solution of $CuSO_4$ (1M) Flux : 386.65 mg	SrS : Cu (0.003M) Flux (0.05M)
S′4	$SrSO_4$: 10 gm, C : 1.4 gm 0.3 ml of stock solution of $CuSO_4$ (1M) Flux : 773.3 mg	SrS : Cu (0.003M) Flux (0.1M)
S′5	$SrSO_4$: 10 gm, C : 1.4 gm 0.3 ml of stock solution of $CuSO_4$ (1M) Flux : 2319.9 mg	SrS : Cu (0.003M) Flux (0.3M)

2.4 Structure of synthesized materials:

In order to determine the structure of the synthesized materials, X-ray diffraction spectra of representative samples (powders) were recorded by Debye Scherrer Method. The results of these investigations are given as follows:

The X-ray diffraction (XRD) spectra of the three alkaline earth sulphides, namely, CaS, BaS, SrS and are shown in Fig 2.1, 2.2 and 2.3 respectively.

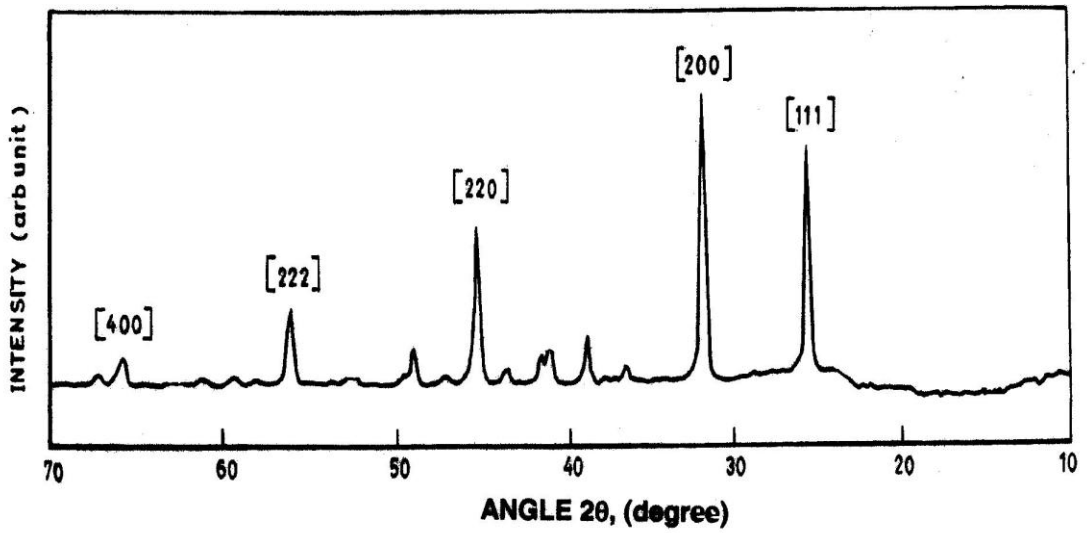

***Fig.2.1**: XRD of CaS:Cu (0.003 M)*

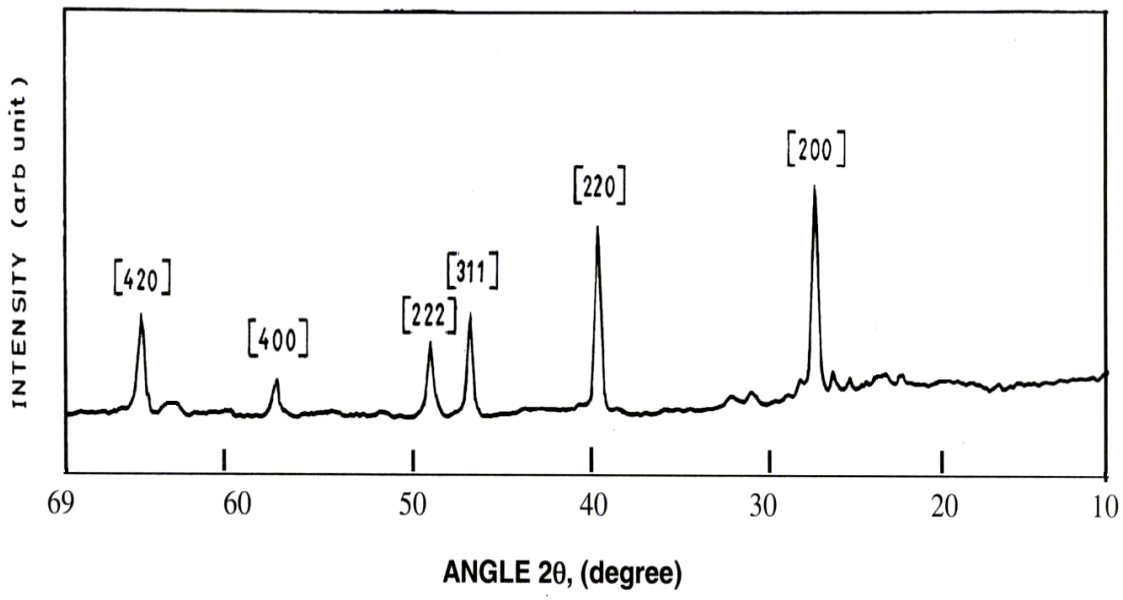

***Fig.2.2**: XRD of BaS:Cu (0.003 M)*

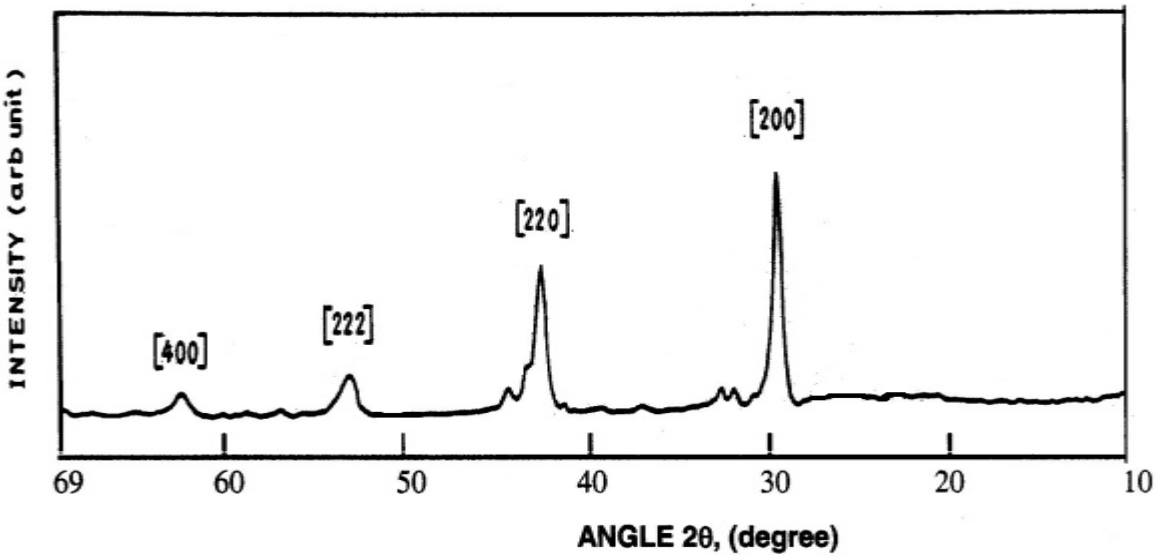

***Fig.2.3**: XRD of SrS:Cu (0.003 M)*

Sharp lines of XRD demonstrate that the sulphates which are used as starting materials have been converted into respective sulphides. The diffraction lines and the related d_{hkl} values match very well with the standard values reported by National Bureau of Standards [21] and approved by Joint Committee for Powder Diffraction Standards (JCPDS) [22]. Following the procedure given below we have obtained the data from XRD of the three sulphides.

1. The value of the diffraction angle θ obtained from the recorded curves were compared with JCPDS values [22] and tentative values of (hkl) were assigned.
2. The interplanar spacing d_{hkl} corresponding to each θ was calculated using the following relation:

$$\theta = \mathrm{Sin}^{-1}\left(\frac{\lambda n}{2d_{hkl}}\right) \qquad (2.1)$$

where λ is the wavelength of reflected X-ray, n is the order of diffraction, d_{hkl} is the interspacing between reflecting planes, hkl are the Miller indices for that plane.

3. Using the tentative values of (hkl) and the actual values of d_{hkl}, the value of 'a' was calculated using equation A 2.1 (in the Appendix 2.1).
4. Average value of the lattice constant 'a' was found from all the experimental values. That average was taken to be equal to d_{100}.

5. From this value of d_{100} , θ was calculated using equation

   $2d \sin\theta = n\lambda$, where n = 1 and λ = 1.544 Å

6. From this value of θ_{100} (= θ_1) we found the ratio of $\sin^2\theta / \sin^2\theta_1$ and then following the procedure described in brief [23] in Appendix 2.1, we confirmed the values of (hkl) corresponding to all values of θ. The same are tabulated in Tables 2.7 to 2.9.

Table 2.7: d_{hkl} and 'a' values for CaS: Cu

Measured value of angle of diffraction (θ)	JCPDS Values of (θ)	Sin θ	Sin ^{2}θ	$\frac{Sin^2\theta}{Sin^2\theta_1}$	(hkl)	d_{hkl} (Å)	Lattice constant (a in Å)
7.76*	-	0.135	0.018	≈ 1	100	5.7120	5.7120 □
13.40	13.58	0.223	0.049	≈ 3	111	3.3312	5.7698
15.64	15.70	0.269	0.072	≈ 4	200	2.8544	5.6791
22.54	22.49	0.380	0.146	≈ 8	220	2.0079	5.6791
26.30	26.65	0.443	0.196	≈ 11	311	1.7378	5.760
27.94	27.94	0.468	0.219	≈12	222	1.6428	5.6910
32.74	32.75	0.540	0.290	≈16	400	1.4233	5.6935

□ Standard value of 'a' = 5.6948Å, Standard deviation σ = 0.0415

Table 2.8: d_{hkl} and 'a' values for BaS: Cu

Measured value of angle of diffraction (θ)	JCPDS Value of (θ)	Sin θ	Sin ^{2}θ	$\frac{Sin^2\theta}{Sin^2\theta_1}$	(hkl)	d_{hkl} (Å)	Lattice constant (a in Å)
6.89§	-	0.120	0.014	≈ 1	100	6.367	6.367 □
12.06	12.05	0.208	0.043	≈ 3	111	3.6853	6.383
13.96	13.95	0.241	0.058	≈ 4	200	3.1917	6.383
19.96	19.94	0.341	0.116	≈ 8	220	2.2556	6.379

* extrapolated value of diffraction angle
§ extrapolated value of diffraction angle

23.56	23.57	0.399	0.159	≈ 11	311	1.9264	6.389
24.71	24.70	0.418	0.174	≈ 12	222	1.8419	6.380
29.20	28.83	0.487	0.238	≈ 16	400	1.578	6.312
32.0	31.71	0.529	0.280	≈19	331	1.453	6.333
32.66	32.62	0.5396	0.291	≈20	420	1.4268	6.381

□ Standard value of 'a' = 6.386Å, Standard deviation σ = 0.0285

Table 2.9*: d_{hkl} and 'a' values for SrS: Cu*

Measured value of angle of diffraction (θ)	JCPDS Value of (θ)	Sin θ	$Sin^2\theta$	$\frac{Sin^2\theta}{Sin^2\theta_1}$	(hkl)	d_{hkl} (Å)	Lattice constant (a in Å)
7.38 ♣	-	0.128	0.016	≈ 1	100	5.987	5.987 □
12.8	12.79	0.221	0.048	≈ 3	111	3.475	6.018
14.9	14.84	0.257	0.066	≈ 4	200	2.994	5.988
21.5	21.21	0.366	0.134	≈ 8	220	2.100	5.939
26.5	26.31	0.446	0.199	≈ 12	222	1.725	5.975
31.3	30.79	0.516	0.266	≈16	400	1.504	6.016

□ Standard value of 'a' = 6.020Å, Standard deviation σ = 0.0325

From the above tables, it is clear that the diffraction data of the synthesized alkaline earth sulphides match very well with the standard JCPDS data. This establishes that the starting host materials CaSO4, BaSO4 and SrSO4 have been fully converted into CaS, BaS and SrS respectively. The values of Miller indices (hkl) found from the indexing method clearly reveal that the converted sulphides crystallize in the cubic lattice form.

♣ extrapolated value of diffraction angle

References

[1] G.F. Alfrey, M.A.S. Sweet, *Proc. Int. Conf. Lumin*, **1**, 1022, (1966).

[2] D. Poelman, R.L. Van Melrhaeghe, B.A. Vermeersch and F Cardon, *J. Phys. D: Appl. Phys.*, **30**, 465, (1997).

[3] Y.S. Kim, S.J. Yun, *J. Phys: Condens. Matter*, **16**, 569 (2004).

[4] N. Yamashita, *Japn. J. Appl. Phys.*, **30**, 3335 (1991).

[5] J.Wu, D. Newman and I. V.F. Viney, *J. Phys. D : Appl. Phys.*, **35**, 968, (2002).

[6] E.I. Anila, Arun Arvind and M.K. Jayraj, *J. of Nanotech.*,**19**, 145604, (2008).

[7] G. Blasse; B.C. Grabmaier, *Luminescent Materials*; Springer: Berlin, Germany, (1994).

[8] W. M. Yen, M. J. Weber, *Inorganic Phosphors: Compositions, Preparation and Optical Properties*; CRC Press: Boca Raton, FL, USA, (2004).

[9] R.P. Khare and J.D. Ranade, *J. Material Sciences*, U.K., **15**, 1868, (1980).

[10] H.W. Leverenz, "*An introduction to luminescence of solids*", John Wiley & Sons (1950).

[11] R. Pandey, S. Sivaraman, *J. Phys. Chem. Solids*, **52**, 211(1991).

[12] F. A. Kroger, *Some aspects of the luminescence of solids*, Elsevier, Amsterdam, (1948).

[13] F. A. Kroger, *Brit. J. Appl. Phys. suppl.* 4-**5**, 58 (1955).

[14] G. F. J. Garlick, "*Preparation and characteristics of solid luminescent materials*", Wiley (1948).

[15] K.N. Kim, J.M. Kim, K.J. Choi, J.K. Park, C.H. Kim, *J. Am. Ceram. Soc.*, **89**, 3413, (2006).

[16] Y.S. Hu, W.D. Zhuang, H.Q. Ye, S.S. Zhang, Y. Fang, X.W. Huang, *J. Lumines.* **111**, 139, (2005).

[17] B.Q. Sun, G.S. Yi, D.P. Chen, Zhou and Y.X. Cheng, *J. Mater. Chem.*, **12**, 1194, (2002).

[18] C.R. Wang, K.B. Tang; Q. Yang, Y.T. Qian, *J. Electrochem. Soc.*, **150**, G163-G166, (2003).

[19] C.R. Wang, K.B. Tang, Yang, C.H. An, B. Hai, G.Z. Shen, Y. T. Qian, *Chem. Phys. Lett.*, **351**, 385-390 (2002).

[20] P.F. Smet and D. Poelman, *J. Phys. D-Appl. Phys.*, **42**, 095306 (2009).

[21] National Bureau of Standards (USA), Circ 539, **7**, **8** & **52** (1957).

[22] JCPDS- International centre for Diffraction Data (1999)

[23] R. P. Khare, "*Analysis Instrumentation: An Introduction*, (CBS, New Delhi), P. 135 (1993).

APPENDIX 2.1

Indexing of cubic Crystal [23]

For cubic crystals, the interplanar spacing, d_{hkl}, is related to the Miller indices (h, k, l) by the following relation:

$$d_{hkl} = \left\{ \frac{1}{\sqrt{(h^2 + k^2 + l^2)}} \right\} a \qquad \text{(A 2.1)}$$

where a is the edge of the cubic lattice (or the unit cell parameter).

Now, consider some families of planes (h, k, l) and note the corresponding values of $h^2 + k^2 + l^2$ (as given in Table A 2.1 below). A close examination of this table reveals that the number 7 is missing. Whatever be the values of h, k, l, the sum of their squares will never be equal to 7. This is known as a forbidden number. Next two such numbers are 15 and 23.

Table A 2.1: Planes (h, k, l) and corresponding values of $h^2 + k^2 + l^2$

Plane represented by (hkl)	$h^2 + k^2 + l^2$
100	1
110	2
111	3
200	4
210	5
211	6
220	8
221	9
300	9
310	10
etc	etc

Another point of interest is that the sum of the squares of the indices 221 and 300 both equal 9. This simply means that the reflections from these planes overlap.

Now combining the expression for d_{hkl} for cubic crystals with the Bragg's equation

$n\lambda = 2d_{hkl} \sin\theta_{hkl}$

and putting n=1, we get

$$\mathrm{Sin}^2\theta_{hkl} = \frac{\lambda^2}{4a^2}(h^2 + k^2 + l^2) \qquad \text{(A 2.2)}$$

For a particular powder pattern, λ and 'a' are constant and hence $\mathrm{Sin}^2\theta_{hkl}$ is proportional to $(h^2 + k^2 + l^2)$. Thus, the above relationship may be used to recognize the powder pattern of the cubic lattice.

The procedure is as follows. Measure the position of the diffraction lines on the chart. Calculate the values of θ and write them in the increasing order and then calculate $\mathrm{Sin}^2\theta$ values. Divide $\mathrm{Sin}^2\theta$ values by $\mathrm{Sin}^2\theta_1$. If these ratios are approximately 1, 2, 3, 4, 5, 6, 8, etc; then the diffraction pattern is that of a cubic crystal. Once the sequence of numbers is established, the Miller indices (hkl) can be assigned. This is called indexing of cubic crystals.

Chapter 3

Excitation and Emission Spectra at Room Temperature

3.1 Introduction

Luminescence is a general term applied to emission of light but is different from incandescence. This is a phenomenon that involves the absorption of energy by matter and its re-emission as visible or near-visible radiation. It has been sub-classified into fluorescence and phosphorescence on the basis of the mechanism by which the atom or molecule undergoes the reverse transition from the excited state to the ground state. Garlick [1] defines fluorescence as the luminescence emitted during excitation while phosphorescence as that emitted after the cessation of excitation. On the basis of physical processes, Pringsheim [2] defines fluorescence as the emission that takes place by one or more spontaneous transitions and phosphorescence as that which occurs with the intervention of a metastable state followed by return to the excited state due to addition of energy.

One often sees terms in literature, such as, photoluminescence, radioluminescence, electroluminescence, cathodoluminescence etc; the classification being based on the type of exciting source employed. Excellent reviews on the subject may be found in the works of Curie [3], Butler [4], Ropp [5], Grattan and Zhang [6] and Shionoya and Yen [7].

3.2 Theory of excitation and emission processes

Several models have been proposed to explain the phenomenon of luminescence. An energy band model based on the "collective electron theory" of Bloch [8] has been used by most researchers [9-20]. According to this theory, qualitatively, when atoms are arranged in an orderly way and in close proximity with each other to form a crystal, the energy states for the electrons in the atoms are distributed by mutual interaction. As a result, the discrete electronic states are broadened into bands of allowed energy separated by bands of forbidden energy. Thus, instead of the discrete energy states there are discrete energy bands for the electrons inside the crystal. The uppermost completely filled band is called the valence band and the next higher allowed band is called the conduction band. The energy levels in an allowed band are so closely spaced that effectively they form a continuum.

The incorporation of an activator atom in a crystalline solid will, in general, give rise to localized energy levels in the normally forbidden energy gap, which produces emission centers for luminescence. L represents the ground state of the centre above the filled band called valence band (VB) and L′ is its excited state. Other impurities, lattice perturbation due to activator or defects and the presence of vacant lattice sites produce unoccupied levels (T) at various depths in the forbidden gap below the conduction band (CB), in which excited electrons can be trapped. These levels are known as electron traps.

Absorption and emission processes in phosphors may be explained on the basis of this model. The excitation of luminescence by photon absorption in the matrix lattice or luminescence centre involves raising of an electron from valence band or from the ground state of the luminescence centre to the conduction band or from a filled activator ground level to some higher activator level. These transitions are shown in Fig. (3.1) by A, B and D respectively. The absorption of energy may also result in transition E of the electron from the filled band directly into trapping states, the positive hole left behind migrating to the luminescence centers and emptying them. The luminescence emission occurs when an excited electron returns to an empty ground state of the luminescence centre.

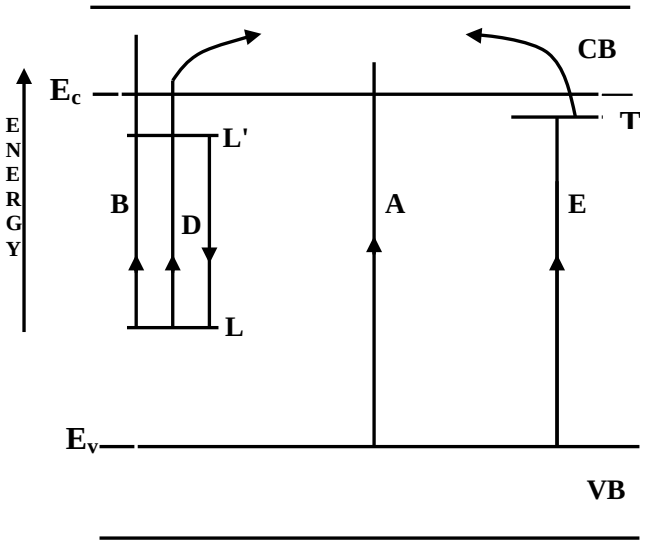

Fig. 3.1*: Energy band model [E_c and E_v are the energies corresponding to the bottom of the conduction band (CB) and top of the valence band (VB)]*

Electrons in the conduction band can return to luminescence centre or may be captured by the traps (T) and phosphorescence is then determined by their activation (thermal, optical or electrical) from traps and subsequent return to the empty luminescence centre.

3.3 Processes in Crystalline Phosphors

The luminescence process involves three stages viz.,

(a) absorption and excitation

(b) transfer and storage of energy and

(c) conversion of stored energy as light i.e. emission.

(a) Absorption and Excitation:

The absorption and excitation characteristics of phosphors are primarily functions of the nature of the host lattice and the activator [3]. Some of the possible modes of excitation [21, 22] are shown in Fig. (3.2) and may be described as follows:

(i) Excitation by fundamental lattice absorption produces a free electron in the conduction band (CB) and a free hole in the valence band (VB) on absorption of each photon.

(ii) Excitation of the normal valence electrons produces a bound electron-hole pair called exciton. In this case, no free electrons or holes are produced and energy transferred by the diffusion of the exciton as one unit.

(iii) Excitation of the luminescence centre produces a free electron in the conduction band and a free hole in the neighborhood of the centre.

(iv) Excitation of valence electrons raises an electron to an unoccupied centre and a free hole in the valence band.

(v) Excitation of the valence electron creates a mobile hole in the valence band and the electron is trapped at 'T'.

(vi) Excitation within a luminescence centre raises an electron to the excited state of the centre. In this case, no free electrons or holes are produced and the luminescence is highly localized, determined only by the centre configuration.

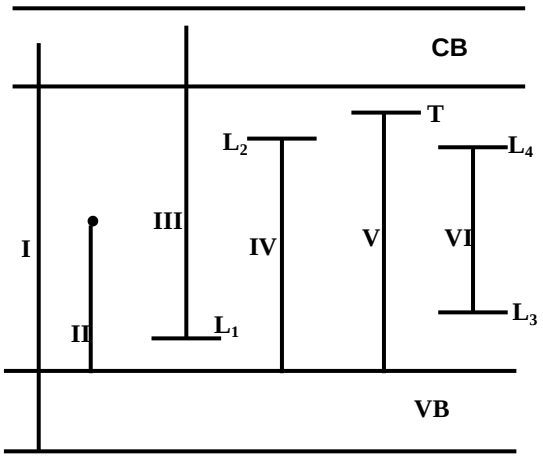

***Fig. 3.2**: Modes of excitation and physical picture of absorption processes (Schematic)*

(*L_1 – Occupied state of luminescence centre, L_2 - Unoccupied state of luminescence centre, L_3 - Ground state of luminescence centre , L_4 – Excited state of luminescence centre, T - Trapping state*)

Corresponding to these transitions the absorption characteristics may be described as follows:

(i) Any radiation of energy greater than the separation between conduction band and valence band raises electrons from the valence band to the conduction band and the absorption due to this is known as a fundamental absorption band. The wavelength corresponding to minimum energy required for the above transition is known as the fundamental absorption edge. For light of energy greater than minimum required, the absorption is continuous and fairly constant up to a certain minimum energy (transition I in Fig. 3.2).

(ii) In the processes of excitation (marked II in Fig. 3.2) where the energy is lower than the band gap energy, the absorption by the lattice creates excitons, which are thermally dissociated at room temperature. These electron-hole pairs move in each other's field in the crystal with no net charge. The absorption is manifested by a series of narrow absorption lines on the low energy side of the absorption edge.

(iii) Other absorption bands at longer wavelength than the absorption edge will be present corresponding to the electronic transitions III, IV and V (in Fig. 3.2)

which are dependent on the matrix and activator or both [5]. These transitions give some structure in the tail of the absorption spectrum lying outside the absorption edge.

(iv) Corresponding to the electronic transition VI (in Fig. 3.2) the absorption band occurs at still longer wavelength and is due to the electronic transition confined to the luminescent centre or impurity centers.

(v) The trapped electrons may be raised by optical stimulation into the conduction band, giving rise to a further set of absorption bands in the long wavelength region. These have been observed in materials in the powder form.

In addition, electron in excited phosphors may be raised into emptied centers, thus giving long wavelength absorption band similar to trapped electrons. Defects and impurities present also give new absorption bands usually on the long wavelength side of the characteristic absorption [23].

In general, the absorption spectrum of a crystalline phosphor may be divided into a short wavelength absorption region associated with the matrix crystal lattice, culminating in the fundamental absorption edge and a longer wavelength region associated with the activators and other impurities.

(b) Transfer and Storage of Energy:

When a luminescence centre absorbs energy, it becomes ionized. This energy is not immediately converted into phonons or photons and may be stored in localized metastable states, first proposed by Jablonski [24] and later adopted by Johnson [25] to explain long decay phosphorescence. As shown in Fig. (3.3) absorption of exciting radiation by a luminescence centre raises an electron into the excited state (F). It may then directly return to the ground state (G) with the emission of fluorescence or it may fall into the metastable state (M) lying just below (F). The transition (M$\leftrightarrow$G) is usually forbidden. The electron in the metastable state requires some activation energy to return to the ground state via (F). The energy is supplied by thermal activation. The resulting delayed emission is phosphorescence.

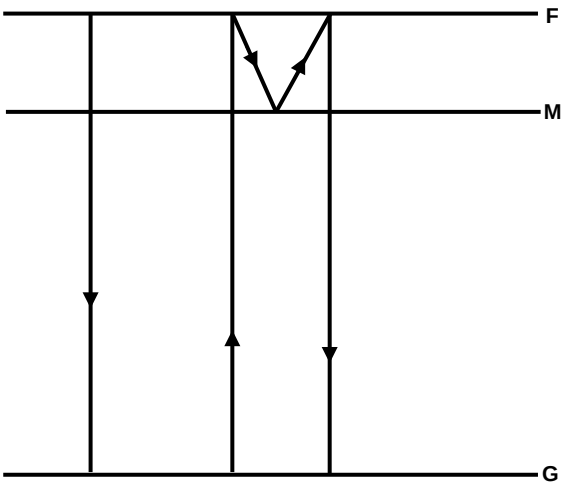

Fig 3.3: Jablonski Model

(c) Emission

Luminescence emission takes place when an excited electron in the conduction band or in the excited state of a centre, returns to the ground state of the luminescence centre. The probability of direct transition from the conduction band to the valence band is low and generally not observable. The temporary storage of energy, by trapping of excited quasi or free electrons, positive holes or excitons in metastable state makes the luminescence emission complicated. The excited electrons may fall into these levels releasing energy as lattice vibrations or phonons. The nature of trapping centers is a major factor in determining the nature of phosphorescence [26].

The ‘anti-stokes’ luminescence, the emission of shorter wavelength than the exciting one, has been observed in some phosphors [27, 28]. This has been explained on the basis of a two-stage excitation process. The first infrared photon ionizes the impurity level into the conduction band and a second one raises a valence electron into the empty level, thus creating an electron-hole pair followed by luminescence emission of shorter wavelength.

3.4 Experimental setup

The experimental setup (schematic) for studying the excitation and emission spectra of synthesized materials is shown in Fig. (3.4). The instrument used is SHIMADZU spectrofluorophotomenter RF-5301PC.

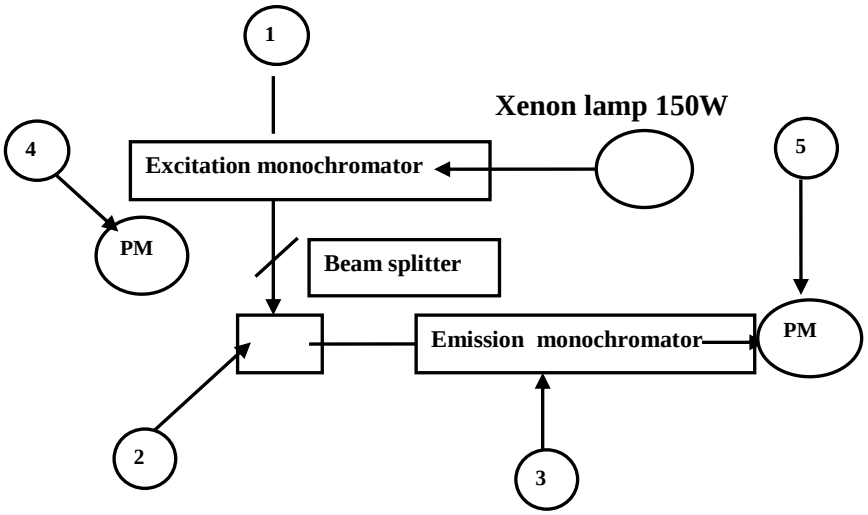

***Fig 3.4**: Block diagram of spectrofluorophotometer*

The excitation monochromator (1) isolates a particular wavelength form the light from the Xenon lamp to obtain excitation light. Since brighter excitation light will contribute to higher sensitivity of the spectrofluorophotometer, the excitation monochromator incorporates a diffraction grating with a larger aperture to collect the largest possible amount of light. The sample holder (2) holds a sample coated on glass substrate. The emission monochromator (3) selectively receives fluorescence emitted from the sample and its photomultiplier tube, PM, (5) measures the intensity of the fluorescence. This monochromator has a diffraction grating whose size is the same as that of the excitation monochromator to collect the greatest possible amount of light. The photomultiplier tube, PM, (4) is for monitoring. Generally, the Xenon lamps used on spectrofluorophotometer are characterized by very high emission intensity and an uninterrupted radiation spectrum. However, their tendency to unstable light emission will result in greater-signal noise if no countermeasure is incorporated. In addition, the non-uniformity in the radiation spectrum of the Xenon lamp and in the spectral sensitivity characteristics of the photomultiplier tube (these criteria are generally called instrument functions) causes distortion in the spectrum. To overcome these factors, the photomultiplier tube (4) monitors a portion of excitation light and feeds the resultant signal back to the photomultiplier tube (5) for fluorescence scanning. (This scheme is called the light-source compensation system).

The optical system of the RF-5301PC instrument is illustrated in Fig. (3.5). A 150 W Xenon lamp (1) serves as the light source. The uniquely designed lamp housing contains generated ozone in it and decomposes the ozone by means of the heat

produced by the lamp. The bright spot on the Xenon lamp is magnified and converged by the ellipsoidal mirror (2) and then further converged on the inlet slit of the slit assembly (excitation side) (3) by the concave mirror (4). A portion of the light isolated by the concave grating (5) passes through the outlet slit, travels through the condenser lens (11) and illuminates the sample. (The concave grating in both the monochromators in a highly efficient ion-blazed holographic grating, a product of Shimadzu's unique optics technology.) To achieve light-source compensation, a portion of the excitation light is reflected by the beam splitter quartz plate (6) and directed to the Teflon reflector plate-1 (7) The diffusely reflected light from the reflector plate-1 (7) then passes through the aperture for light quantity balancing (21) and illuminates the Teflon reflector plate-2 (8). Reflected by the reflector plate-2 (8), the diffuse light is attenuated to a specific ratio by the optical attenuator (9) and then reaches the photomultiplier for monitoring (10).

The fluorescence occurring on the sample surface is directed through the lens (13) to the emission monochromator that comprises the slit assembly (14) and the concave grating (15). Then, the isolated light is introduced through the concave mirror (16) into the photomultiplier for photometry (17) and the resultant electrical signal is fed to the preamplifier.

The optical system of this instrument is primarily designed for studying the liquid samples. In order to study our samples we made a paint of the powdered phosphor with the help of a non-luminescent adhesive and painted on the glass substrates and dried. The painted slide was kept at an angle of 37° with respect to the excitation beam in the sample holder.

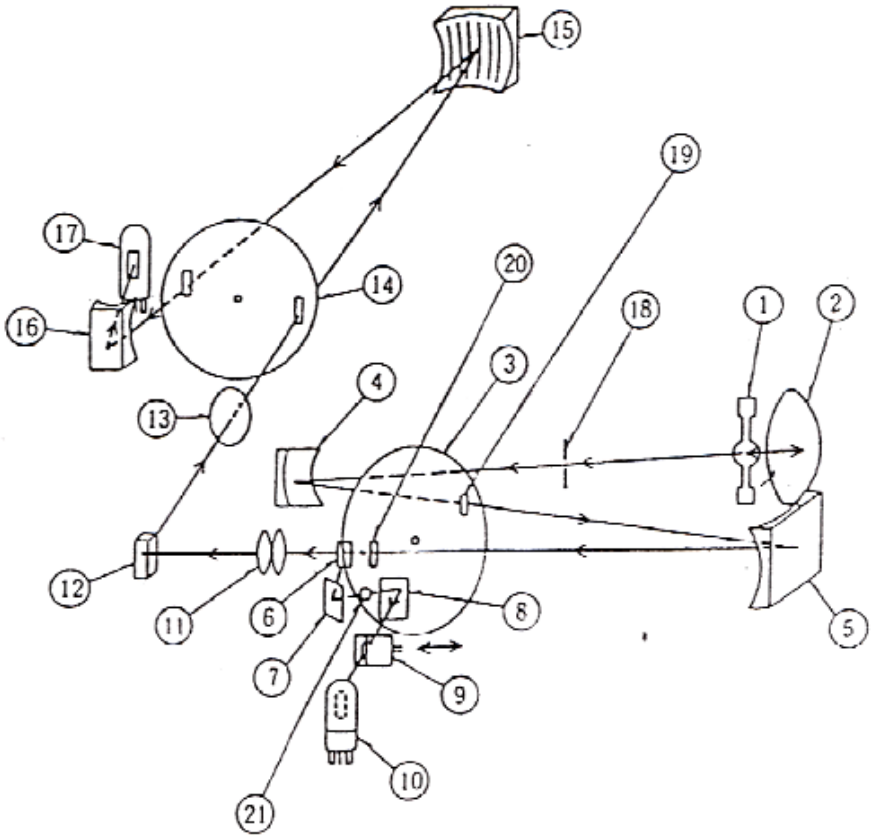

***Fig 3.5**: The optical system of the RF-5301PC instrument*

1. Xenon lamp, 150 W
2. Ellipsoidal mirror, SiO_2 –coated
3. Slit Assy., excitation side
4. Concave mirror
5. Concave grating (for excitation)
6. Beam splitter quartz plate
7. Teflon reflector plate 1
8. Teflon reflector plate 2
9. Optical attenuator
10. Photomultiplier for monitoring, R212-14
11. Condenser lens (dual-lens)
12. Sample Holder
13. Condenser lens
14. Slit Assy., emission side
15. Concave grating (for emission)
16. Concave mirror
17. Photomultiplier for photometry, R3788-02
18. Focal point
19. Inlet slit
20. Outlet slit
21. Aperture for light quantity

3.5 Results: CaS:Cu - The record of excitation and emission spectra of CaS:Cu (without flux) phosphors is shown in Figs 3.6 and 3.7 respectively. In nearly all the samples the excitation peak is observed around 310 nm and the emission peak is observed around 480 nm.

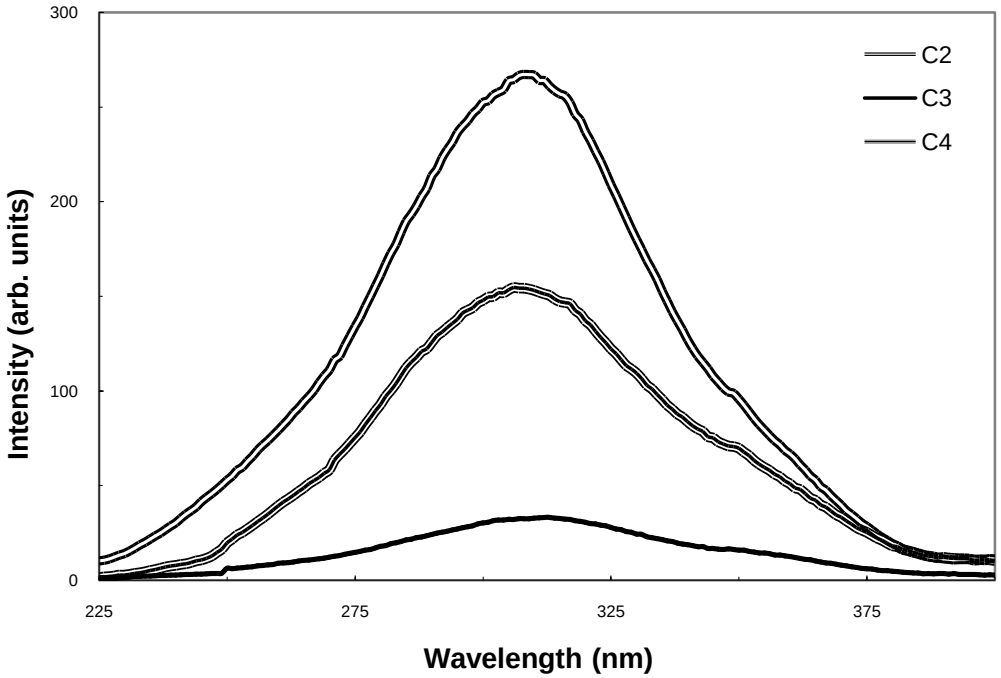

Fig 3.6*: Excitation spectra of representative CaS:Cu(without flux) phosphors*

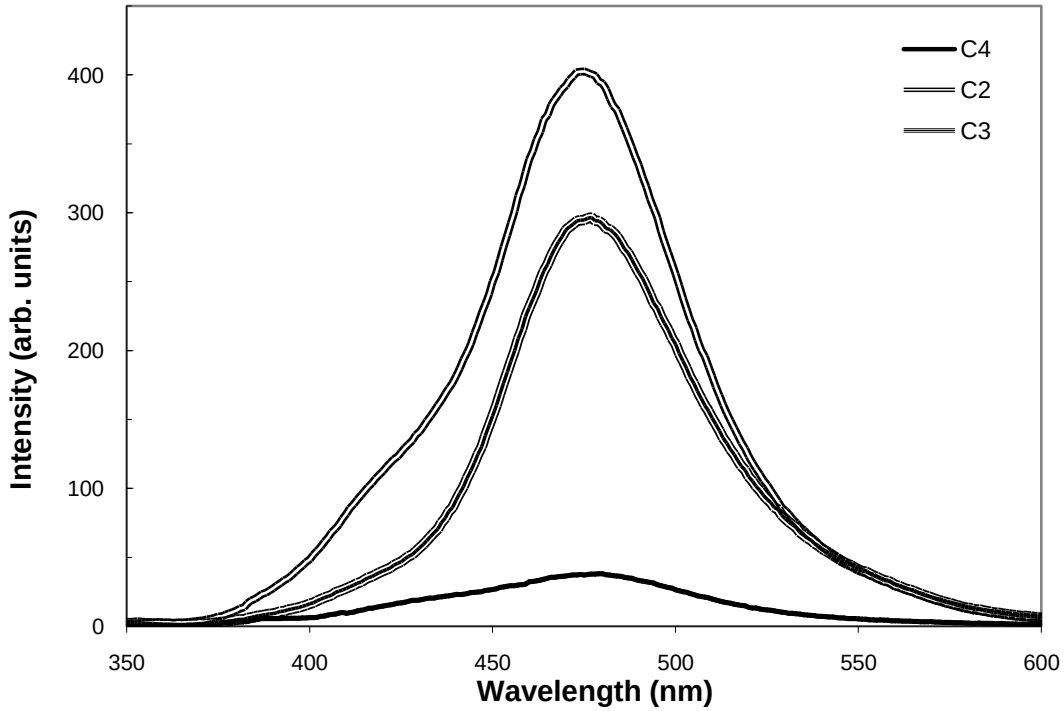

Fig 3.7: *Emission spectra of representative CaS:Cu(without flux) phosphors*

Addition of flux gives rise to two excitation peaks, one at 310 nm (as in the previous case) and second, at 345 nm. But the emission peak remains at 480 nm. However, the brightness of these phosphors increases almost three – fold as can be seen from Figs. 3.8 and 3.9.

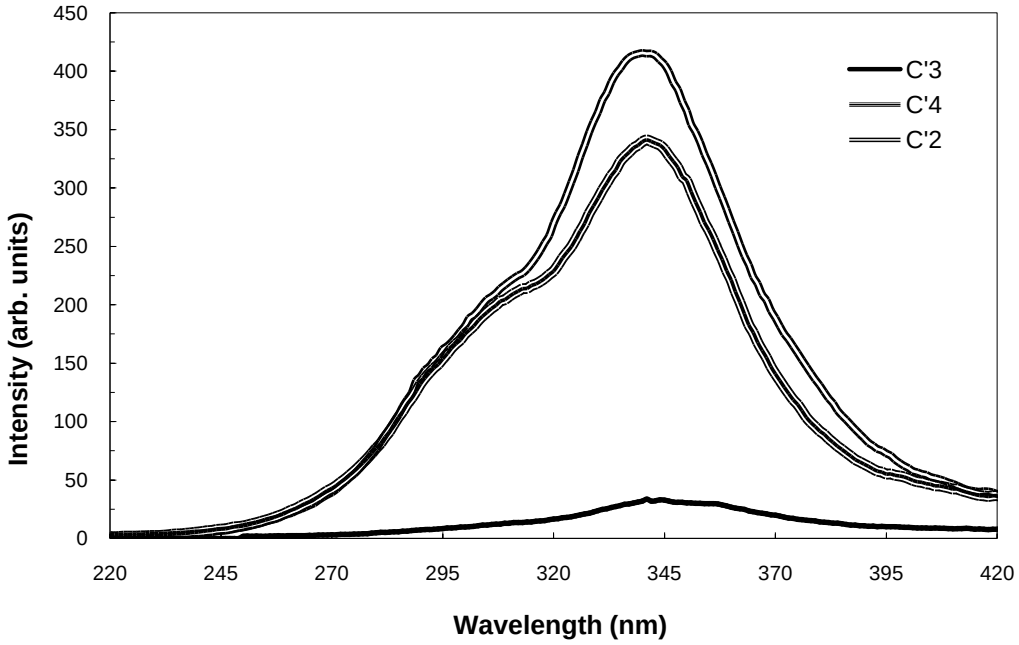

***Fig 3.8**: Excitation spectra of representative CaS:Cu(with flux) phosphors*

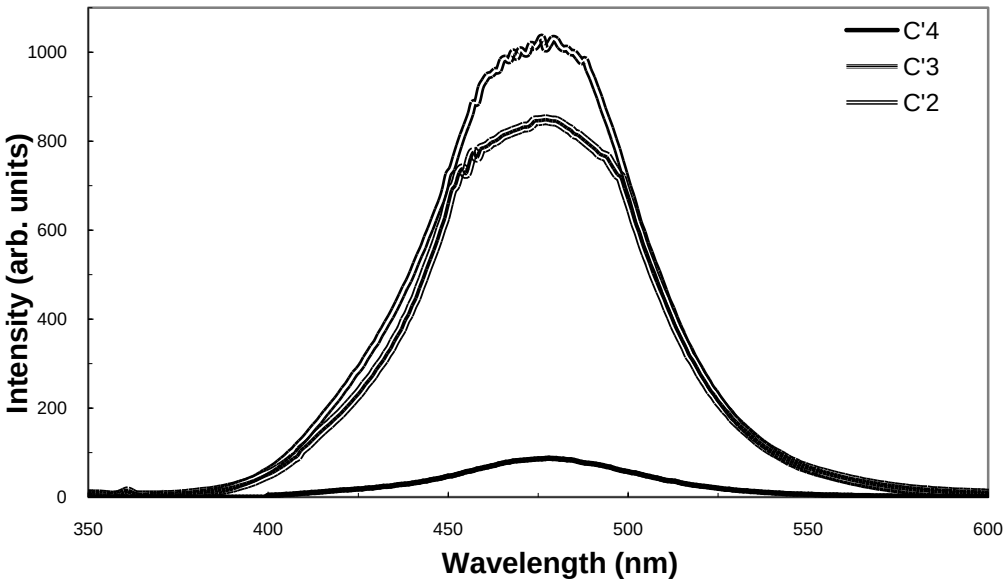

***Fig 3.9**: Emission spectra of representative CaS:Cu(with flux) phosphors*

BaS:Cu- In the case of copper doped Barium Sulphide phosphors two peaks are observed in the excitation spectra in all the samples as shown in Fig. 3.10. Although, the excitation peaks slightly vary with concentration of copper but, in general, the

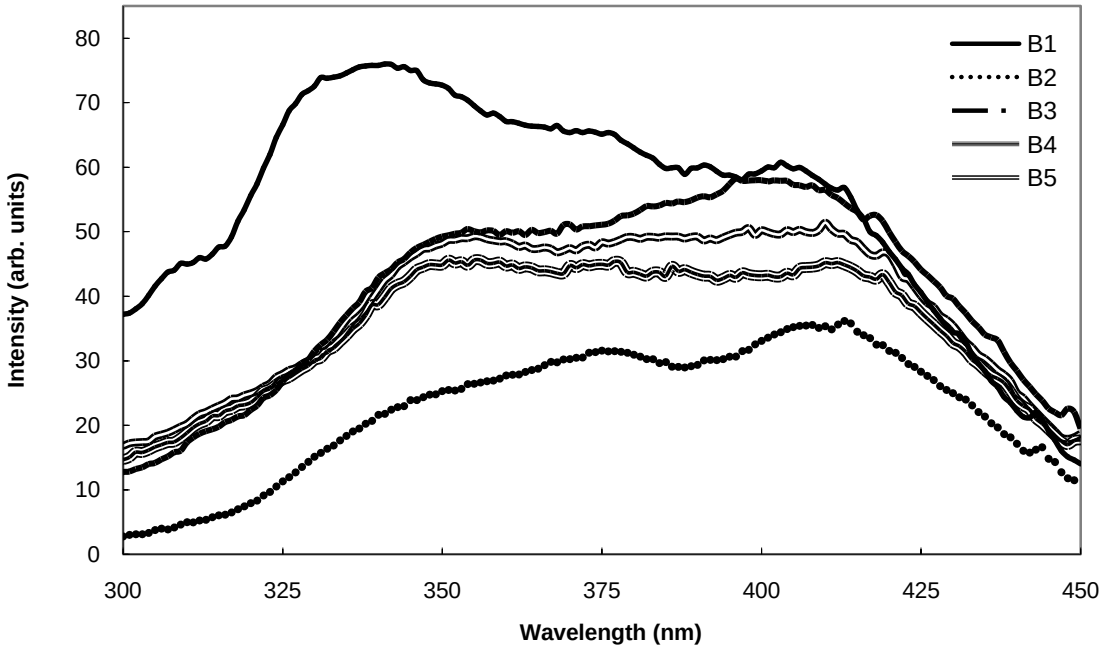

***Fig 3.10**: Excitation spectra of representative BaS:Cu(without flux) phosphors*

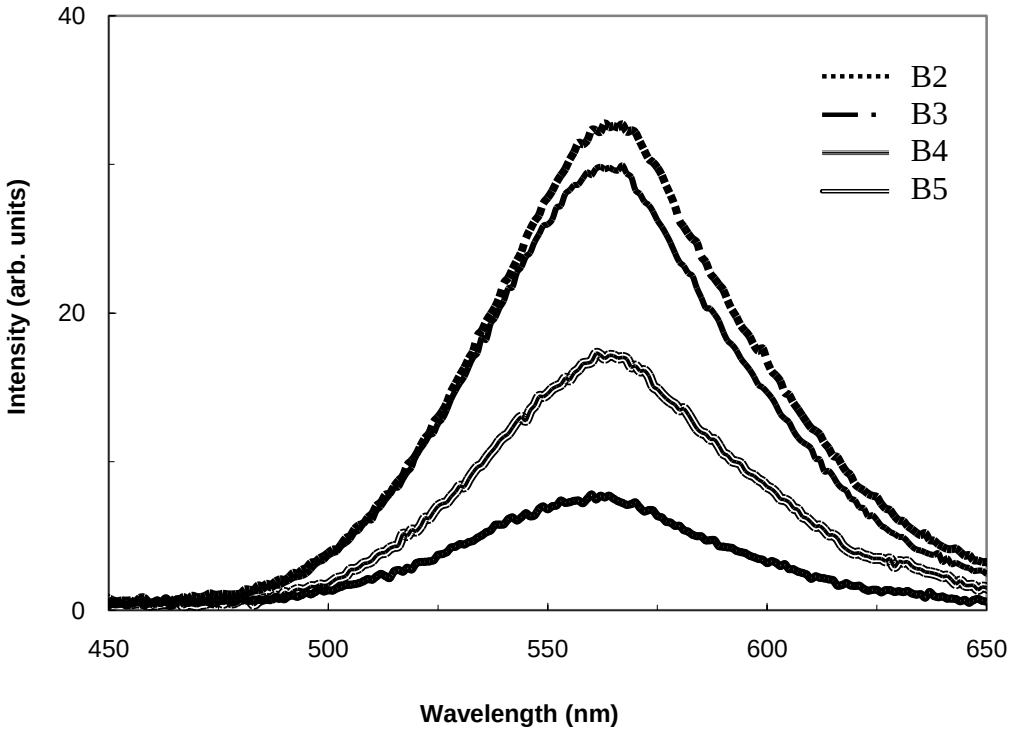

***Fig 3.11**: Emission spectra of representative BaS:Cu(without flux) phosphors*

The addition of flux in these phosphors neither changes excitation peaks (340 nm and 410 nm) nor emission peak (560 nm). However, the emission intensity increases two –fold as is evident by comparing Figs. 3.11 and 3.13.

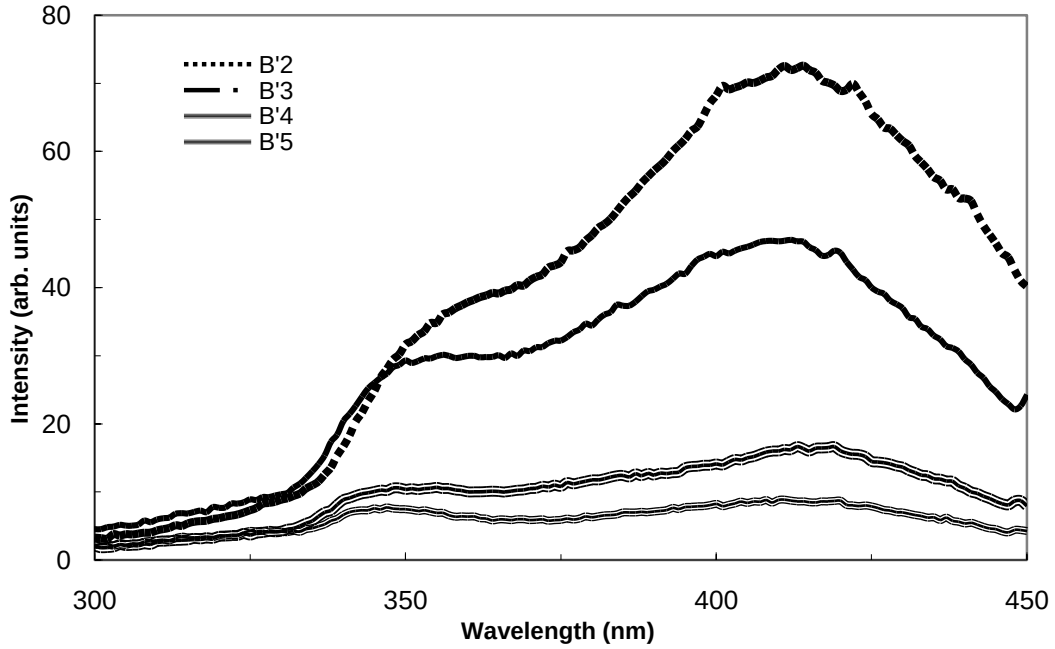

***Fig 3.12**: Excitation spectra of representative BaS:Cu(with flux) phosphors*

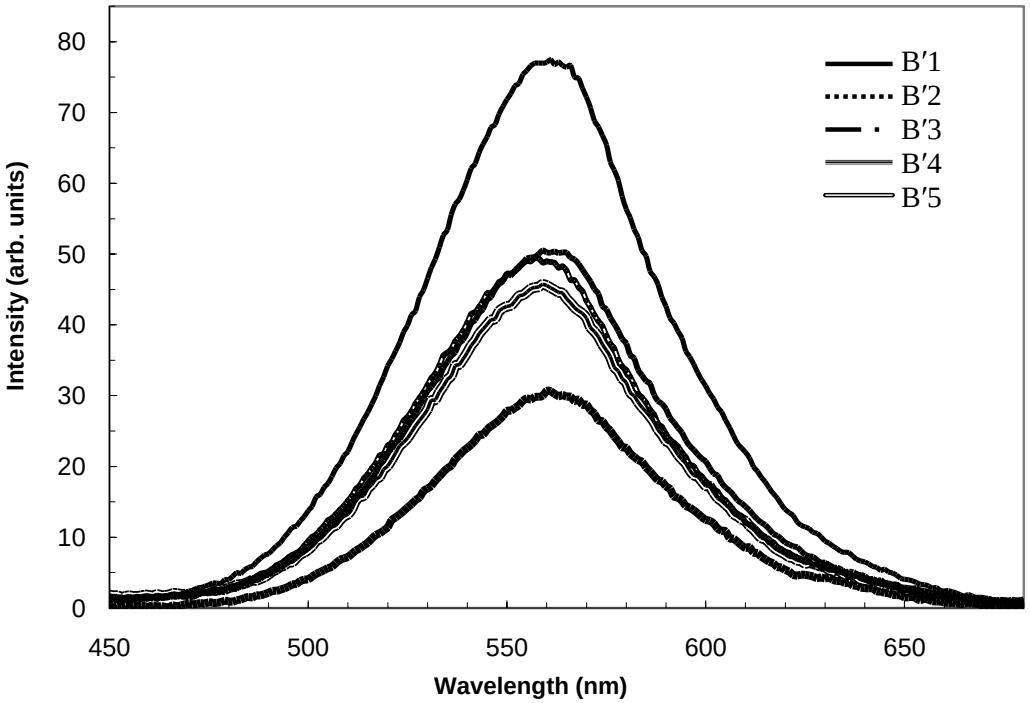

***Fig 3.13**: Emission spectra of representative BaS:Cu(with flux) phosphors*

SrS:Cu- In copper doped strontium sulphide phosphors (without flux), excitation spectra shows two prominent peaks around 310 and 345 nm, as shown in Fig. 3.14. However, the emission peak is observed around 500 nm (see Fig. 3.15).

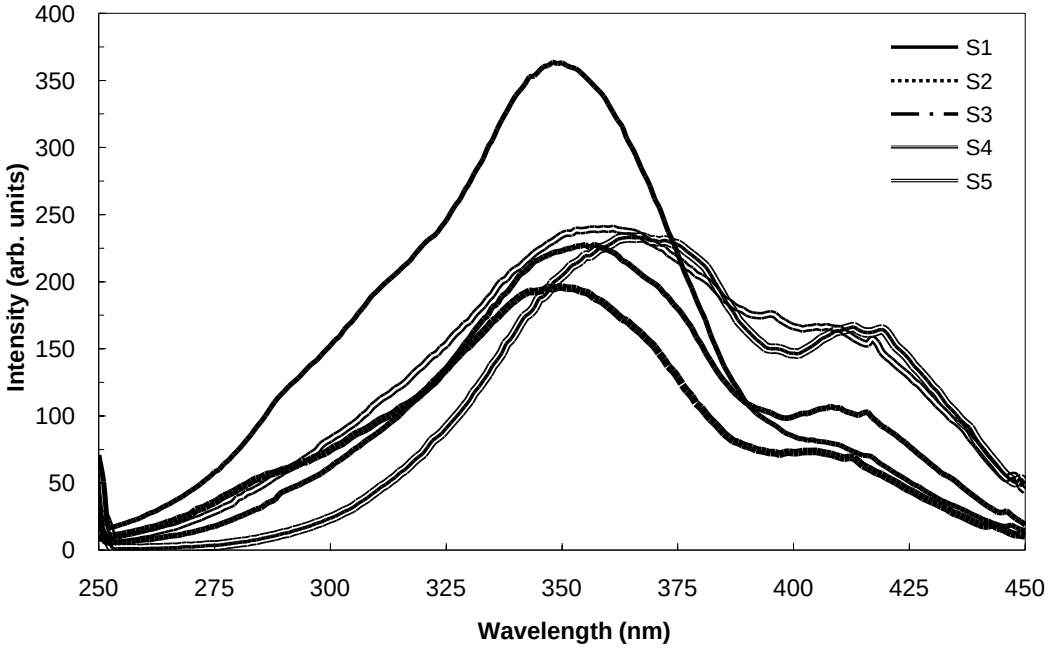

***Fig 3.14**: Excitation spectra of representative SrS:Cu(without flux) phosphors*

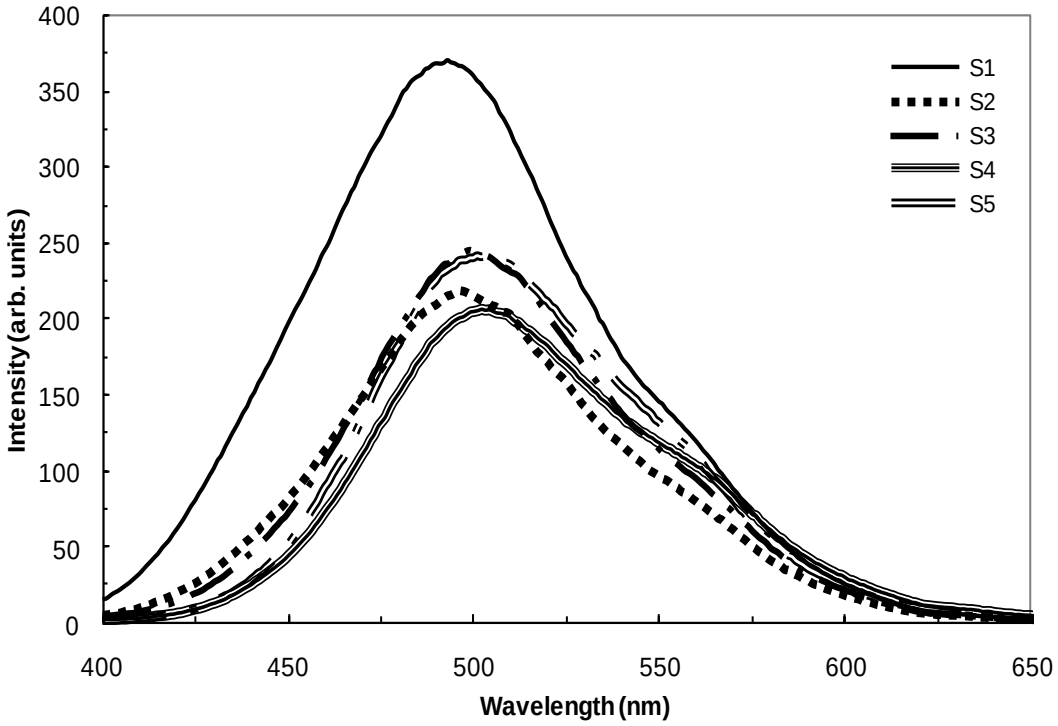

***Fig 3.15**: Emission spectra of representative SrS:Cu(without flux) phosphors*

The addition of flux in this case shifts the excitation peaks to 350 and 410 nm (see Fig. 3.16), but the emission peak remains at the same position, 500 nm (as can be seen in Fig. 3.17). The fluorescence intensity, in this case too, increases considerably.

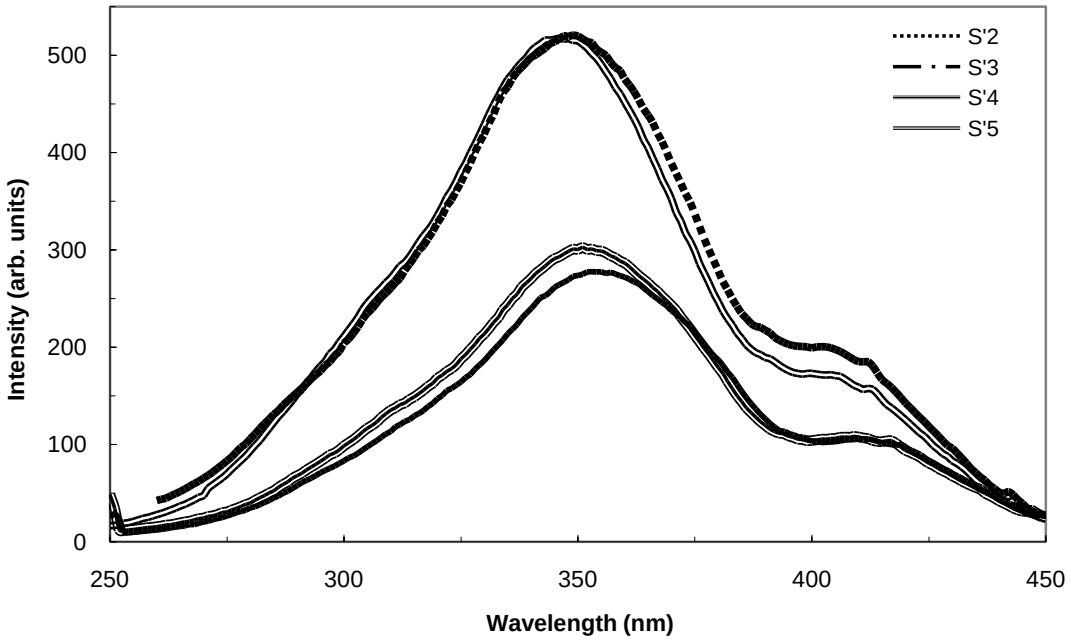

***Fig 3.16**: Excitation spectra of representative SrS:Cu(with flux) phosphors*

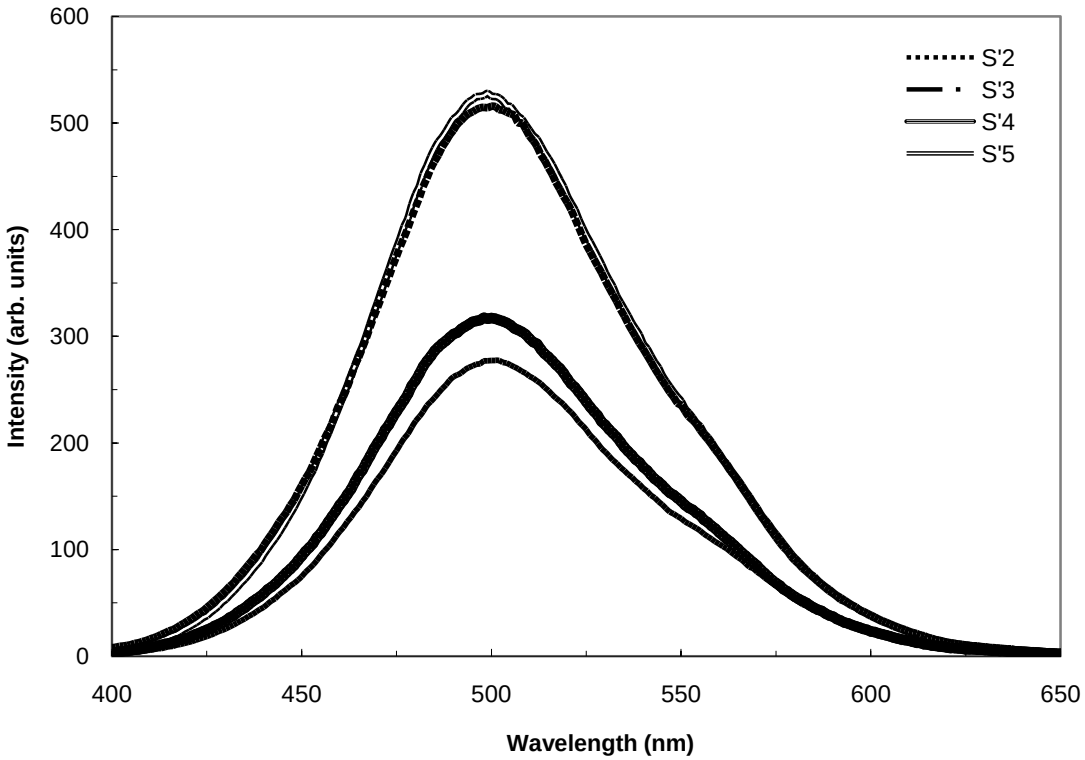

***Fig 3.17**: Emission spectra of representative SrS:Cu(with flux) phosphors*

These results have been compared with those of other investigators and further discussed in the light of existing theories in Chapter 6.

References

[1] G. F. J. Garlick, "*Luminescent Materials*", Oxford Univ. Press, London (1949).

[2] P. Pringsheim, "*Fluorescence & Phosphorescence*", Interscience, New York (1949).

[3] D. Curie, "*Luminescence in Crystals*" translated by G.F.J. Garlick, Methuen & Co. Ltd., London (1963).

[4] K. H. Butler, "*Fluorescent Lamp phosphors*", Pennsylvania State University press, University Park, PA, (1980).

[5] R. C. Ropp, "*Luminescence and the Solid State*", Studies in Inorganic Chemistry **12,** Elsevier, Amsterdam, (1991).

[6] K.T.V Grattan, Z. Y. Zhang, "*Fiber Optic Fluorescence Thermometry*, Chapman and Hall, London, (1995).

[7] S. Shionoya and W. M. Yen (Eds), "*Handbook of Phosphors*" CRC Press, NY. (1999).

[8] F. Bloch, *Z. Phys.*, **52,** 555 (1928).

[9] M. Lax and E. Burstein, *Phys. Rev.*, **100**, 592 (1955).

[10] J. Lambe & C.C. Klick, Phys. Rev. **98**, 909 (1955). *J. Phys. Rad.*, **17**, 663 (1956).

[11] H. A. Klasens, *J. Phys. Chem. Solids*, **9**, 185 (1959).

[12] K. S. K. Rebane, *Opt. & Spec.* (USA) **13**, 3330 (1962).

[13] S. Shionoya, T. Koda, K. Era & H. Fujiwara, *J. Phys., Soc.* (Japan) **19** 1157 (1964).

[14] J. Kramer, *J. Electrochem. Soc.*, **123**, 85 (1976).

[15] F. Decker, B. Pettinger, and H. Gericher, *J. Electrochem. Soc.*, **130**, 1335 (1983).

[16] N. Yamashita, Y. Michitsuji, and S. Asano, *J. Electrochem. Soc.*, **134**, 2932 (1987).

[17] G. Nogami, K. Murakami, S. Ohkubo, and Y. Hamasaki, *J. Electrochem. Soc.*, **139**, 1777 (1992).

[18] W. K. Chang and K. K. Gleason, *J. Electrochem. Soc.*, **144**, 1441 (1997).

[19] M. Ihara, T. Igarashi, T. Kusunoki, and K. Ohno, *J. Electrochem. Soc.* **149**, H72 (2002)

[20] C. Feldmann, T. Justel, C.R. Ronda and P.J. Schimdt, *Adv. Funct. Mater*. **13,** 511 (2003)

[21] G. F. J. Garlick, "*Progress in Semiconductors*", Vol. I Heywood & Co. Ltd., London (1956).

[22] R. H. Bube, "*Photoconductivity in Solids*", John Wiley, N.Y. (1968).

[23] R. Pandey and S. Sivaraman, *J. Phys. Chem. Solids*, **52,** 211(1991).

[24] A. Jalonski, *Z. Phys.*, **94**, 38 (1935).

[25] R. P. Johnson, *J. Opt. Soc. Am.*, **29**, 387 (1939).

[26] J.T. Randall and M. H. F. Wilkins, *Proc. Roy. Soc., London*, **A184**, 366 (1945).

[27] R. E. Halsted, E. F. Apple and J. S. Prener, *Phys. Rev. Letters*, **2**, 420 (1959).

[28] George G. Guilbault (Ed): "*Practical Fluorescence*" 2nd Edition, Marcel Dekker, NY, 9 (1990).

Chapter 4

Temperature Dependence of Fluorescence

4.1 Introduction:

In past few decades the temperature dependent characteristics of fluorescence of "thermographic phosphors" have been used for remote (or noncontact) measurement of temperature of both static and moving surfaces and have performed many other tasks that standard sensors (thermocouple, thermistors, etc) cannot. The range of usefulness of this class of materials extends from cryogenic temperatures to those approaching 2000°C [1-7]. The study of temperature dependent luminescence is also important from the point of view of its stability and applicability in other devices [8-17]. In addition such systems have also been successfully employed to make contact measurements of temperature. It is from this point of view that the temperature dependence of fluorescence intensity was studied in detail in our system of phosphors. This chapter presents the temperature dependence of fluorescence of phosphors under investigation after briefly reviewing the prevalent theory.

4.2 Theory of Temperature Dependence of Fluorescence:

The intensity of fluorescence during excitation falls if the temperature is raised sufficiently due to the emission of phonons in competition with photon emission. If P_r is the probability of radiative transition and P_{nr} the probability of a non-radiative transition, then the fluorescence is proportional to the ratio [18]

$$\eta = \frac{P_r}{P_r + P_{nr}} \qquad (4.1)$$

where η is called fluorescence efficiency. It is assumed that P_r is sensibly independent of temperature, while P_{nr} rises rapidly with temperature. The latter is given by

$$P_{nr} = s\, exp\left(\frac{-W}{kT}\right) \qquad (4.2)$$

where s is called the frequency factor (which is of the order of magnitude of 10^9 s^{-1}); W is the thermal activation energy; k is Boltzmann constant and T is the temperature (K).

Rearranging eq. (4.1), we get

$$\eta = \frac{1}{1+\frac{P_{nr}}{P_r}}$$

and substituting for P_{nr} from eq. (4.2) we see that

$$\eta = \frac{1}{1+(\frac{s}{P_r})\exp(-\frac{W}{kT})}$$

$$\text{or } \eta = \frac{1}{1+C\exp(-\frac{W}{kT})} \qquad (4.3)$$

where C (= s/P_r) is a constant. In most phosphors, the nature of fluorescence efficiency is adequately described by equation (4.3). In some cases, it may be more complex.

Based on the band theory of solids, Klasens [19] has given a satisfactory model for thermal quenching in sulphide phosphors. When electrons are in the conduction band, the holes in the luminescence centers may be filled up by electrons from the valence band. This process requires a certain activation energy W (energy necessary to remove an electron from the valence band) which can be supplied thermally above a certain temperature. The electron previously removed from the center by optical excitation now cannot return to it and after wandering in the conduction band for a short time may be captured by a non-radiative recombination center. If sufficient numbers of such centers are available, the thermal activation process will determine the probability of non-radiative transitions.

4.3 Some Relevant Parameters Related to Thermal Quenching:

In order to assess the suitability of a phosphor for thermographic application, some parameters are worth considering. These have been defined as follows:

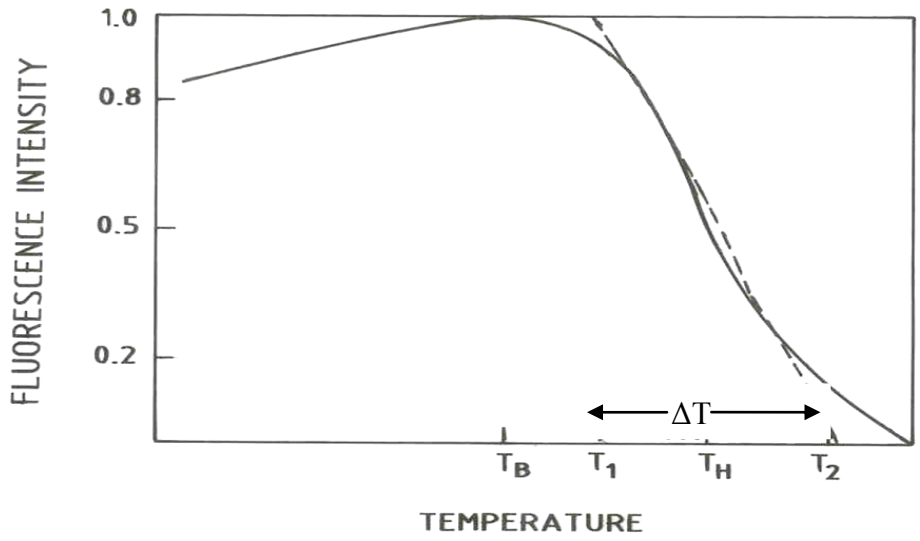

***Fig 4.1**: Definition of thermal quenching parameters (Schematic)*

Quenching Range, ΔT

Following Kroger [20], Mishra and Sharma [21], quenching range is defined as the temperature range within which the fluorescence intensity decreases with temperature after non-radiative transitions begin to dominate and is given by

$$\Delta T = T_2 - T_1 = \left(\frac{5W}{3k}\right)\{(\ln C - \ln 4)^{-1} - (\ln C + Ln\ 4)^{-1}\} \qquad (4.4)$$

This parameter gives an estimate of the span of thermographic sensor.

Quenching Temperature, T_Q

It is defined as the point of intersection of the abscissa and a straight line drawn through the points at which the intensity has fallen to 80 and 20% of the maximum value. In Fig.4.1, T_2 is the quenching temperature and is often denoted as T_Q and is given by the expression.

$$T_Q = \frac{W}{3k}\{4(\ln C - \ln 4)^{-1} - (\ln C + \ln 4)^{-1}\} \qquad (4.5)$$

This gives the end point of the range. The span of the sensor will be limited by T_Q.

Breaking Point Temperature, T_B

It is the temperature at which non-radiative transitions set in; that is, the fluorescence intensity starts to decrease. It is approximately given by:

$$T_B = \frac{W/k}{\ln C + 0.9} \qquad (4.6)$$

The starting of the sensor span will be decided by this parameter.

Half-Value Temperature, T_H

It is the temperature at which the intensity has decreased to half its maximum value within the quenching range ΔT. It is given by the expression:

$$T_H = \frac{W/k}{\ln C} \qquad (4.7)$$

Experimental Setup:

In order to study the variation of fluorescence intensity with temperature the experimental setup, shown block-diagrammatically, in Fig 4.2 was employed. The xenon arc lamp – excitation monochromator combination provides the excitation wavelength, λ_{exc}, which excites fluorescence in the phosphor kept in the sample holder. The mechanical chopper was not used in this experiment and hence the excitation was continuous. The sample holder is fitted with a heating element which provides a controlled temperature to the phosphor.

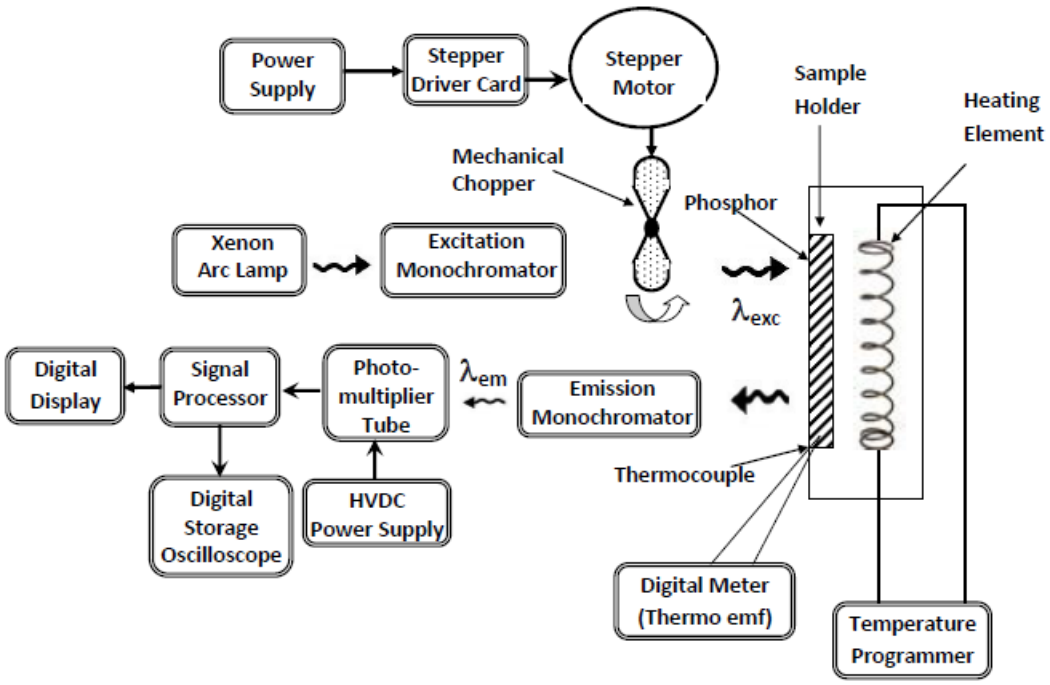

Fig. 4.2: *Experimental Setup for studying temperature dependence of fluorescence*

The fluorescence emitted by the phosphor is focused onto the entrance slit of the emission monochromator. The latter disperses the emission spectrum into its constituent lines or bands. The isolated emission wavelengths, λ_{em} are obtained at the

exit slit, which are then allowed to fall on the photomultiplier tube. The output photocurrent is processed and displayed on the digital meter. The digital storage oscilloscope is not used in this experiment. The temperature of the phosphor can be read using a copper-constantan thermocouple attached to the sample holder.

4.4 Results:

4.4.1Variation of Fluorescence Intensity with Temperature:

The record of the variation of fluorescence intensity at λ_{max} (the wavelength of maximum intensity at RT) as a function of temperature for all the alkaline earth sulphides activated by copper (with and without flux) are shown in Figs. 4.3-4.8. As is evident, the fluorescence intensity decreases in all the cases with increase in temperature. However, the addition of flux in these phosphors improves the slope of the curves. In some cases we did not observe the break temperature T_B. It is possible that it lies beyond the range of temperatures studied in this investigation.

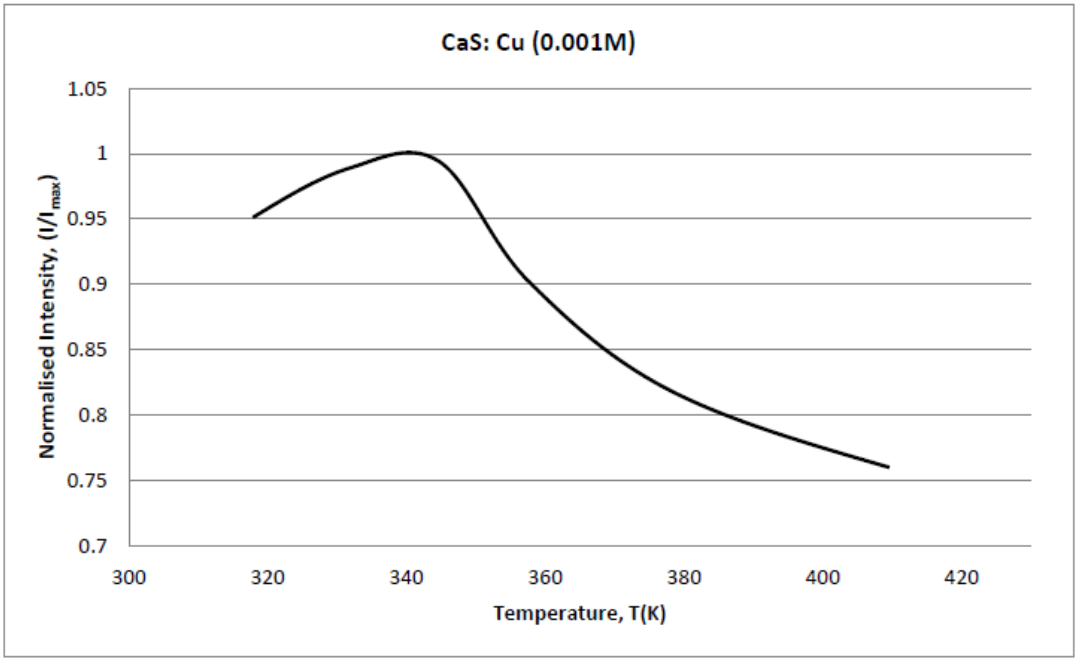

Fig: 4.3(a): Temperature dependence of fluorescence intensity of CaS:Cu(0.001 M)(without flux)

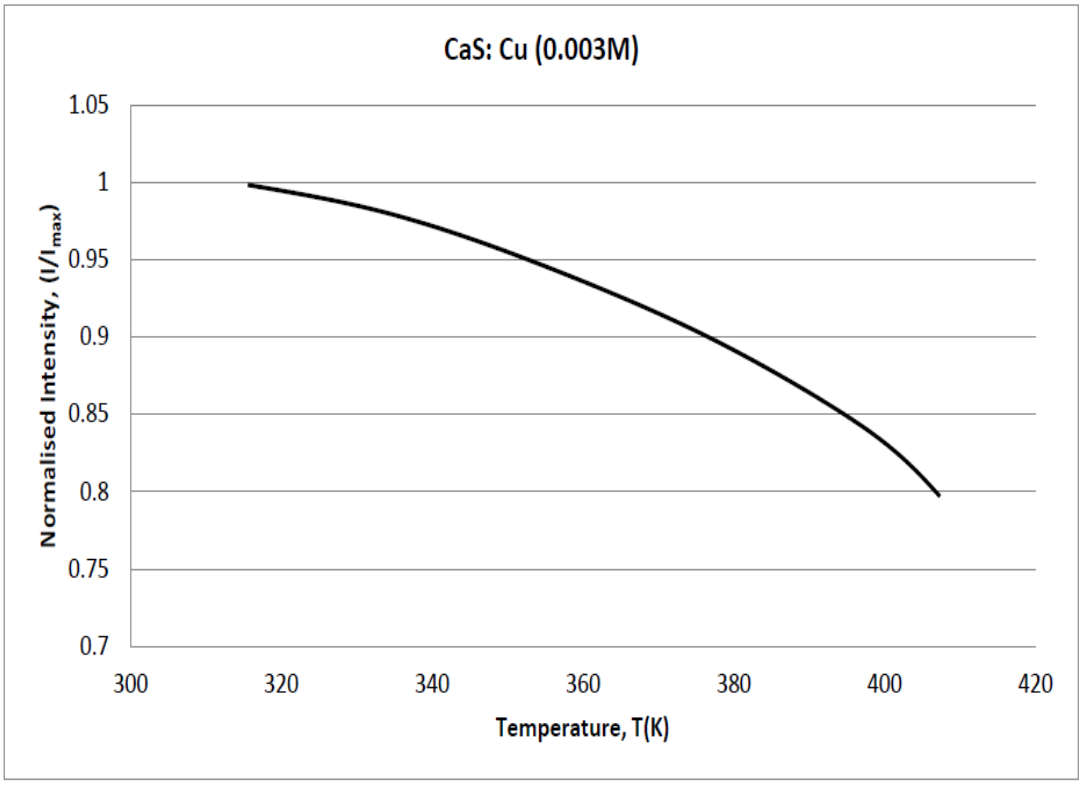

Fig: 4.3(b): Temperature dependence of fluorescence intensity of CaS:Cu(0.003 M)(without flux)

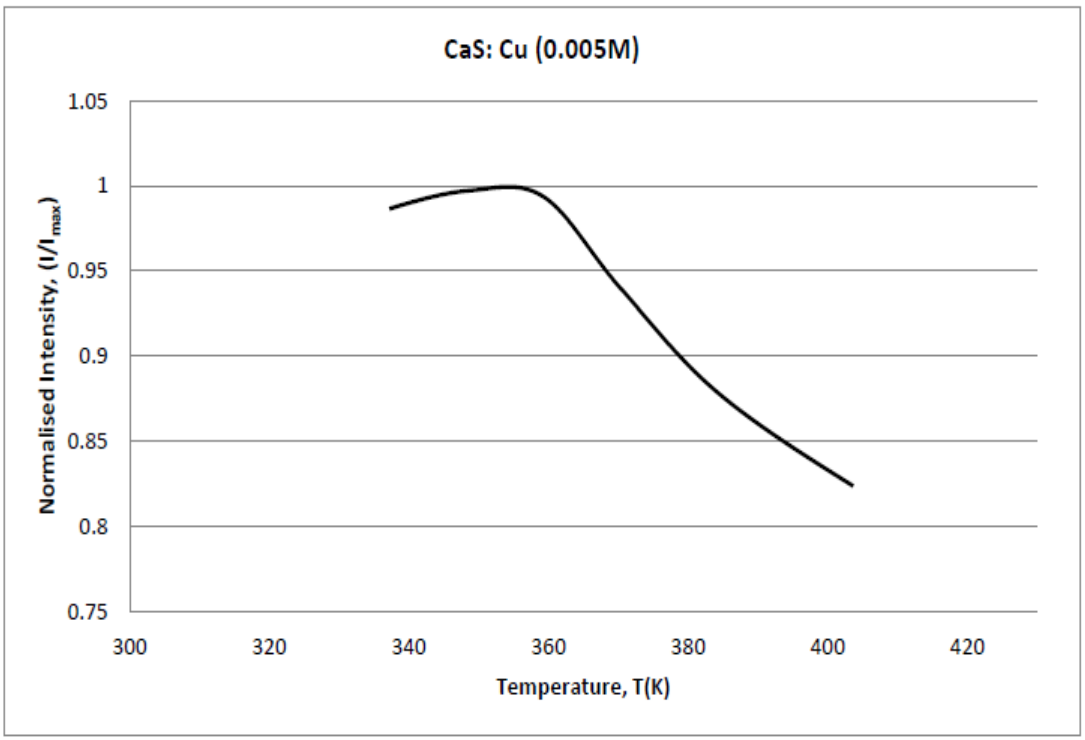

Fig: 4.3(c): Temperature dependence of fluorescence intensity of CaS:Cu(0.005 M)(without flux)

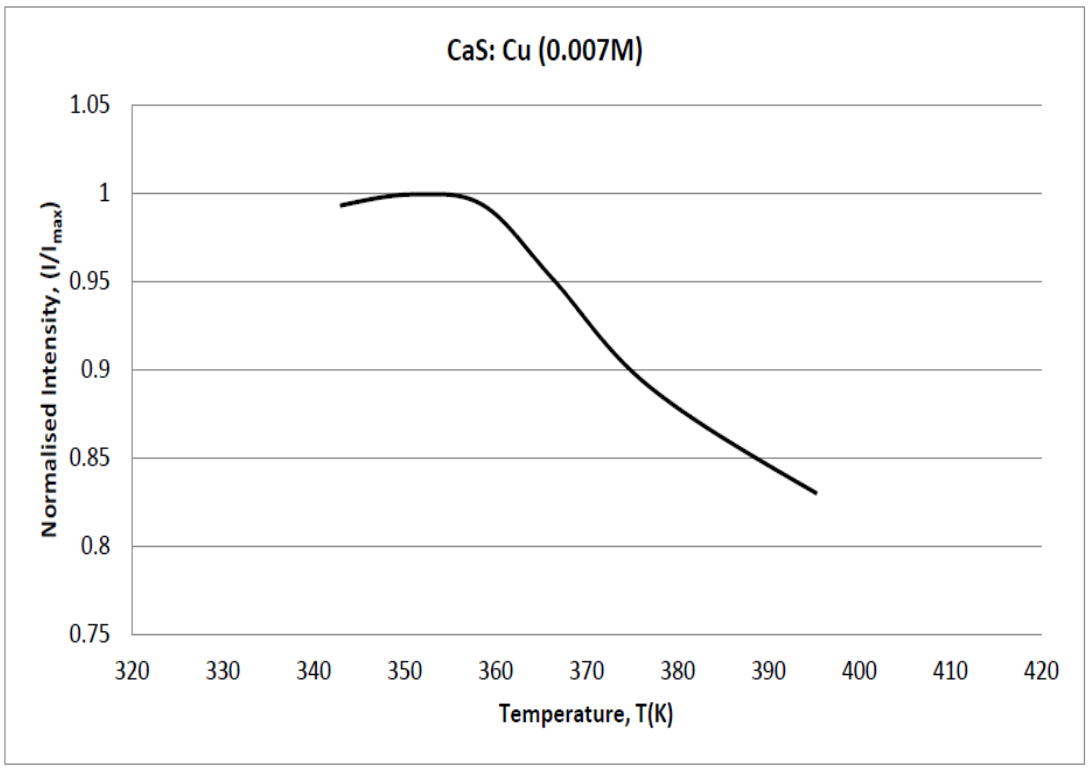

Fig: 4.3(d): Temperature dependence of fluorescence intensity of CaS:Cu(0.007 M)(without flux)

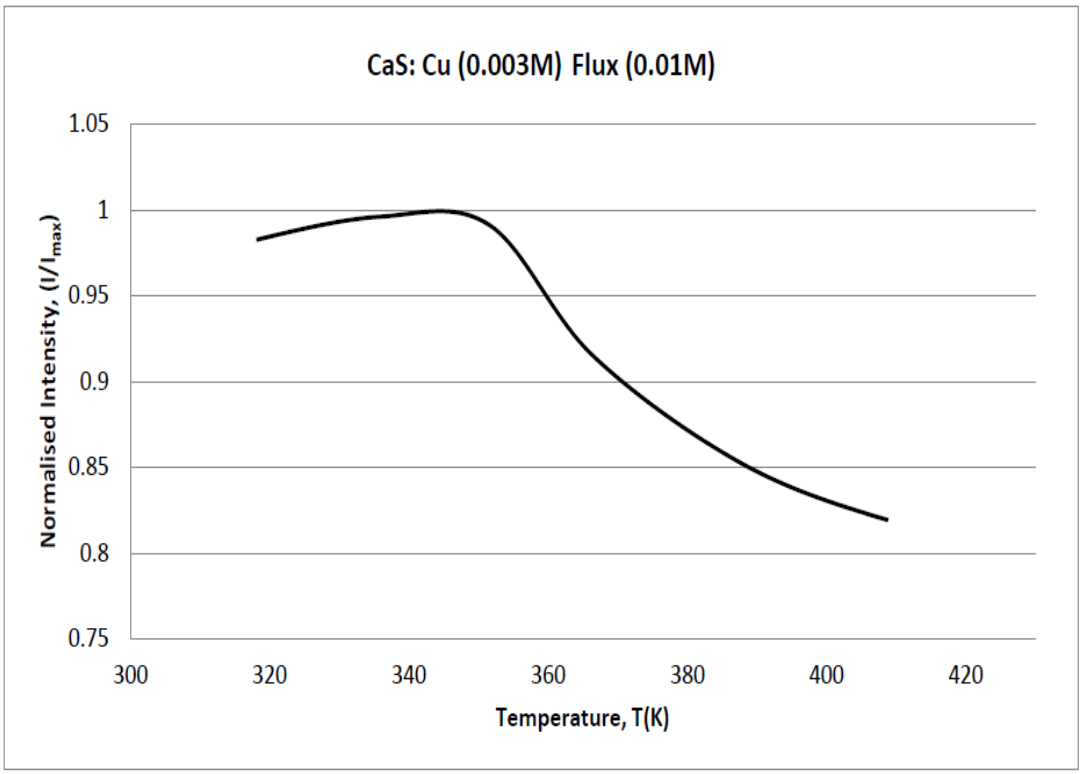

Fig: 4.4(a): Temperature dependence of fluorescence intensity of CaS:Cu(0.003M)(Flux:0.01M)

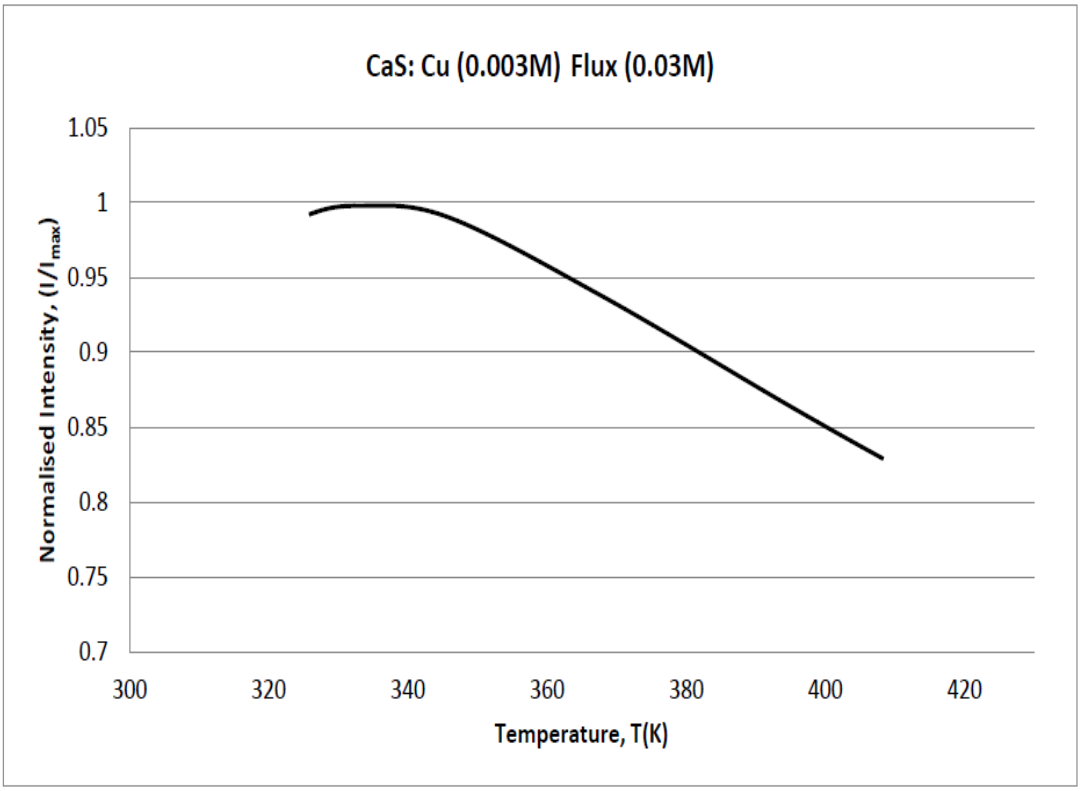

Fig: 4.4(b): Temperature dependence of fluorescence intensity of CaS:Cu(0.003M)(Flux:0.03M)

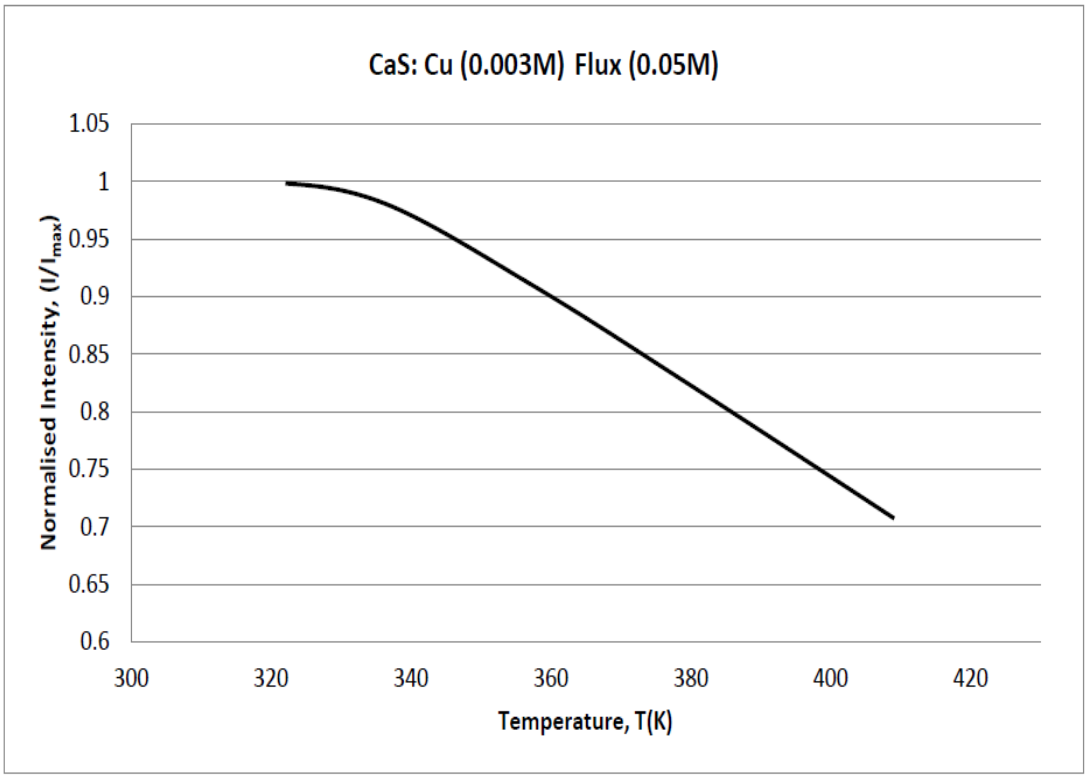

Fig: 4.4(c): Temperature dependence of fluorescence intensity of CaS:Cu(0.003M)(Flux:0.05M)

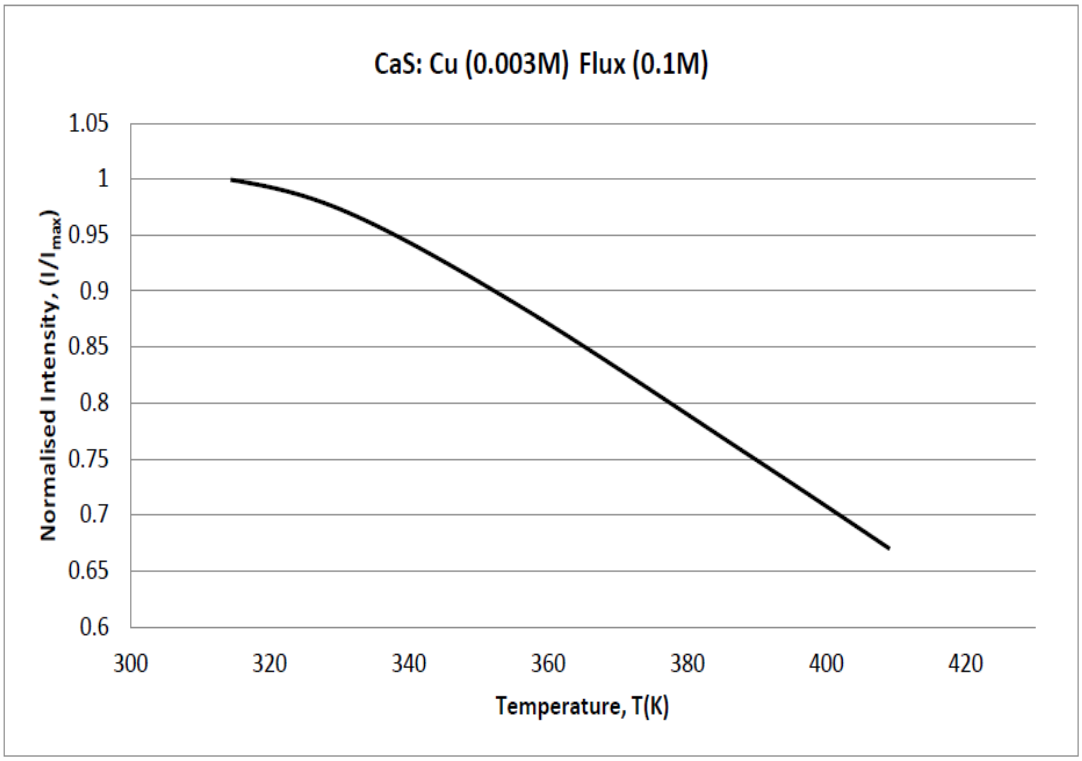

Fig: 4.4(d): Temperature dependence of fluorescence intensity of CaS:Cu(0.003M)(Flux:0.1M)

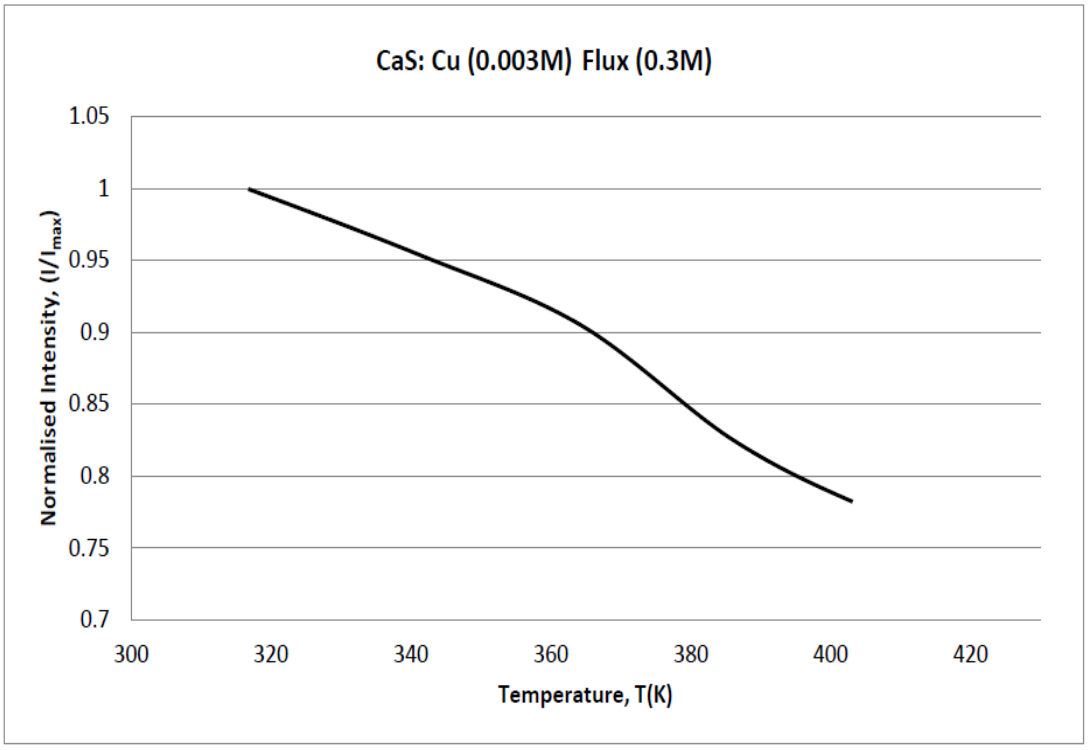

Fig: 4.4(e): Temperature dependence of fluorescence intensity of CaS:Cu(0.003M)(Flux:0.3M)

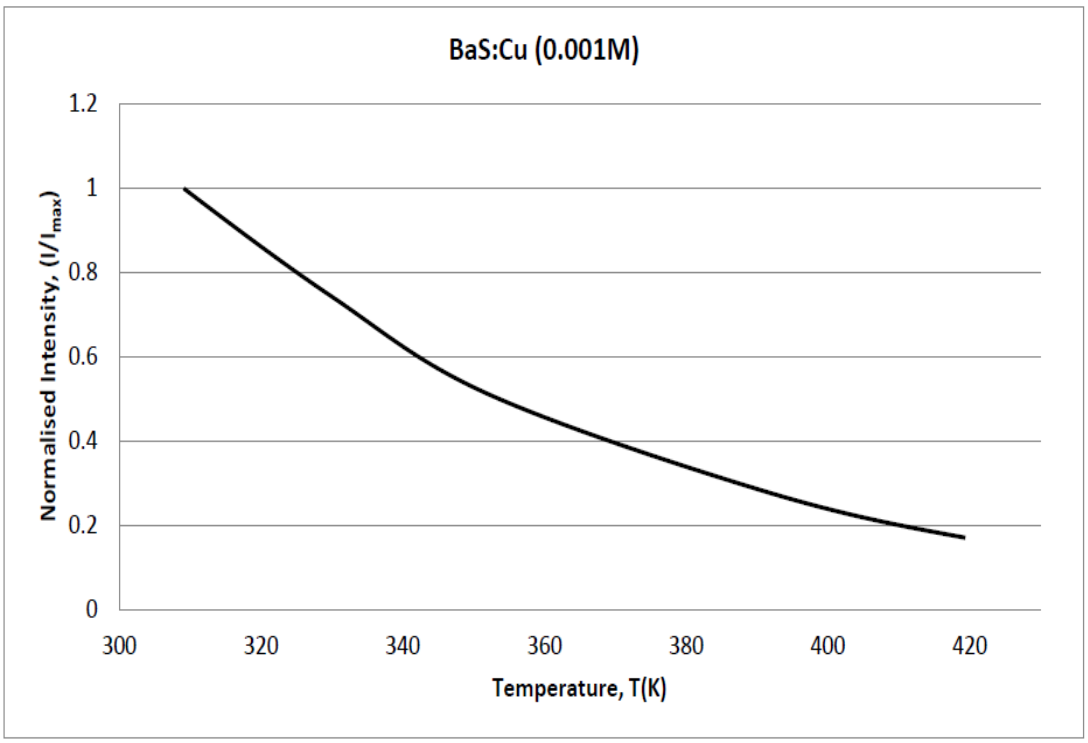

Fig: 4.5(a): Temperature dependence of fluorescence intensity of BaS:Cu(0.001M)(without flux)

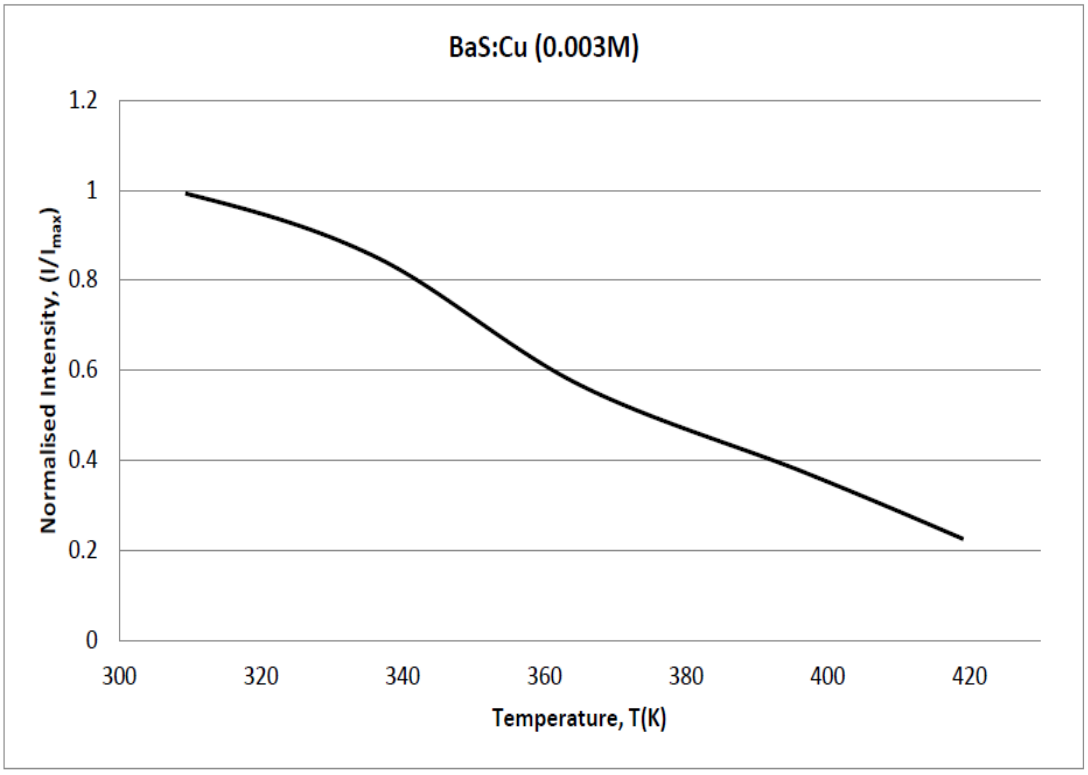

Fig: 4.5(b): Temperature dependence of fluorescence intensity of BaS:Cu(0.003M)(without flux)

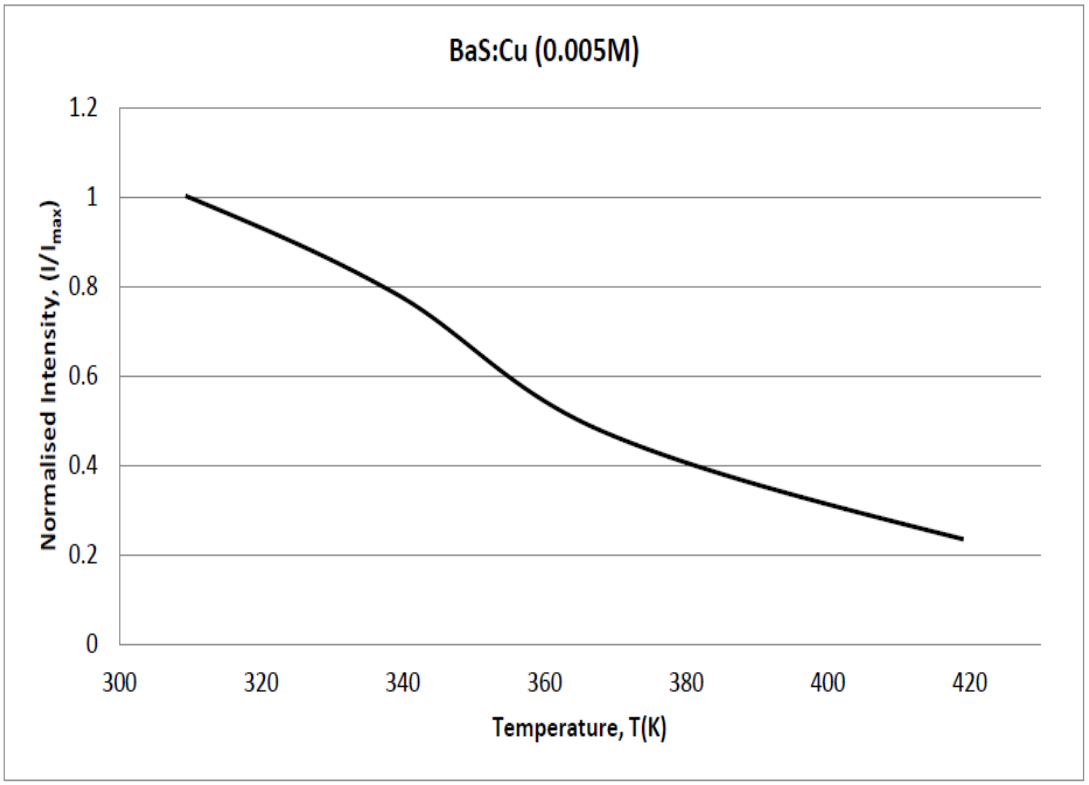

Fig: 4.5(c): Temperature dependence of fluorescence intensity of BaS:Cu(0.005M)(without flux)

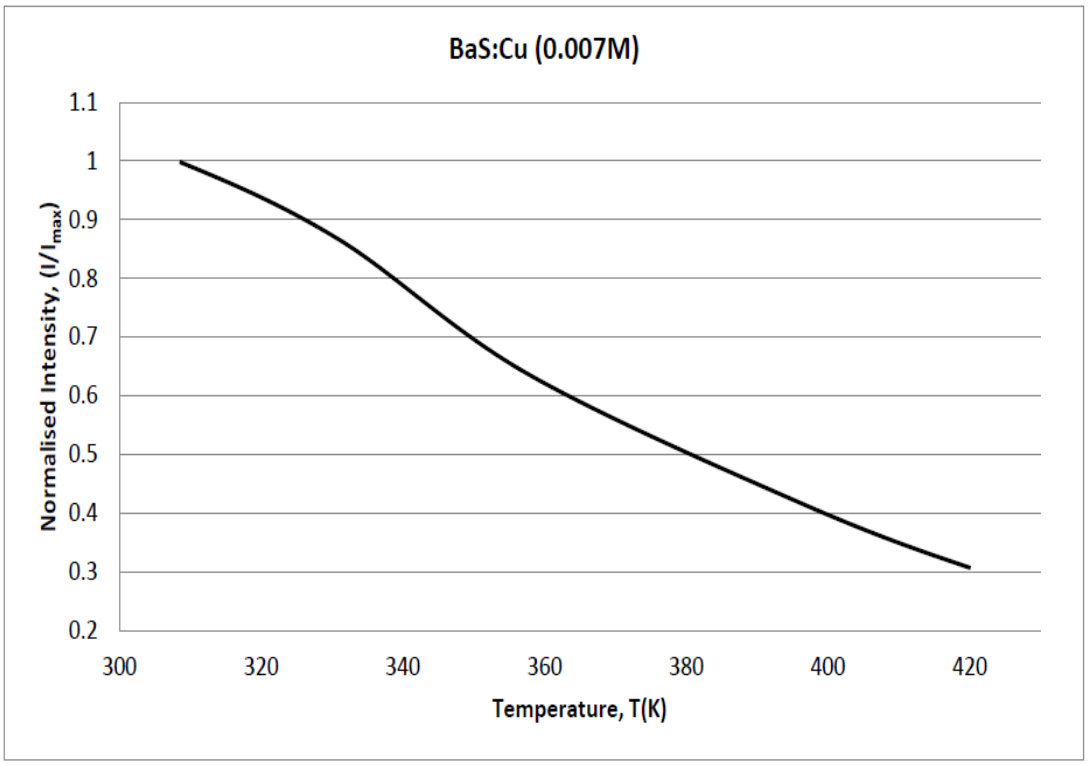

Fig: 4.5(d): Temperature dependence of fluorescence intensity of BaS:Cu(0.007M)(without flux)

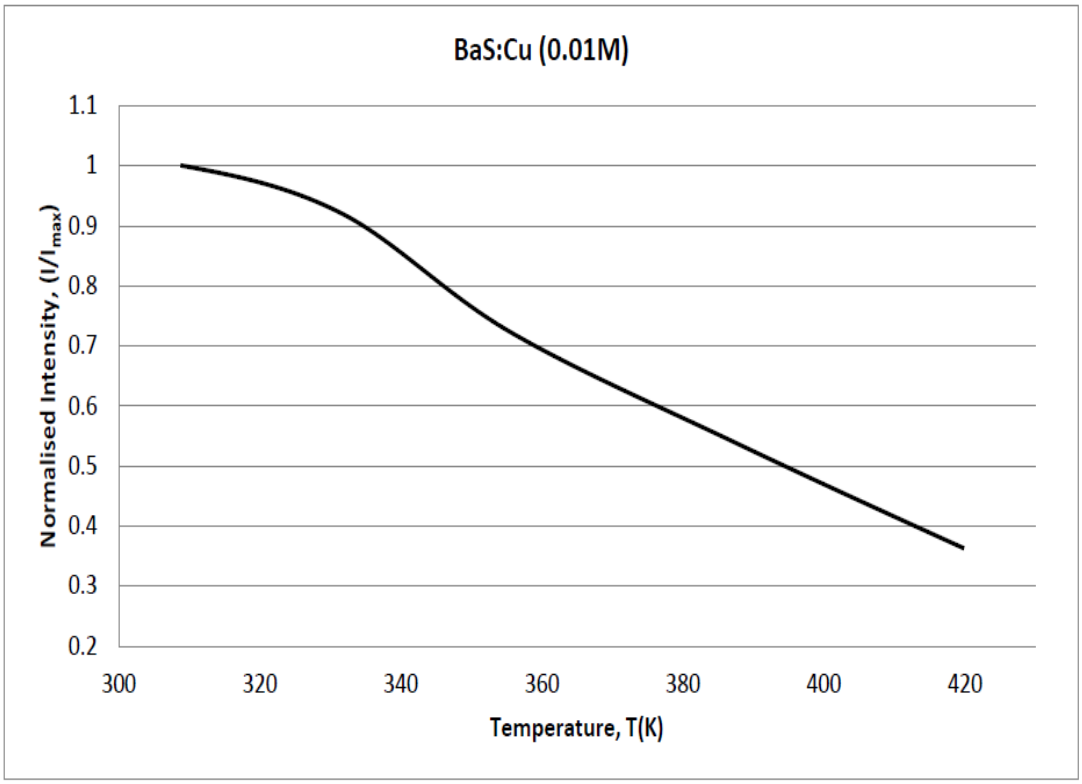

Fig: 4.5(e): Temperature dependence of fluorescence intensity of BaS:Cu(0.01M)(without flux)

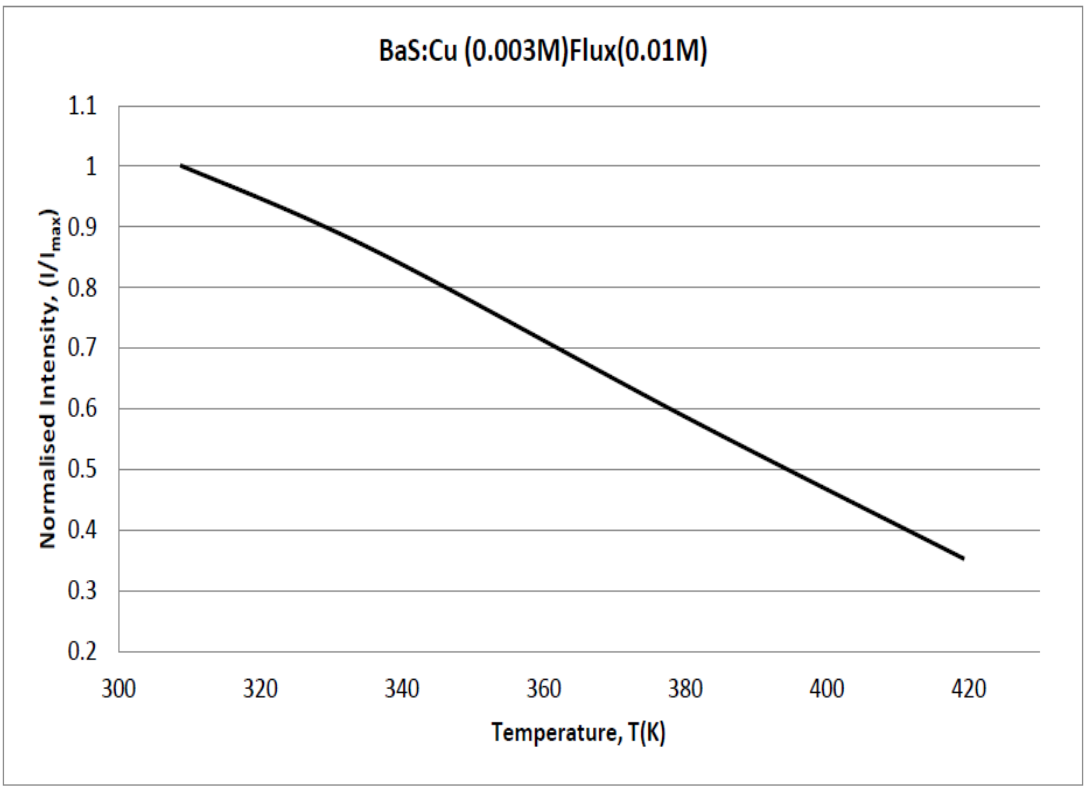

Fig: 4.6(a): Temperature dependence of fluorescence intensity of BaS:Cu(0.003M)(Flux:0.01M)

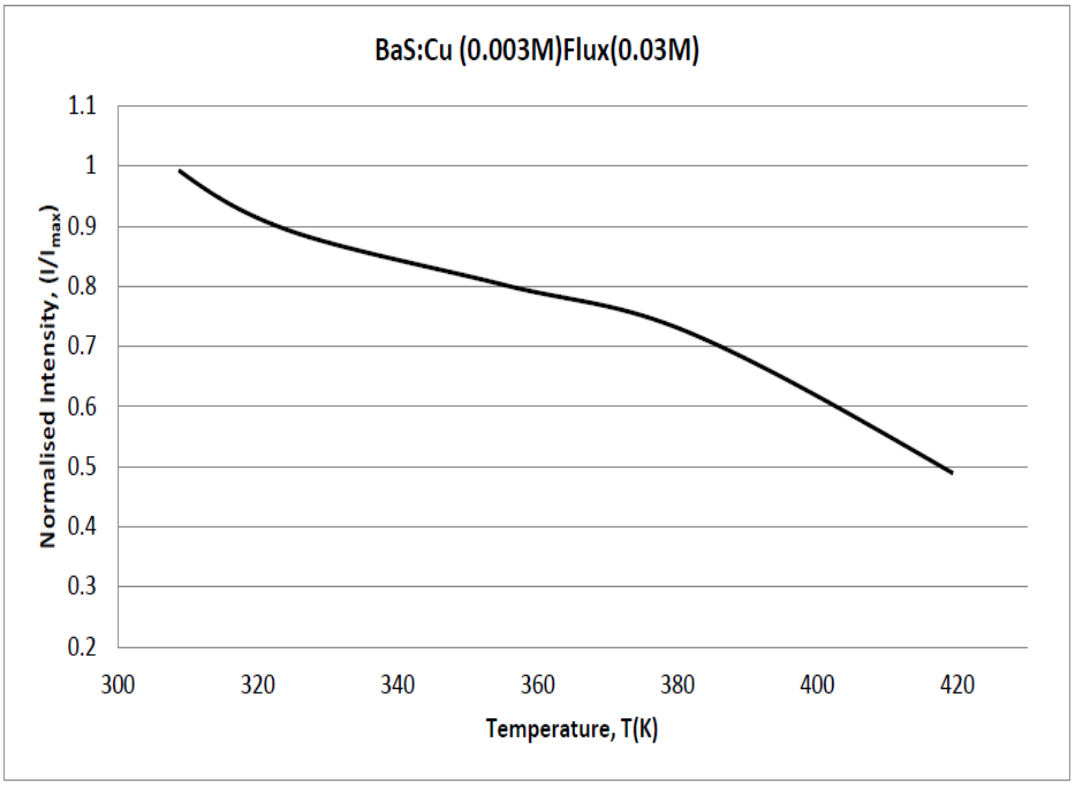

Fig: 4.6(b): Temperature dependence of fluorescence intensity of BaS:Cu(0.003M)(Flux:0.03M)

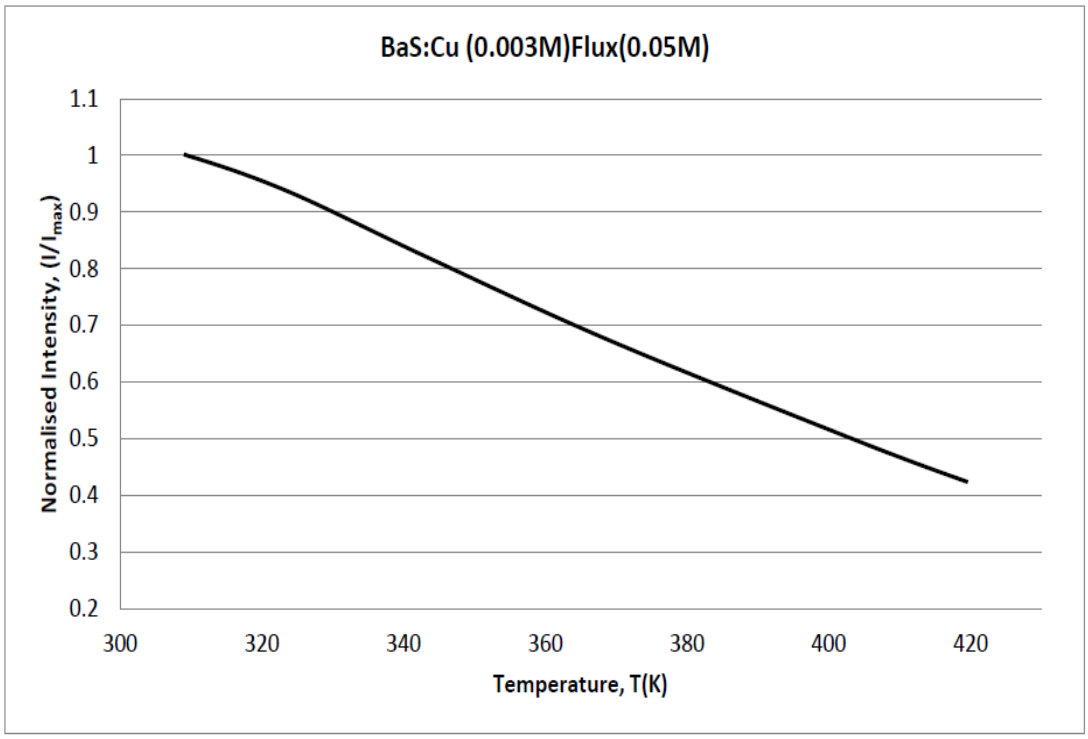

Fig: 4.6(c): Temperature dependence of fluorescence intensity of BaS:Cu(0.003M)(Flux:0.05M)

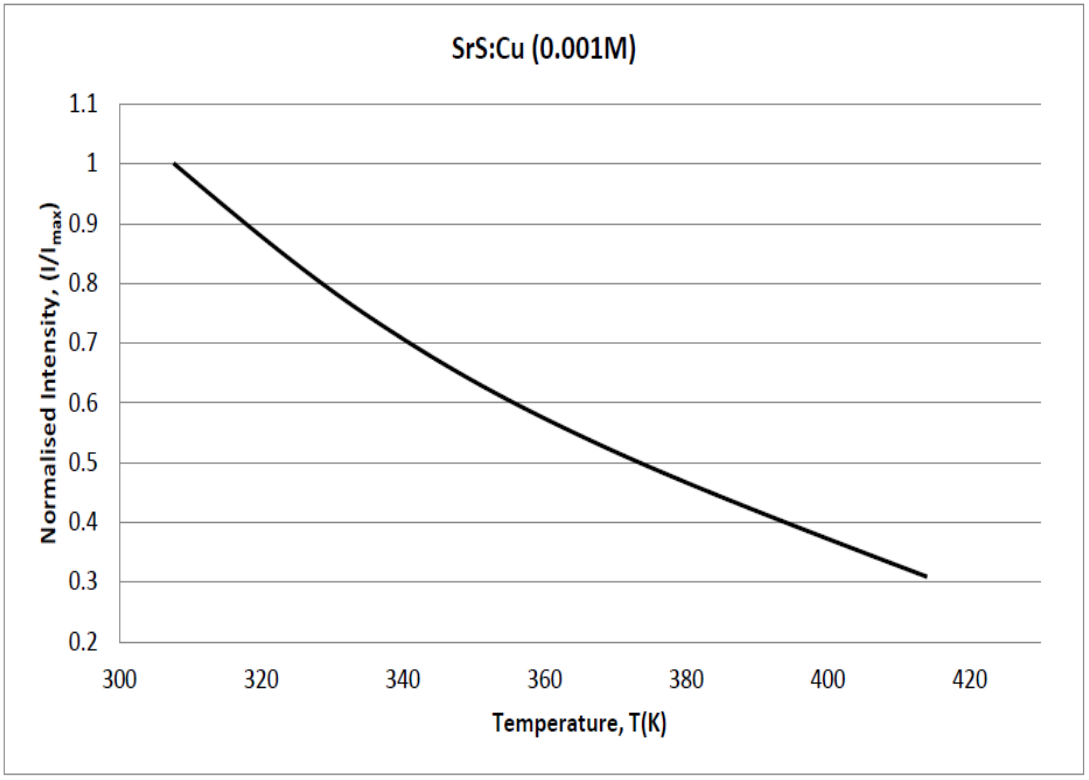

Fig: 4.7(a): Temperature dependence of fluorescence intensity of SrS:Cu(0.001M)(without flux)

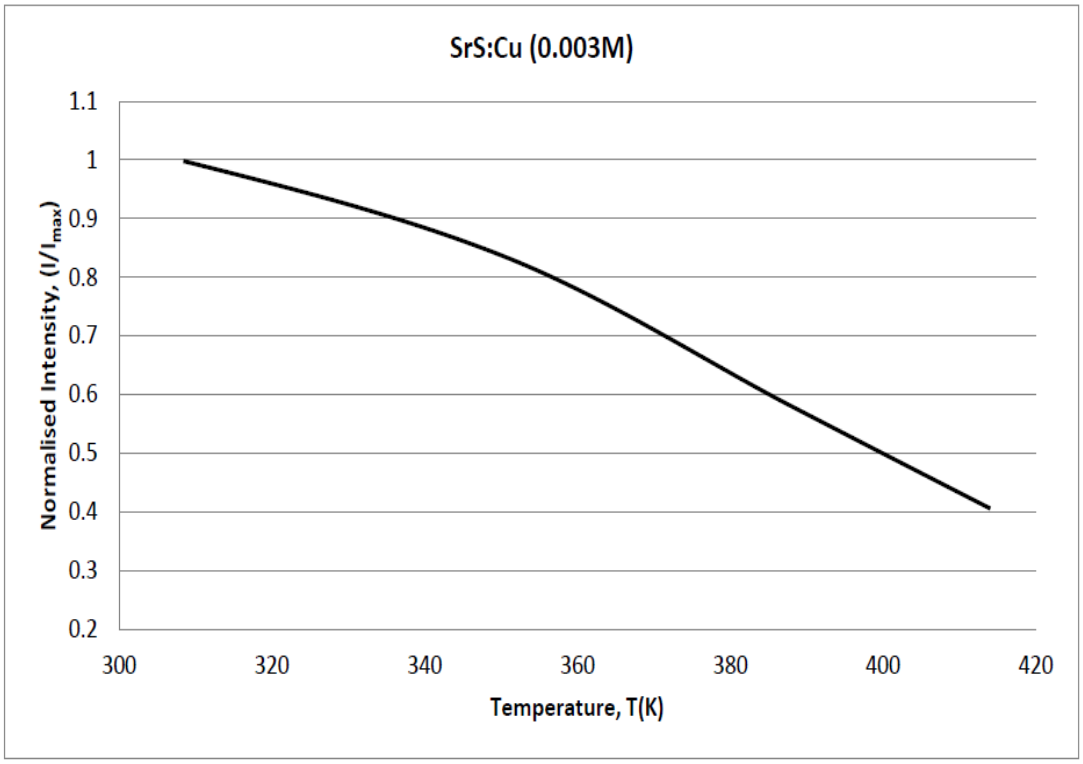

Fig: 4.7(b): Temperature dependence of fluorescence intensity of SrS:Cu(0.003M)(without flux)

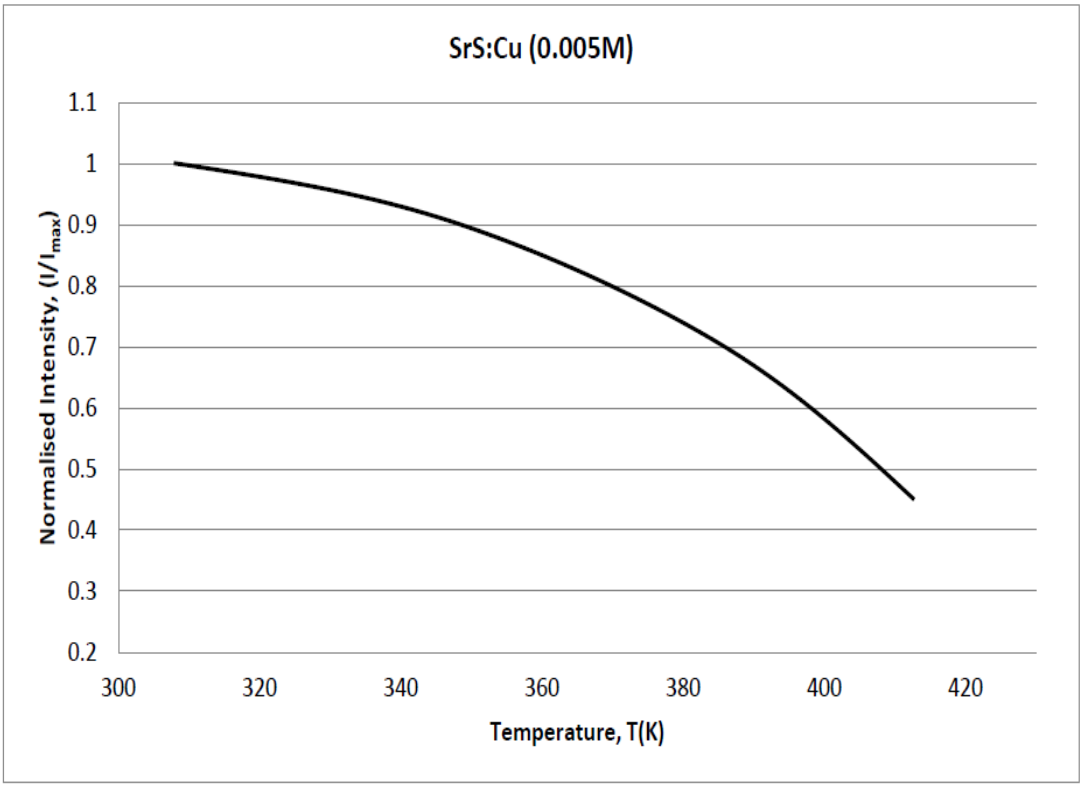

Fig: 4.7(c): Temperature dependence of fluorescence intensity of SrS:Cu(0.005M)(without flux)

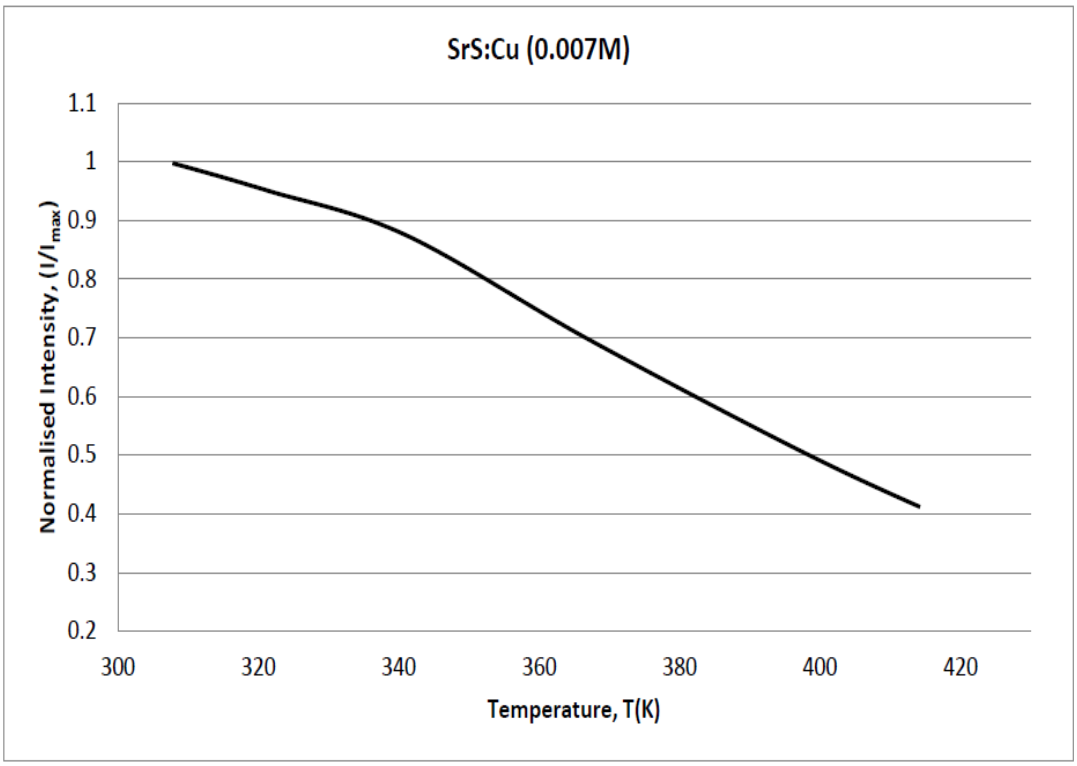

Fig: 4.7(d): Temperature dependence of fluorescence intensity of SrS:Cu(0.007M)(without flux)

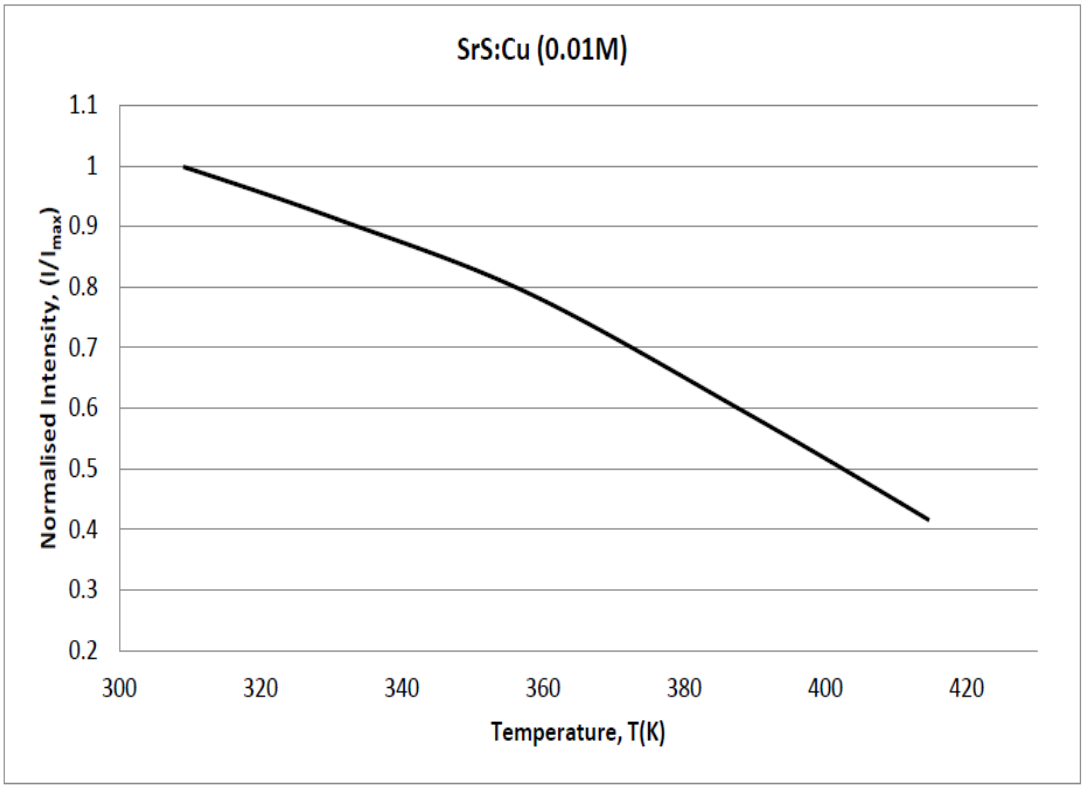

Fig: 4.7(e): Temperature dependence of fluorescence intensity of SrS:Cu(0.01M)(without flux)

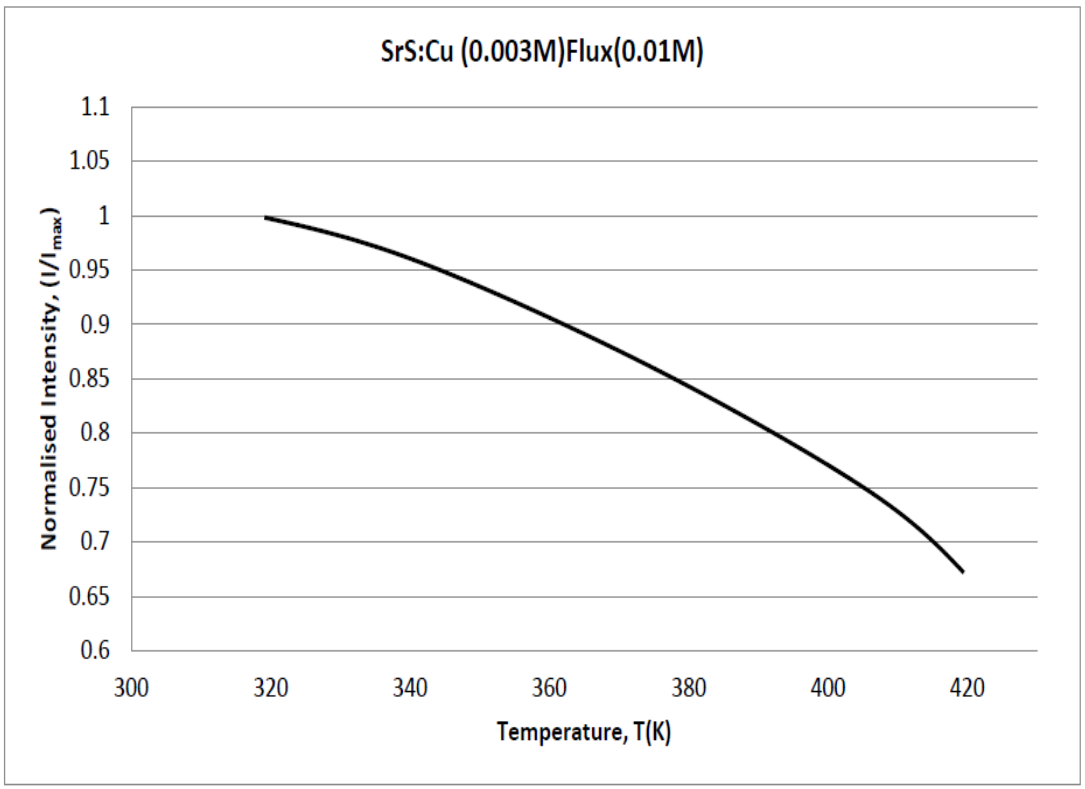

Fig: 4.8(a): Temperature dependence of fluorescence intensity of SrS:Cu(0.003M)(Flux:0.01M)

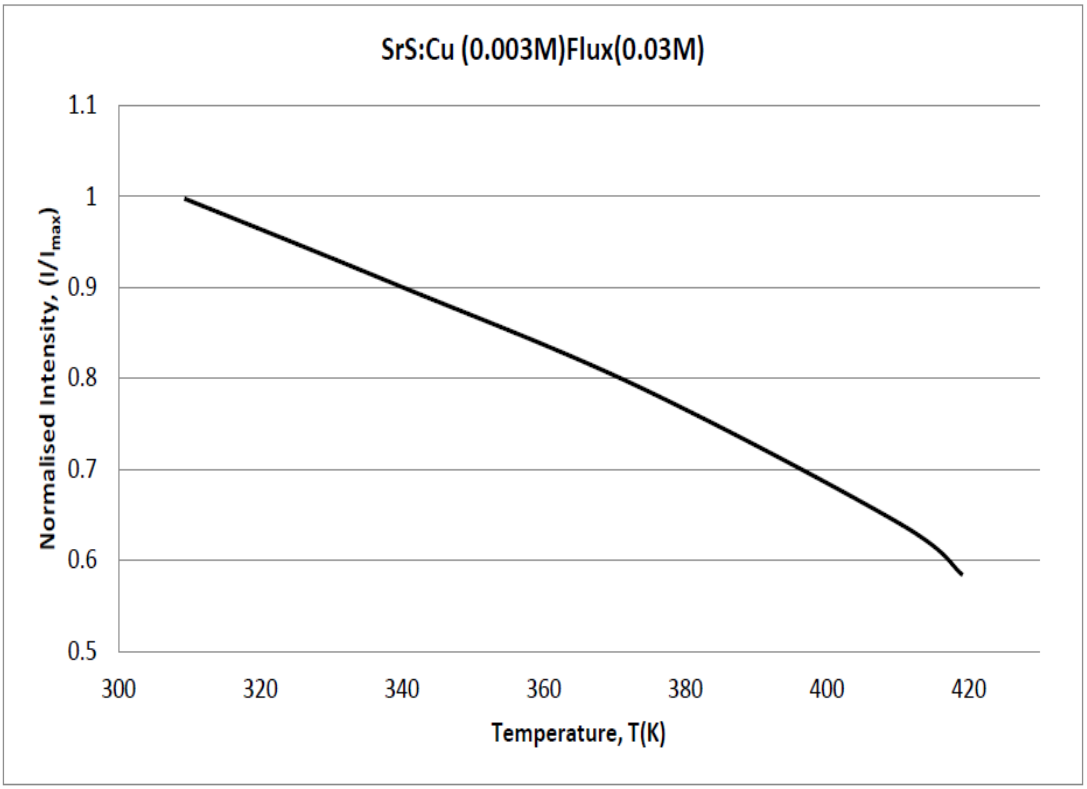

Fig: 4.8(b): Temperature dependence of fluorescence intensity of SrS:Cu(0.003M)(Flux:0.03M)

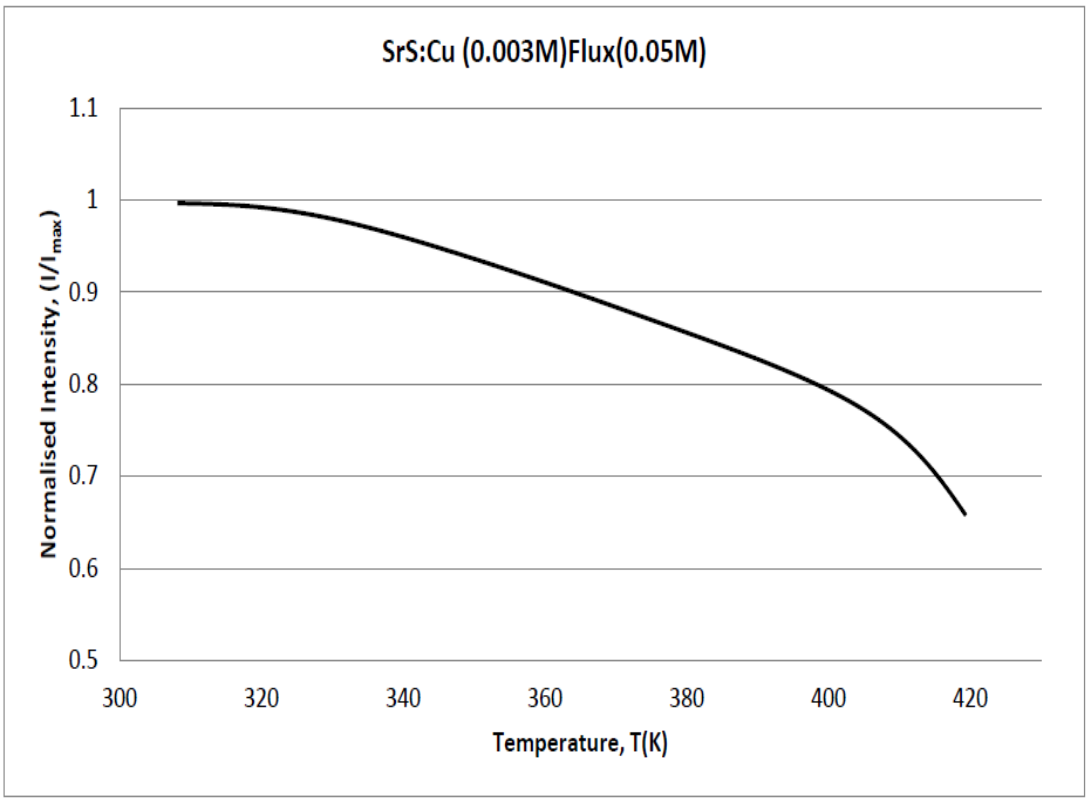

Fig: 4.8(c): Temperature dependence of fluorescence intensity of SrS:Cu(0.003M)(Flux:0.05M)

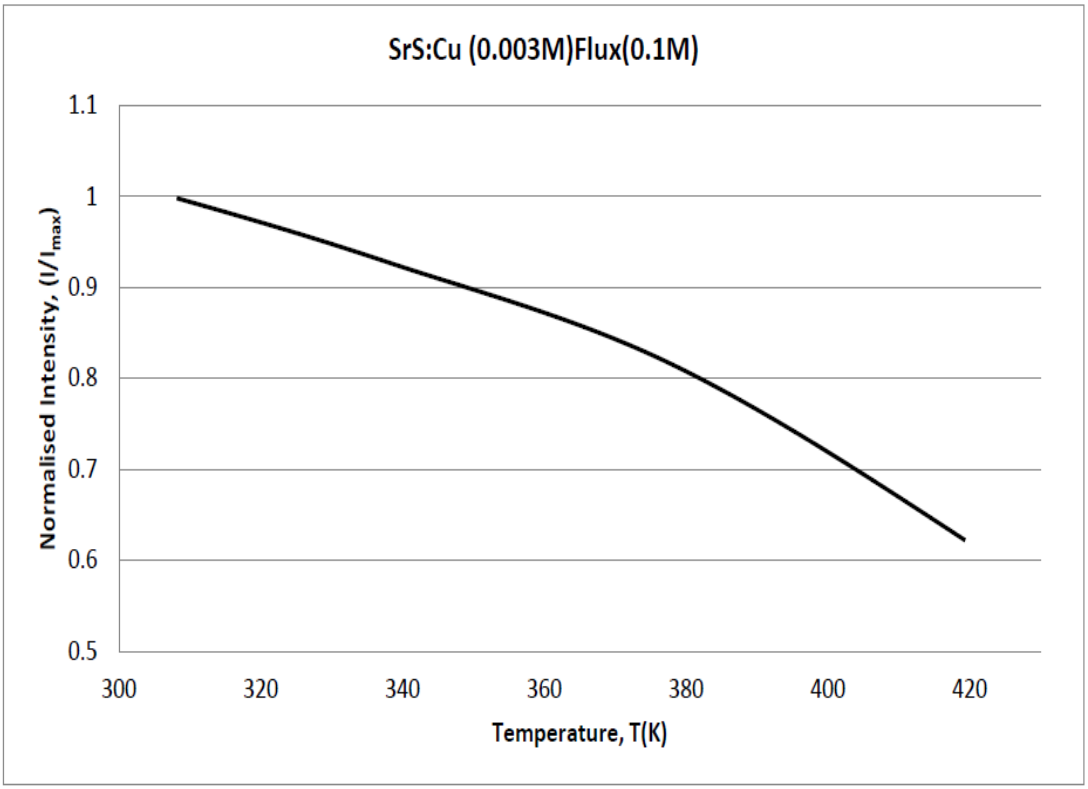

Fig: 4.8(d): Temperature dependence of fluorescence intensity of SrS:Cu(0.003M)(Flux:0.1M)

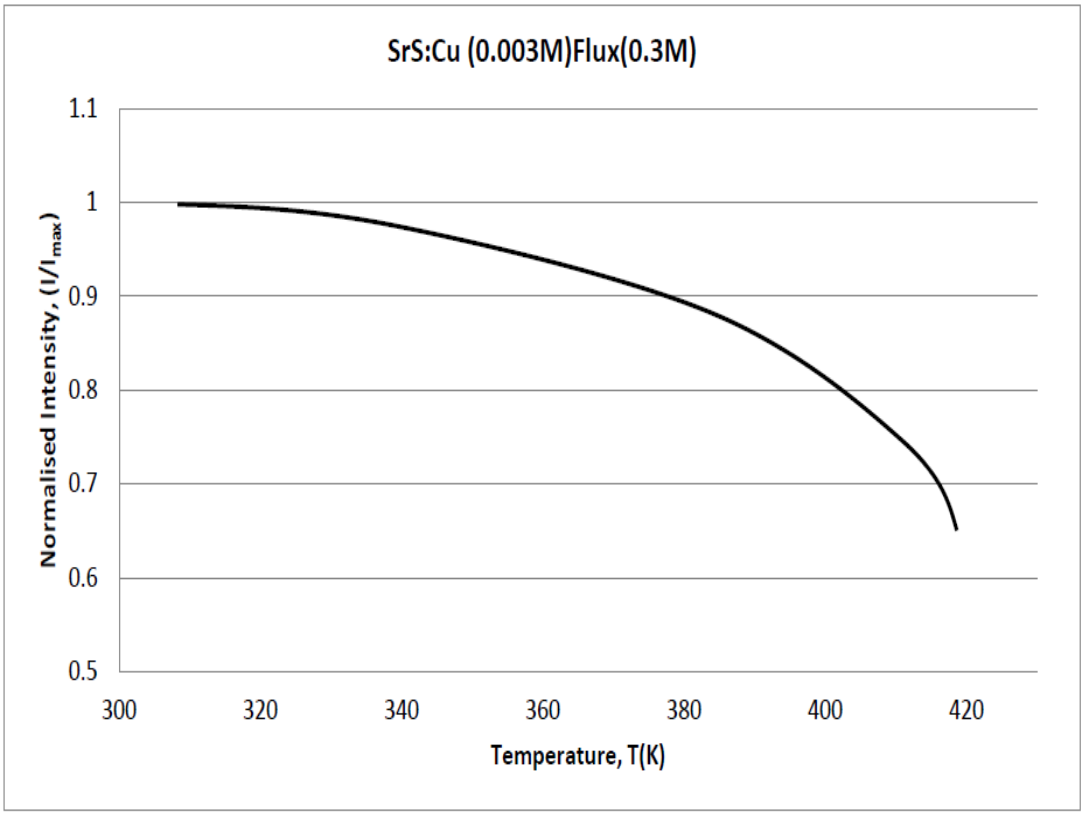

Fig: 4.8(e): Temperature dependence of fluorescence intensity of SrS:Cu(0.003M)(Flux:0.1M)

4.4.2 Calculation of different parameters

Different quenching parameters were calculated employing eqs. (4.4 to 4.7). These are tabulated in Table 4.1.

TABLE 4.1

Thermal Quenching Parameters obtained from intensity versus temperature curves

Sample	Concentration of Activator/Flux	T_B (K)		ΔT (K)	
		Theoretical	Experimental	Theoretical	Experimental
CaS:Cu (without flux)	0.002M	343	342	60	60
	0.003M	313	314	84	80
	0.005M	314	314	88	80
	0.007M	313	314	88	80
CaS:Cu (with flux)	0.003M	314	320	95	80
	0.007M	314	312	95	80
	0.009M	315	312	94	80
	0.01M	343	344	62	60
	0.02M	313	314	96	88
BaS:Cu (without flux)	0.002M	309	312	110	84
	0.003M	309	316	110	90
	0.005M	309	316	110	96
	0.007M	309	312	110	100
	0.009M	309	312	110	100
BaS:Cu (with flux)	0.005M	309	312	110	100
	0.01M	309	312	110	100
	0.015M	309	312	110	100
SrS:Cu (without flux)	0.001M	309	308	105	100
	0.002M	309	308	105	100
	0.003M	309	308	105	100
	0.005M	309	308	105	100
	0.007M	309	308	105	100

	0.009M	309	308	105	100
SrS:Cu (with flux)	0.003M	307	312	112	100
	0.007M	307	308	112	104
	0.01M	307	308	112	100
	0.02M	307	308	112	100
	0.03M	307	308	112	100

From the above table, the values of T_B and ΔT appear to be consistent for all the three types of materials. There is minor difference in the theoretical and experimental values, which is obvious considering the ideal assumptions made in the theoretical derivations. The span, ΔT, over which these materials can be used for temperature measurement, is also quite good; in CaS:Cu, it is around 80 K and in BaS and SrS, it is around 100 K. In conclusion, the temperature dependence of fluorescence of alkaline earth sulphides doped with copper may be used for measurement of temperature of hot surfaces in this temperature range.

References

[1] S.W. Allison, G.T. Gillies, *Rev. Sci. Instrum*. **68**, 2615 (1997)

[2] S.W. Allison, M.R. Cates, B.W. Noel, G.T. Gillies, *IEEE Trans. Instrum. Meas.* **37**, 637 (1988)

[3] K.W. Tobin, S.W. Allison, M.R. Cates, G.J. Capps, D.L. Beshears, M. Cyr, B.W. Noel, *Am. Inst. Aeronaut. Astronaut. J.* **28**, 1485 (1990)

[4] B.W. Noel, H.M. Borella, W. Lewis, W.D. Turley, D.L. Beshears, G.J. Capps, M.R. Cates, J.D. Muhs, K.W. Tobin, *Trans. ASME* **113**, 242 (1991)

[5] A. Omrane, F. Ossler, M. Ald´en, U. Görannson, G. Holmstedt, *Proc. 7th Int. Symp. in Fire Safety Sci.* (2002), p. 141–152

[6] J.P. Feist, A.L. Heyes, S. Seefelt, *Proc. Inst. Mech. Eng*. **217**, 193 (2003)

[7] A. Omrane, F. Ossler, M. Ald´en, J. Svenson, J.B.C. Pettersson, *Fire Mater.* **29**, 39 (2005)

[8] B. A. Baukol, J. C. Hitt, P. D. Keir and J. F. Wager, *Appl. Phys. Lett.* **76,** 185 (2000).

[9] N. E. Karsunskaya, T. V. Torchinskaya, B. R. Dzhumaev, B. R. Khomenkova, I. Yu, B. M. Bulakh, A. Many, Y. Goldstein, E. Savir, *Semiconductor conference*, **2,** 511 (2000).

[10] R. P. Khare, A. Subodh, and S. Geetha, *J. Opt*., **30**, 29, (2001).

[11] D. C. Morton, E. W. Forsythe, S. S. Sun, M. C. Wood, M. H. Ervin and K. Kirchner, *Appl. Phys. Lett.* **78**, 1400, (2001).

[12] M. Gaft, R. Reisfeld, G. Panczer, G. Boulon, T. Saraidarov, S. Erlish, *Opt. Mater*., **16,** 279 (2001).

[13] B. L. Abrams, L. Williams, J. S. Bang, P. H. Holloway, *J. Electrochem. Soc.* **150,** H105 (2003).

[14] J. C. Lee, D. H. Park, *Mater. Lett.*, **57,** 2872 (2003).

[15] J. M. Fitzgerald, J. G. Hoekstra, R. K. Bansal, J. D. Fowlkes, P. D. Rack, *Mat. Res. Soc. Symp. Proc.*, **780,** Y1.4.1, (2003).

[16] P. F. Smet, J. V. Gheluwe, D. Poleman, R. L. V. Meirhaeghe, *J. Lumin.* **104,** 145 (2003).

[17] P. F. Smet, I. Moreels, Z. Hens and D. Poelman, *Materials*, **3**, 2834 (2010).

[18] D Curie, "Luminescence in Crystals", Methuen & Co. Lt., New York (1963).

[19] H. A. Klasens, *J. Phys. Chem. Solids*, **9,** 185 (1959).

[20] F. A. Kroger, "*Some aspects of luminescence of solids*", Elsevier, Amsterdam, (1948).

[21] M. M. Mishra and D. Sharma, *Indian J. Pure Appl. Phys.* **17,** 419 (1979).

Chapter 5

Temperature Dependence of Phosphorescent Lifetime

5.1 Introduction

It is well known that photoluminescence exhibits in two different forms, namely, fluorescence and phosphorescence. While fluorescence has very short lifetimes (typically on the order of nanoseconds), phosphorescence usually has much longer time and may last from microseconds to minutes and even hours. Since the lifetime of phosphorescence decay of some substances is dependent on temperature, it can be used for the measurement of temperature. Therefore, the study of variation of phosphorescent lifetime of the synthesized materials with temperature was undertaken in the present work.

5.2 Theory of decay of phosphorescence

According to quantum theory [1], the intensity of decay of phosphorescence process can be expressed in the form

$$I = I_0 e^{-t/\tau} \qquad (5.1)$$

Where the lifetime τ refers to the time when the intensity drops to 37% (i.e. 1/e) of the initial intensity I_0 at t = 0.

For an excited state, the deactivation process may involve both radiative and non-radiative pathways. The lifetime of the phosphorescence process τ, is determined by the sum of all deactivation rates:

$$\tau^{-1} = k_r + k_{nr} \qquad (5.2)$$

where k_r and k_{nr} are the radiative and non-radiative rate constants, respectively. These rate constants are, in general, dependent on temperature [2, 3] and, in general, give rise to thermal quenching of lifetime. Such a thermal quenching has been reported by many investigators [4-7]. This basis has been used for exploring the temperature dependence of phosphorescence of the synthesized materials in the present investigation.

5.3 Experimental setup

The experimental setup used for studying the temperature dependence of phosphorescence is the same (as shown in Fig 4.2) and is reproduced below as Fig 5.1 for convenience of discussion.

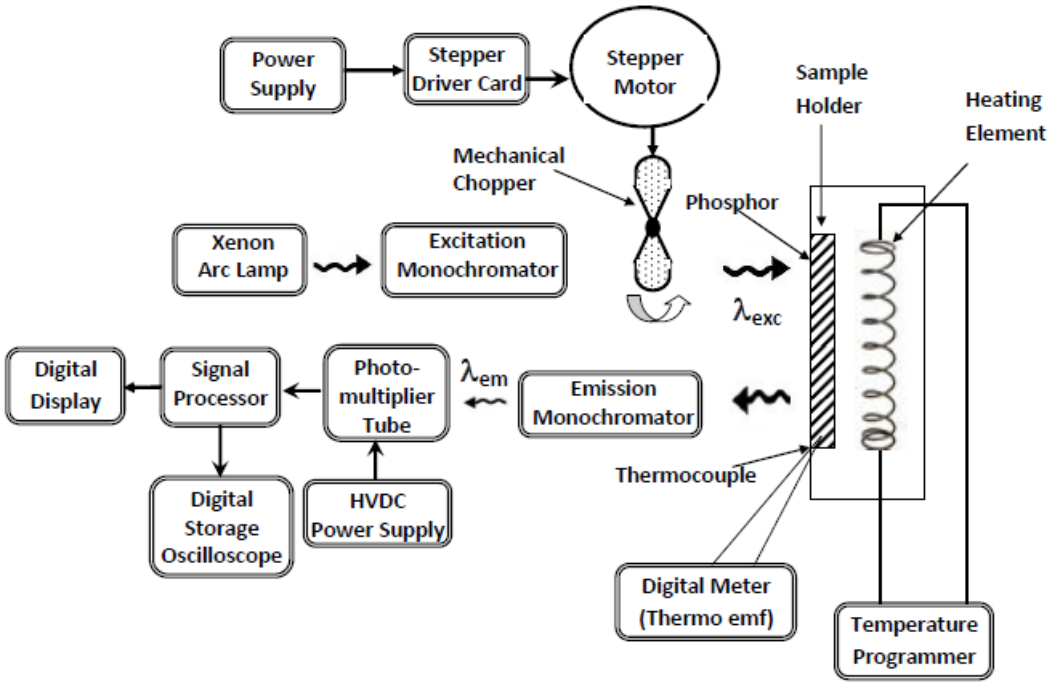

Fig. 5.1: Experimental Setup

The Xenon arc lamp followed by the excitation monochromator provides the excitation wavelength (λ_{exc}). The excitation beam falling on the sample is chopped by the mechanical chopper. The chopper frequency is adjusted, using a stepper motor and stepper driver card, according to the lifetime of phosphorescence. The resultant phosphorescence decay time is detected by the emission monochromator and PMT combination. The signal is recorded by the digital storage oscilloscope. Such decay patterns are recorded at different temperatures. The temperature variation is achieved using a heating element in the sample holder whose temperature is controlled by a temperature controller. Thermocouple is used for measuring the temperature.

5.4 Results:

Variation of Lifetime of Phosphorescence as a Function of Temperature:

At λ_{max}, with pulsed excitation the decay of phosphorescence was recorded at different temperatures for all the phosphors. A few typical records of rise and decay of phosphorescence at different temperatures are shown in Fig. 5.2.

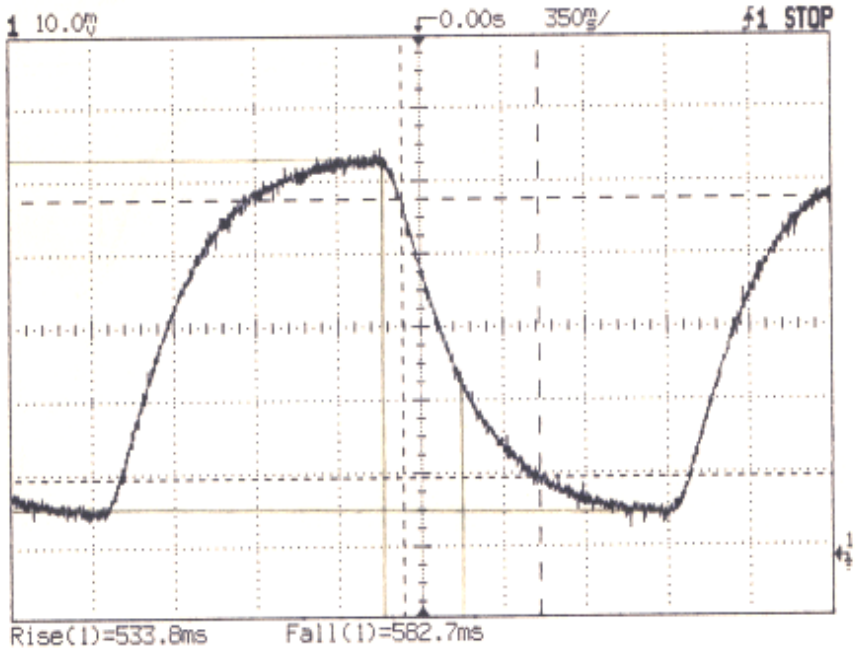

Fig. 5.2 (a): Record of rise and decay of phosphorescence of SrS:Cu (With flux) at RT

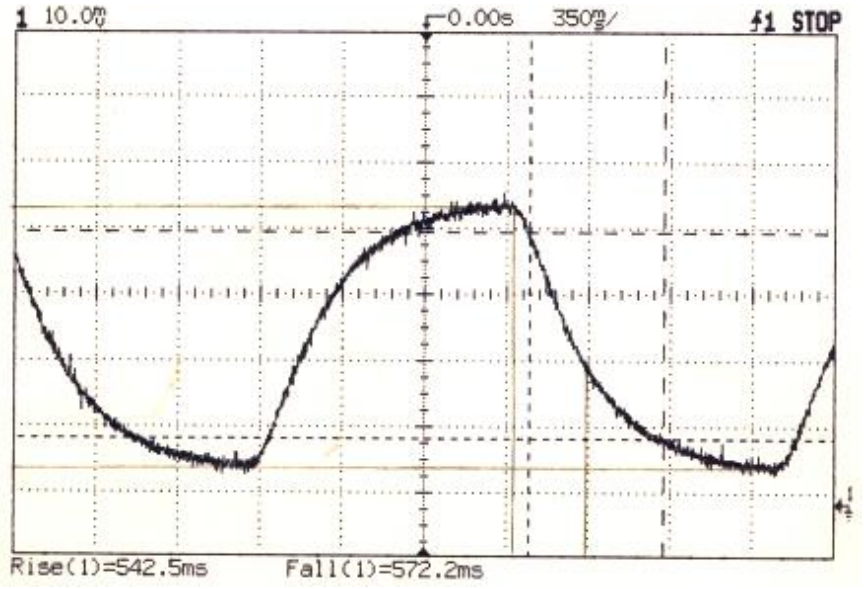

Fig. 5.2 (b): Record of rise and decay of phosphorescence of SrS:Cu (With flux) at 80℃

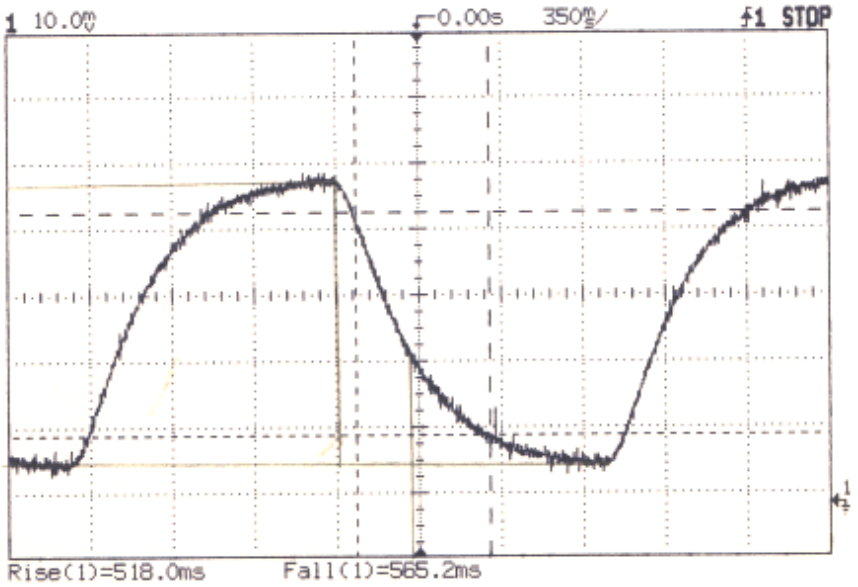

Fig. 5.2 (c): Record of rise and decay of phosphorescence of SrS:Cu (With flux) at 107.2℃

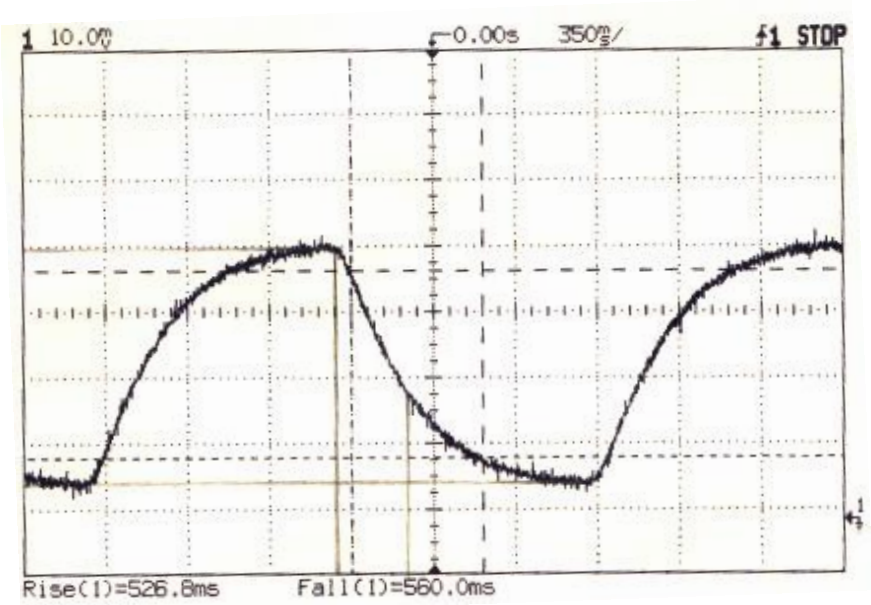

Fig. 5.2 (d): Record of rise and decay of phosphorescence of SrS:Cu (With flux) at 140°C

From such records, the lifetime of phosphorescence at different temperature was determined using eq. 5.1. The variation of lifetime as a function of temperature is shown in Fig 5.3 for CaS:Cu, Fig 5.4 for BaS:Cu and Fig 5.5 for SrS:Cu.

CaS:Cu (without flux)

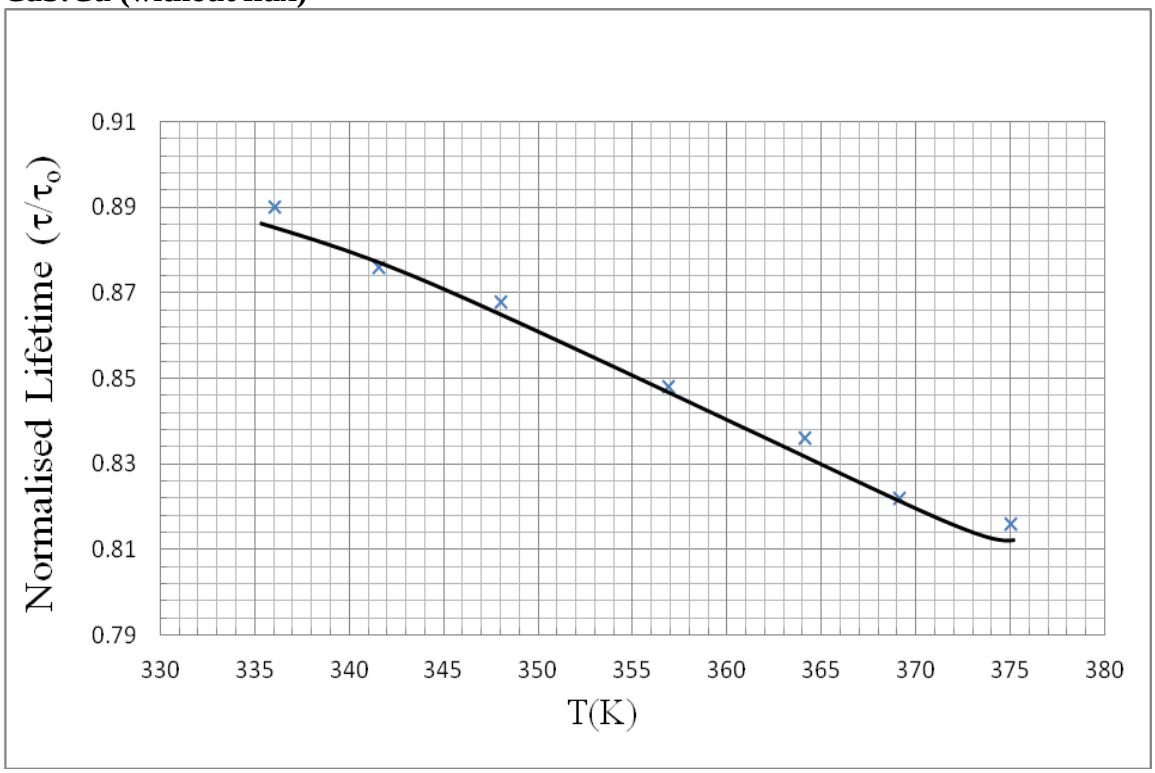

Fig. 5.3 (a) Variation of lifetime with temperature of CaS:Cu (0.003M) (without flux)

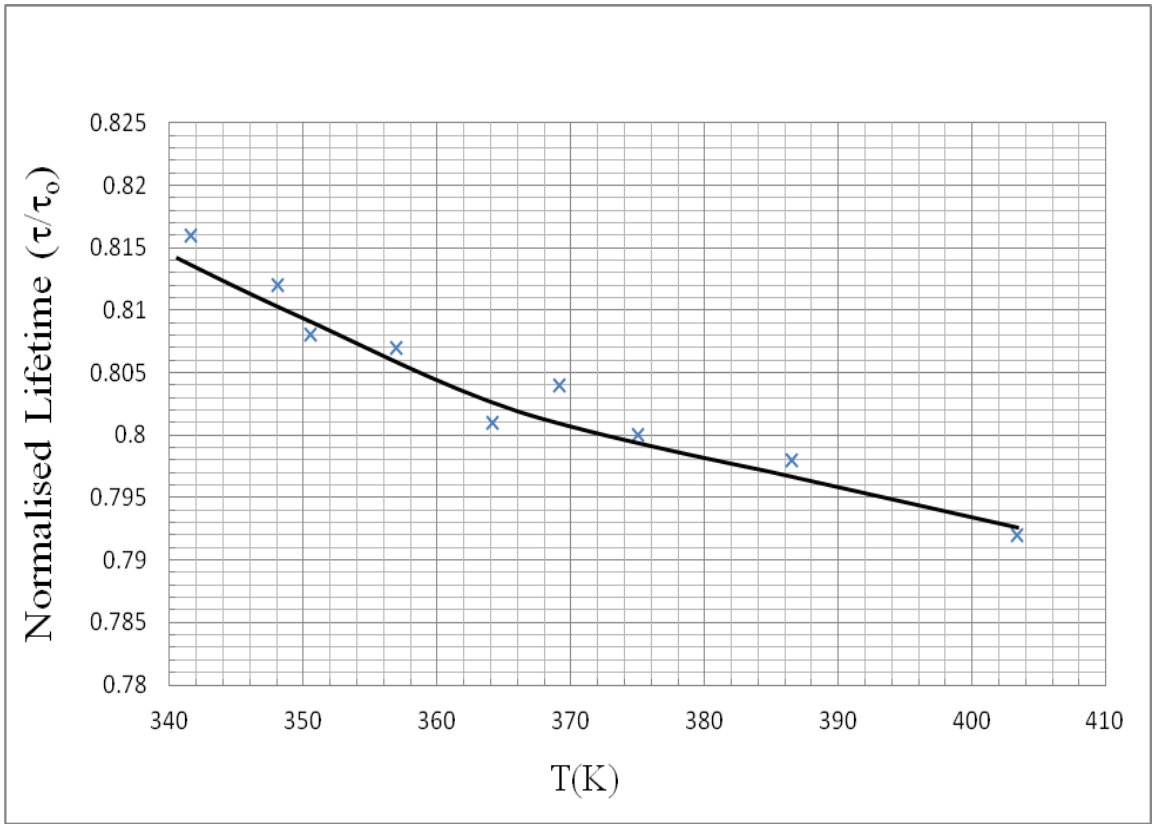

Fig. 5.3 (b) Variation of lifetime with temperature of CaS:Cu (0.005M) (without flux)

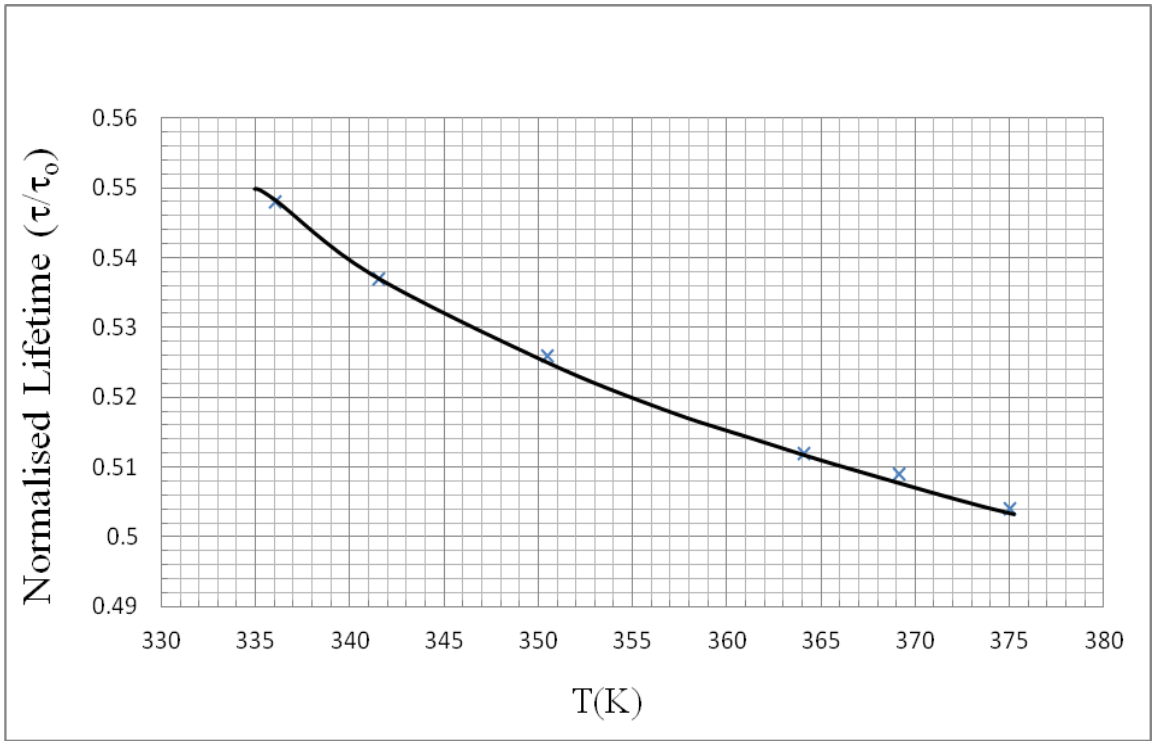

Fig. 5.3(c) Variation of lifetime with temperature of CaS:Cu (0.009M) (without flux)

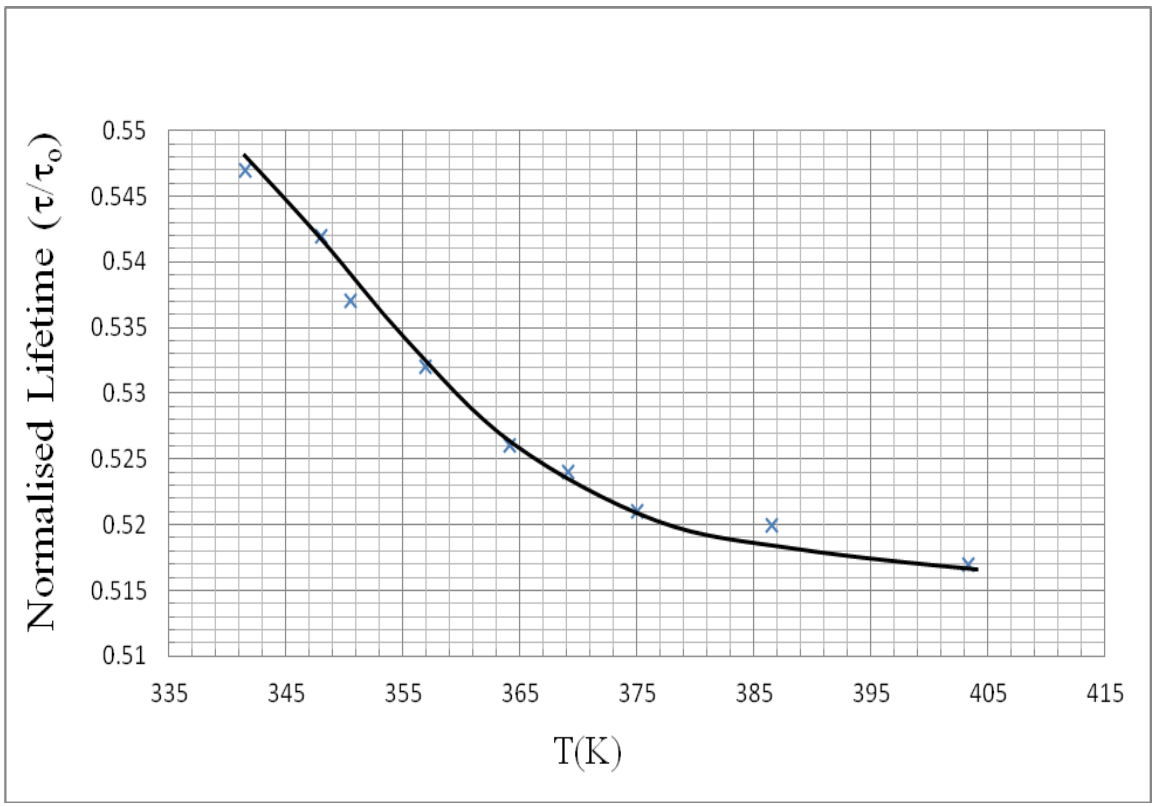

Fig. 5.3(d) Variation of lifetime with temperature of CaS:Cu (0.01M) (without flux)

CaS:Cu (with flux)

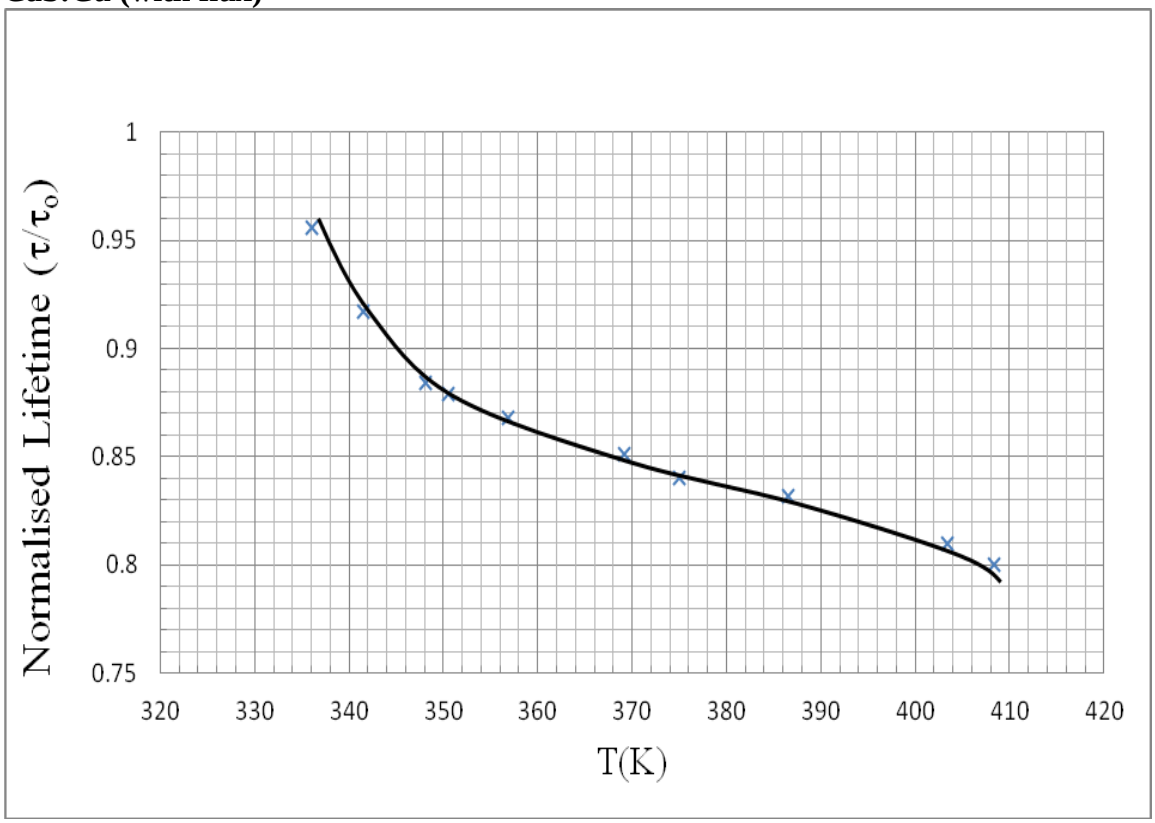

Fig. 5.3 (e) Variation of lifetime with temperature of CaS:Cu(0.003M)(Flux:0.003M)

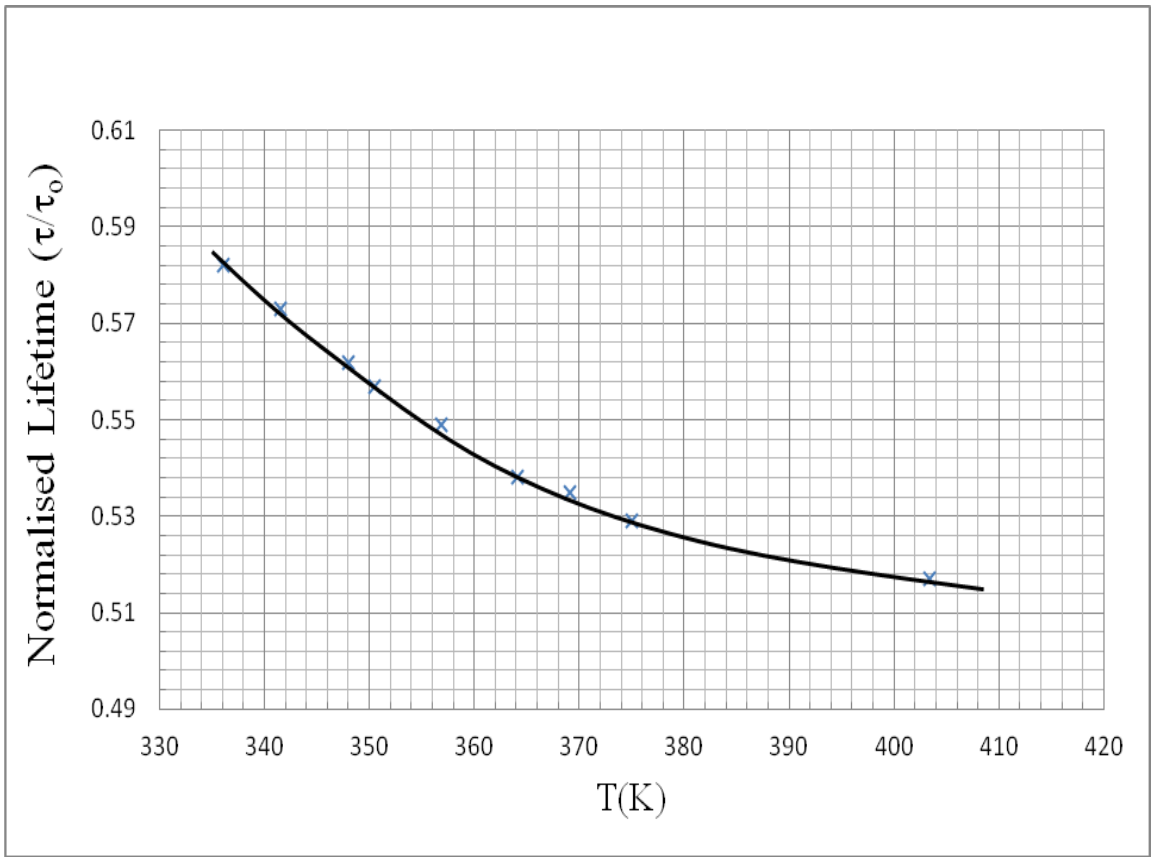

Fig. 5.3 (f) Variation of lifetime with temperature of CaS:Cu (0.003M)(Flux:0.005M)

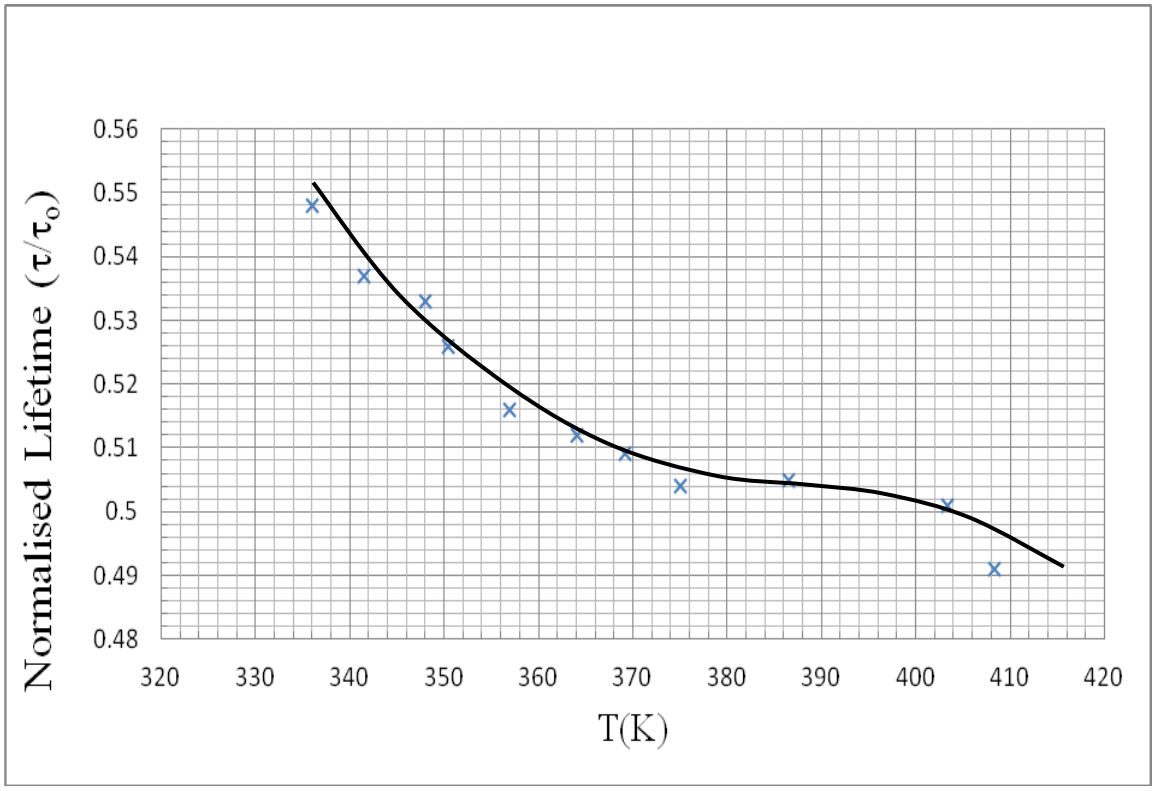

Fig. 5.3 (g) Variation of lifetime with temperature of CaS:Cu (0.003M)(Flux:0.01M)

BaS:Cu (without flux)

`

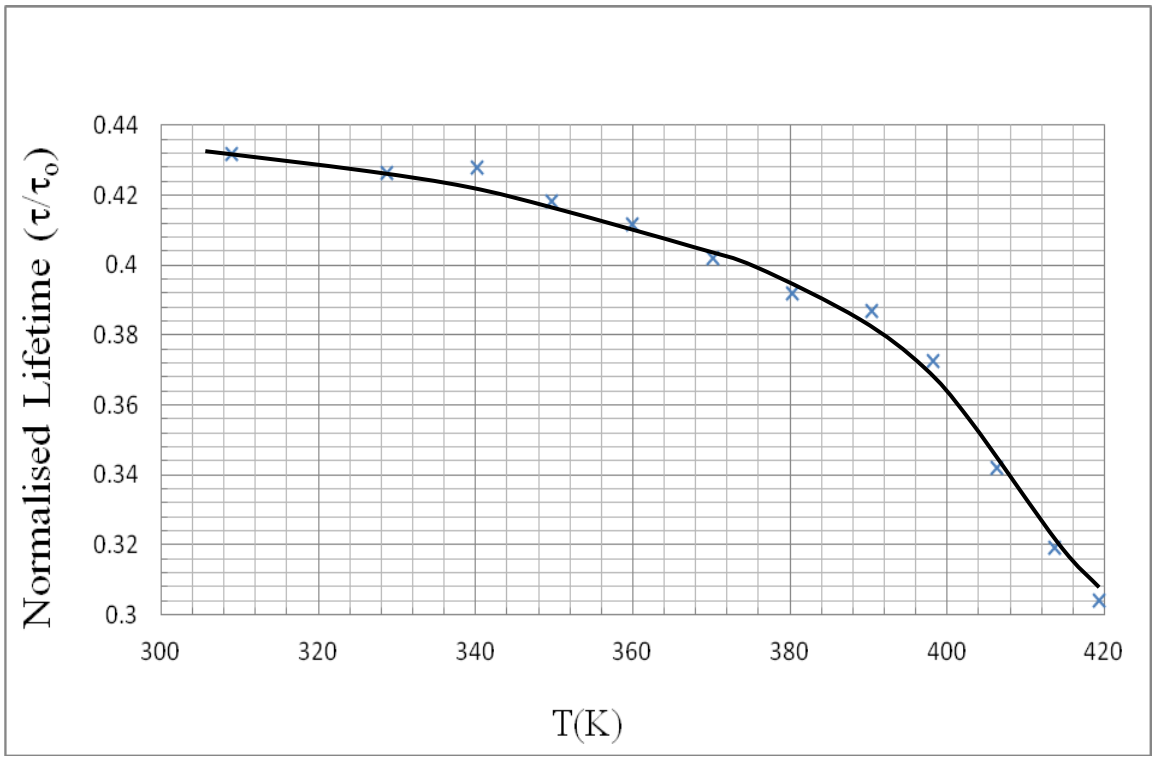

Fig. 5.4 (a) Variation of lifetime with temperature of BaS:Cu (0.001M) (without flux)

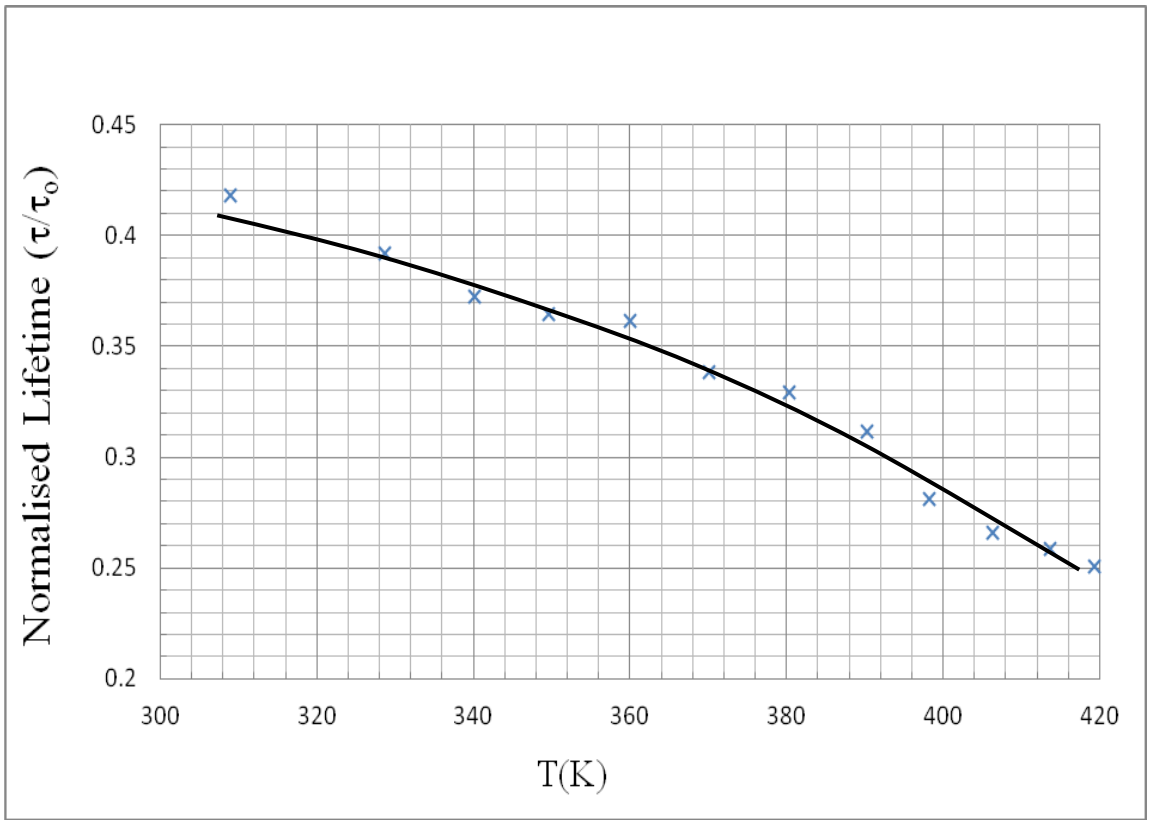

Fig. 5.4 (b) Variation of lifetime with temperature of BaS:Cu (0.002M) (without flux)

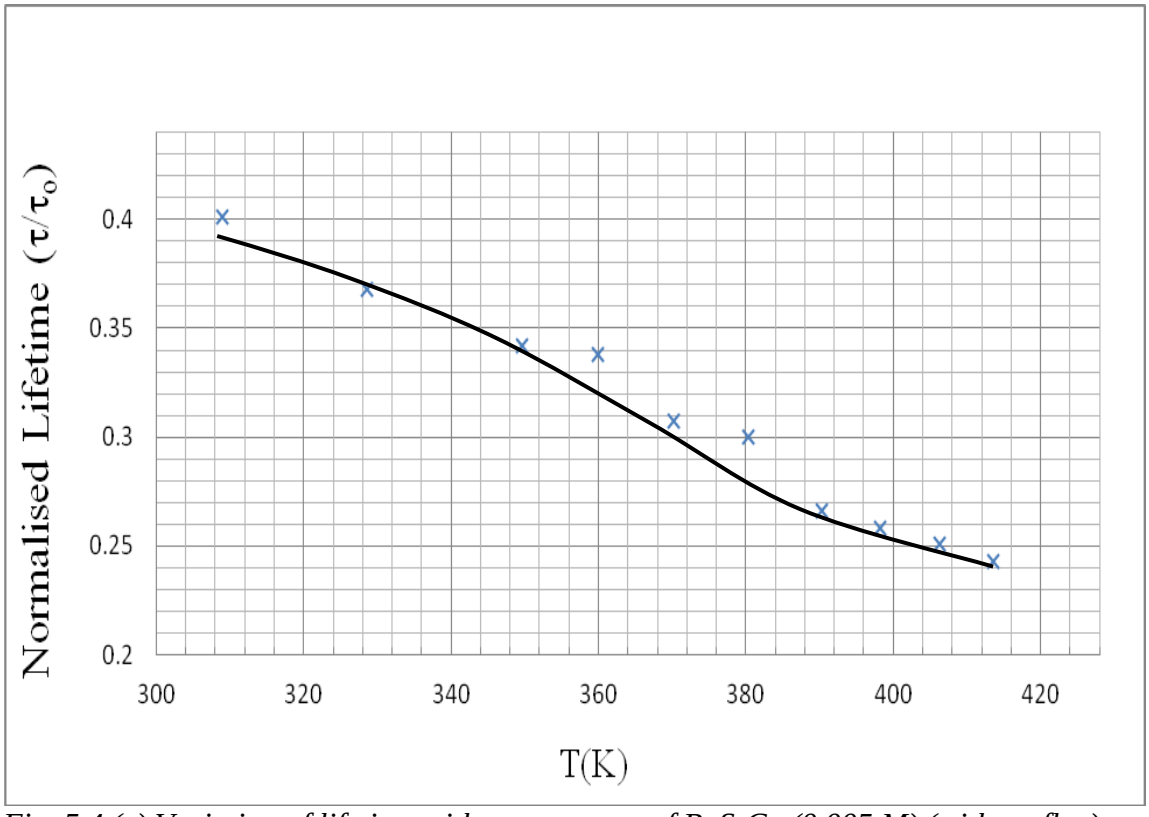

Fig. 5.4 (c) Variation of lifetime with temperature of BaS:Cu (0.005 M) (without flux)

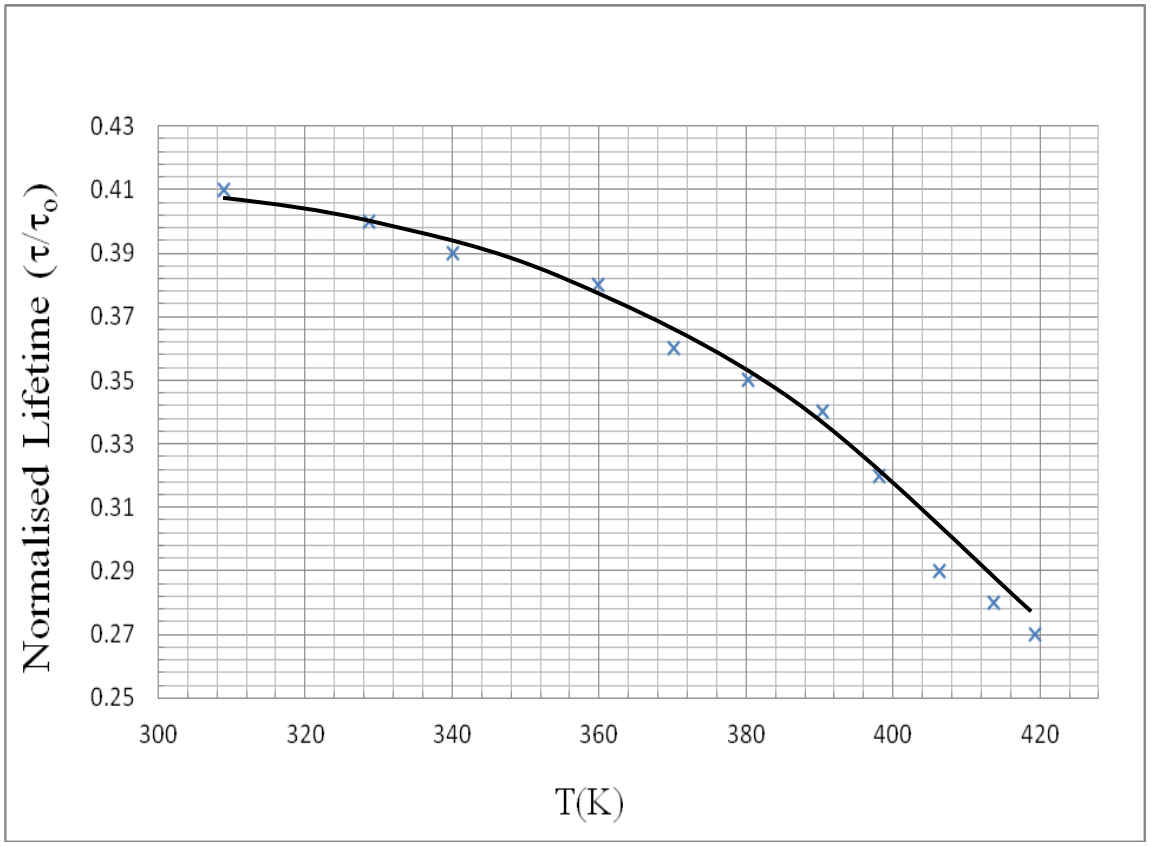

Fig. 5.4 (d) Variation of lifetime with temperature of BaS:Cu (0.007M) (without flux)

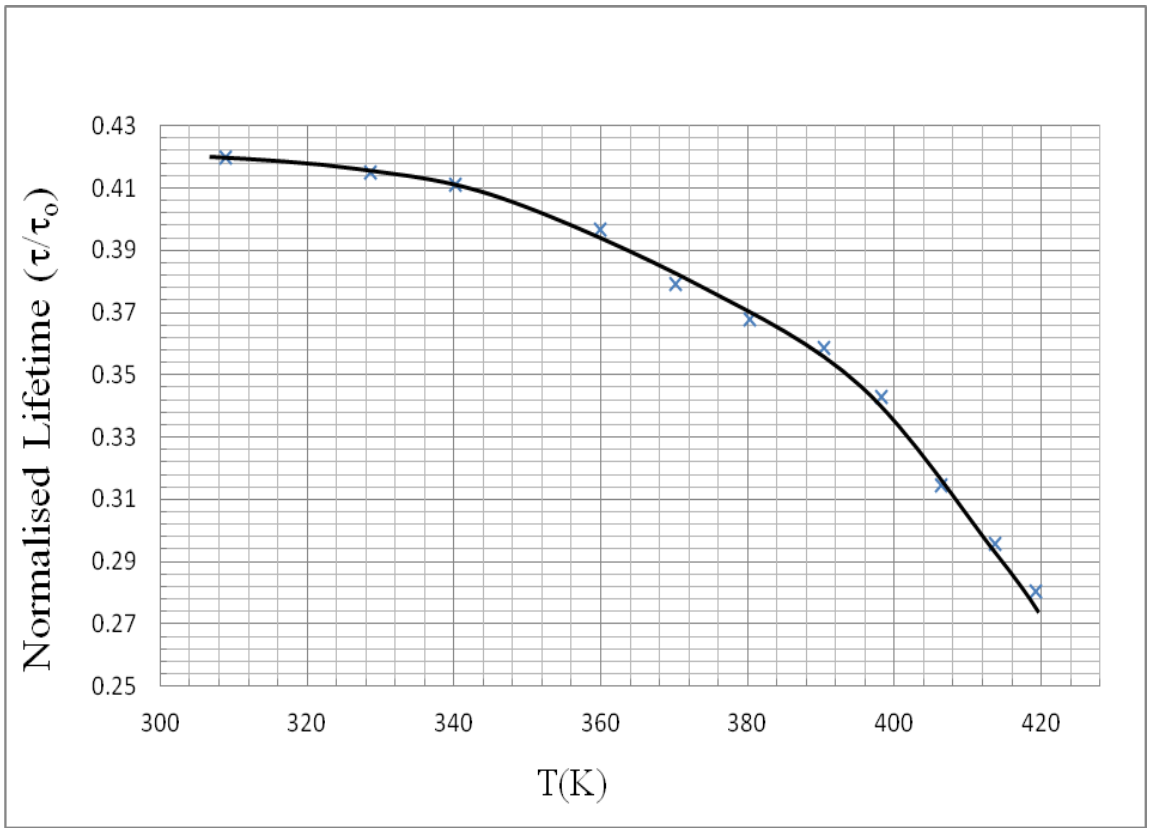

Fig. 5.4 (e) Variation of lifetime with temperature of BaS:Cu (0.009M) (without flux)

BaS:Cu (with flux)

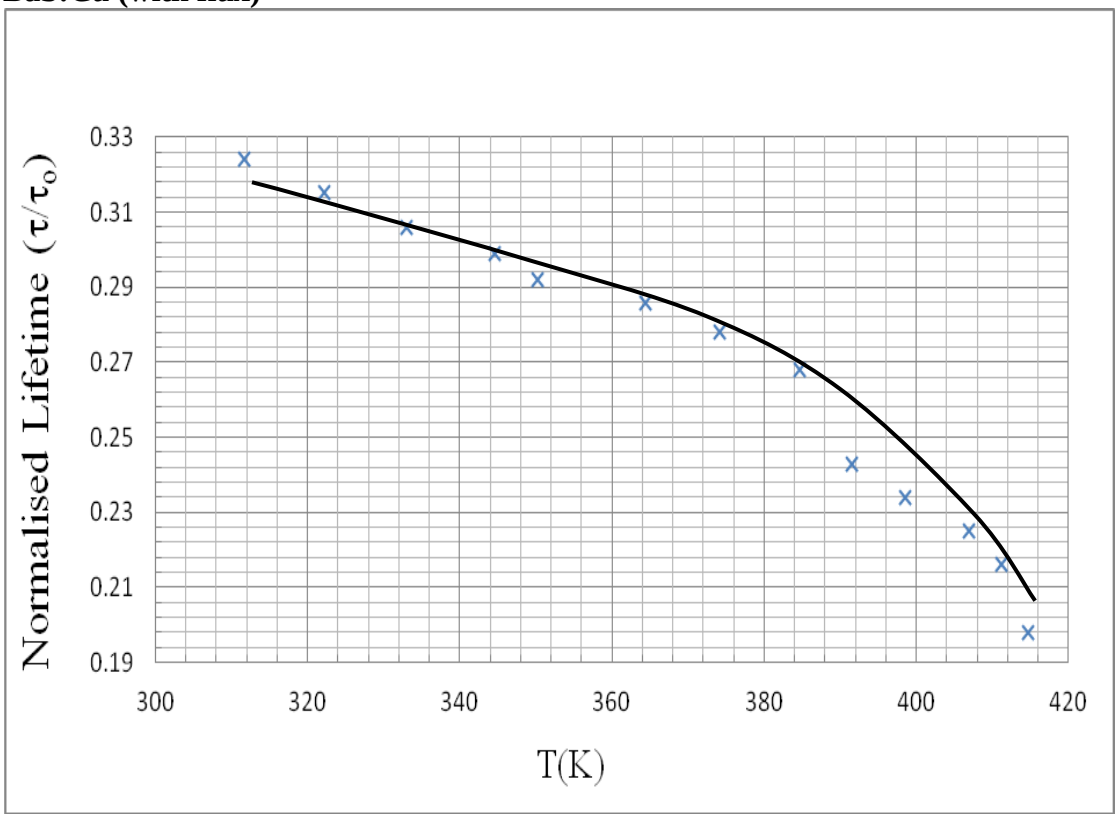

Fig. 5.4 (f) Variation of lifetime with temperature of BaS:Cu (0.001M) (Flux:0.01M)

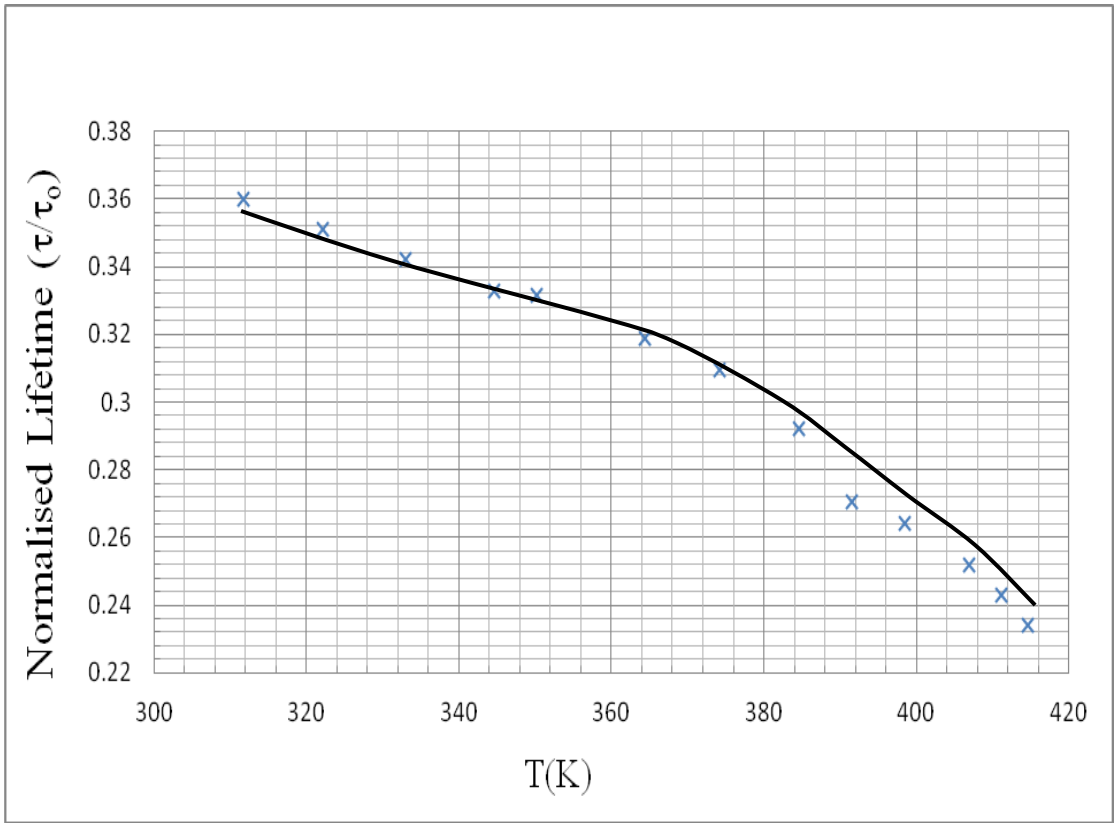

Fig. 5.4 (g) Variation of lifetime with temperature of BaS:Cu(0.001M)(Flux:0.015M)

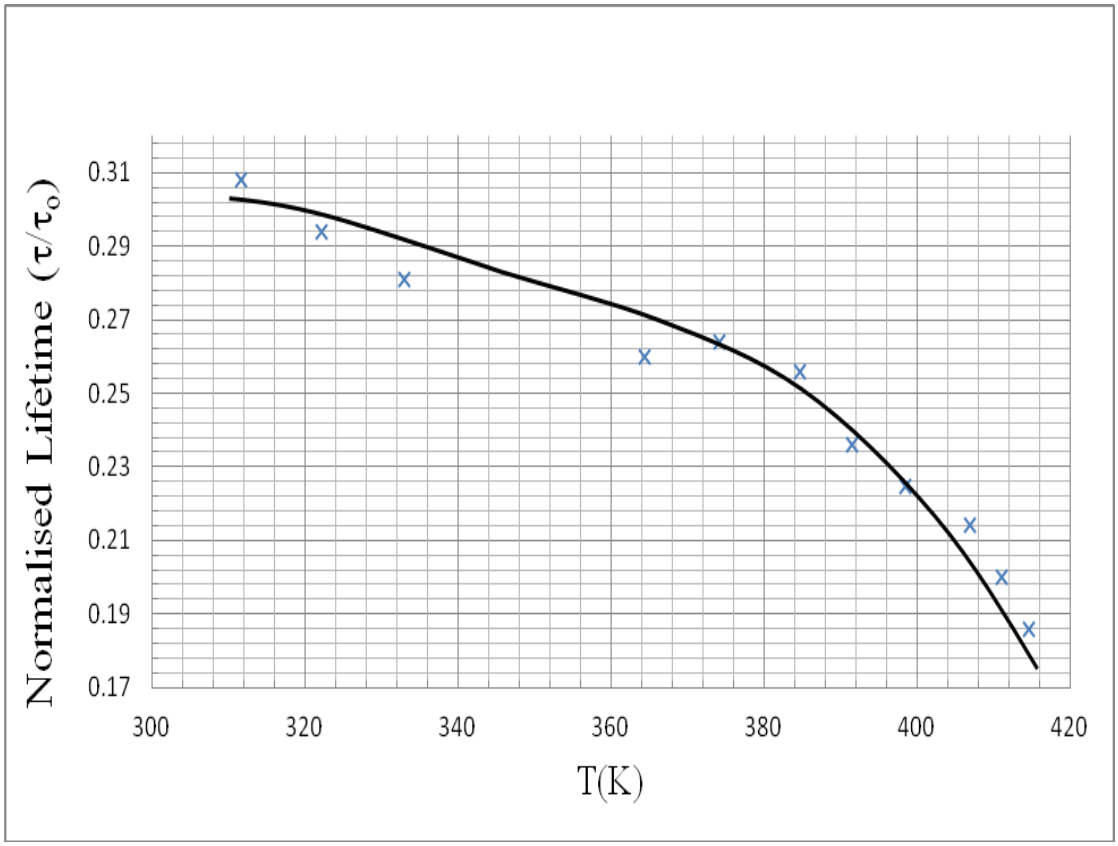

Fig. 5.4 (h) Variation of lifetime with temperature of BaS:Cu (0.001M)(Flux:0.005M)

SrS:Cu (without flux)

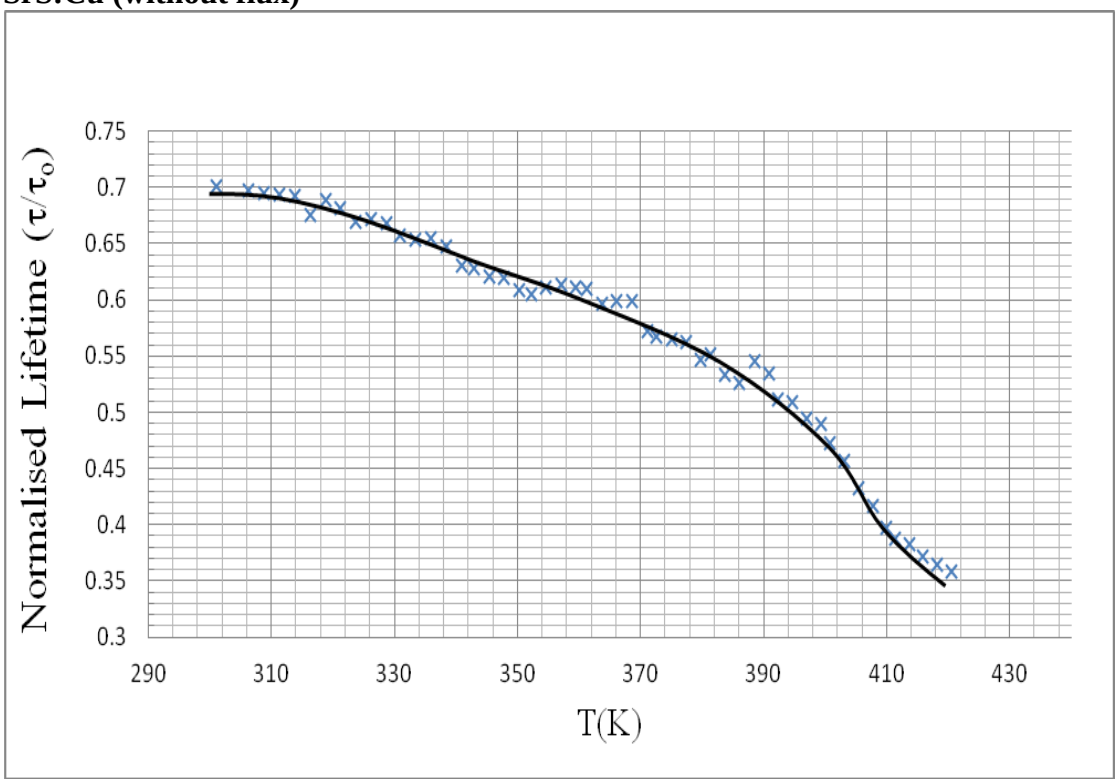

Fig. 5.5 (a) Variation of lifetime with temperature of SrS:Cu (0.001M)(without flux)

SrS:Cu (with flux)

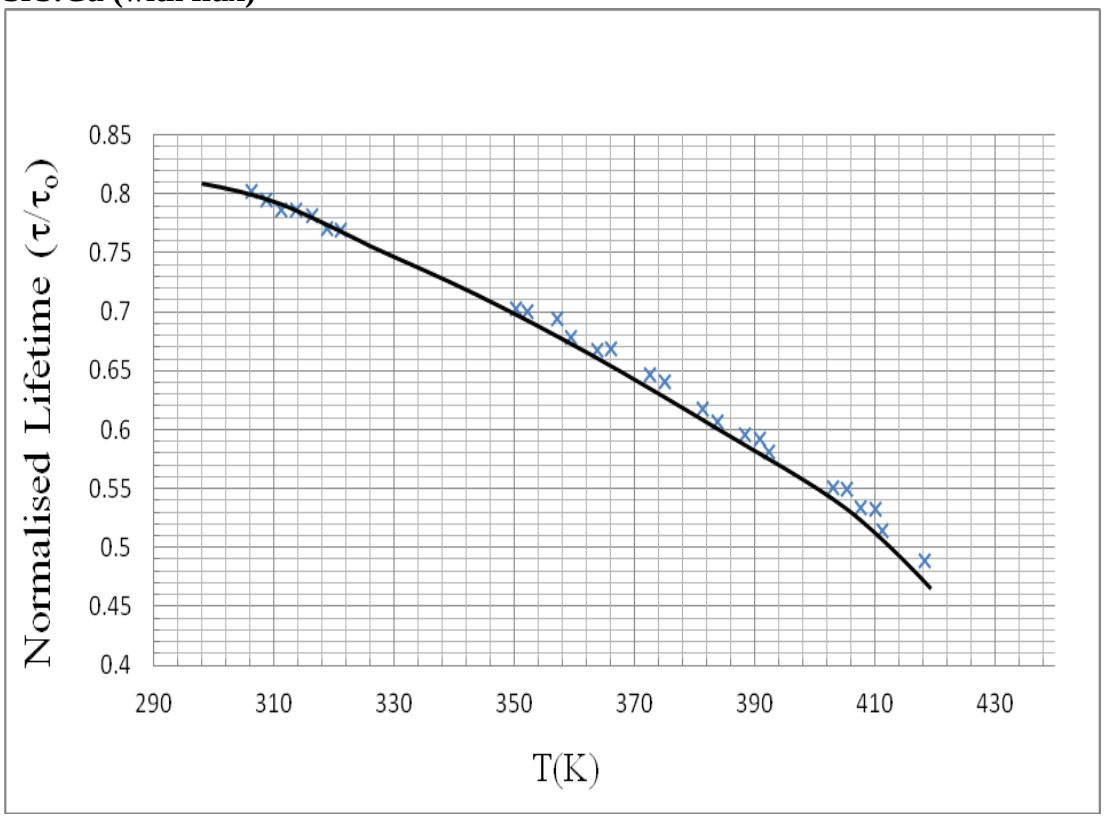

Fig. 5.5 (b) Variation of lifetime with temperature of SrS:Cu (0.003M)(without flux)

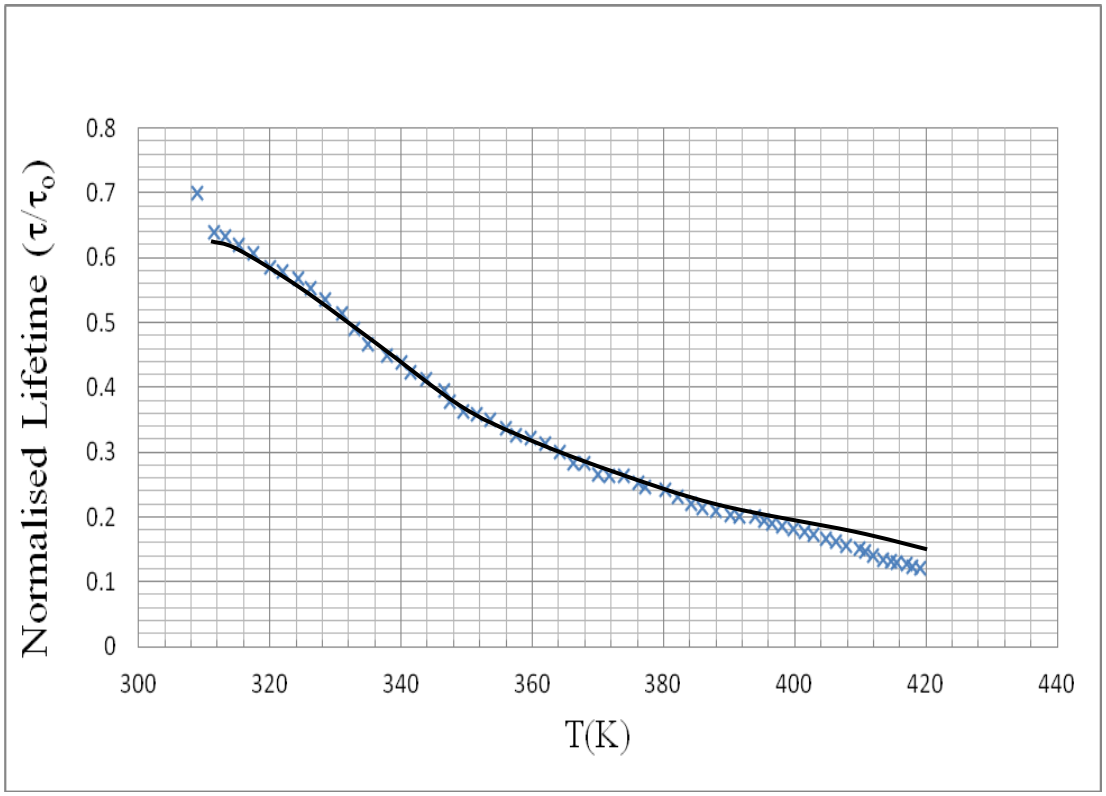

Fig. 5.5 (c) Variation of lifetime with temperature of SrS:Cu (0.003M)(Flux:0.001M)

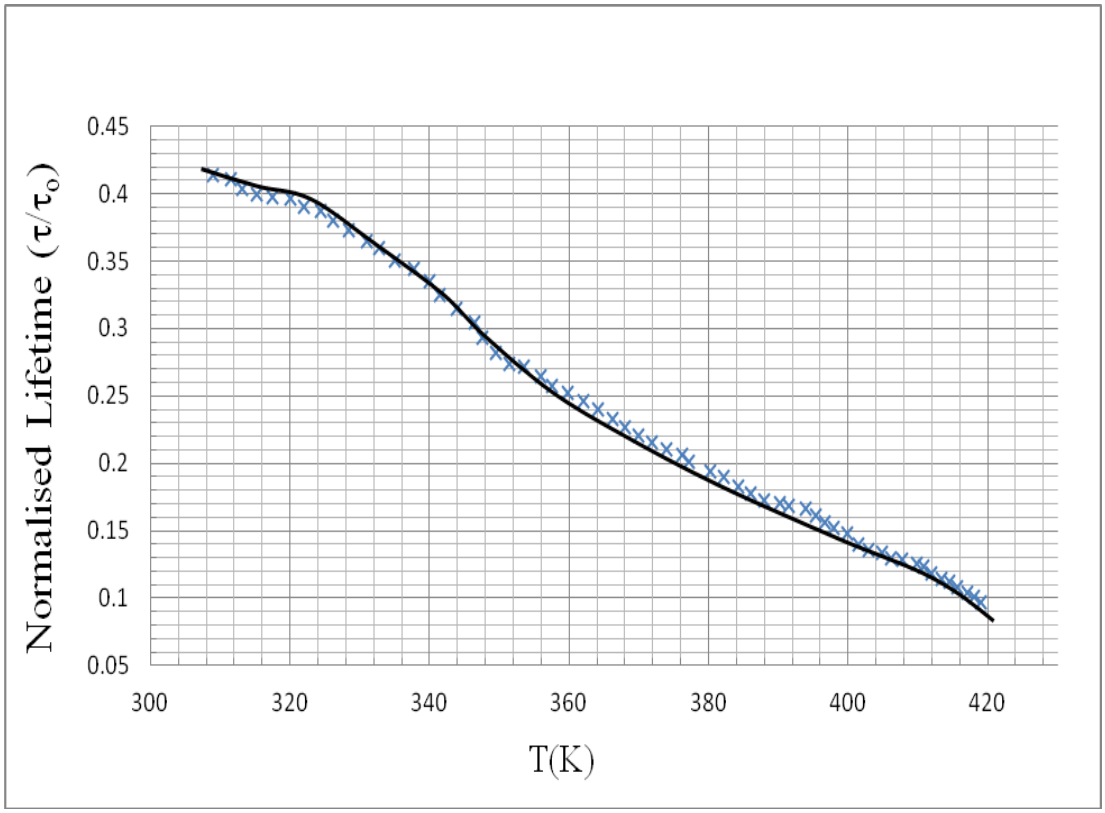

Fig. 5.5 (d) Variation of lifetime with temperature of SrS:Cu (0.003M)(Flux:0.002 M)

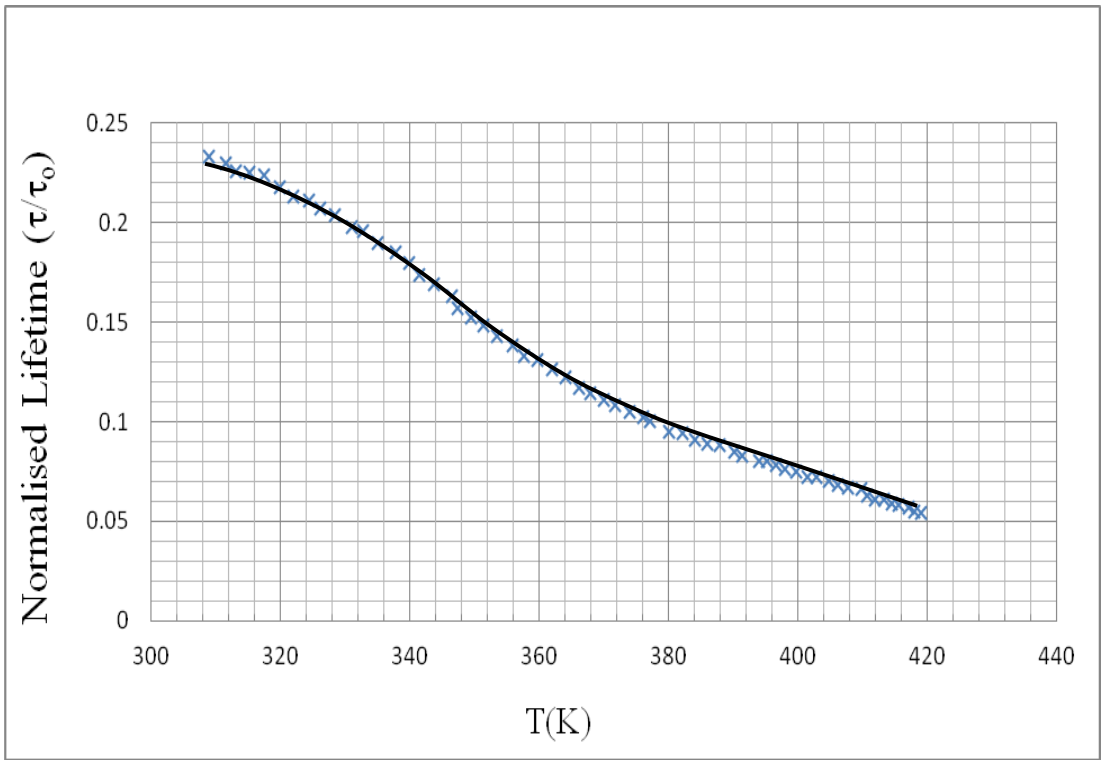

Fig. 5.5 (e) Variation of lifetime with temperature of SrS:Cu (0.003M)(Flux :0.003 M)

We utilized these experimental curves to assess approximate values of T_B and ΔT. These are listed in Table 5.1.

Table 5.1: Thermal quenching parameters of different phosphors as obtained from lifetime variation with temperature

Sample	Concentration of Activator/Flux(M)	T_B (K)	ΔT (K)
CaS:Cu (without flux)	0.003	335	40
	0.005	335	40
	0.009	340	44
	0.01	341	40
CaS:Cu(with flux)	0.003	336	60
	0.005	336	--
	0.01	336	60
BaS:Cu(without flux)	0.001	308	100
	0.002	308	100
	0.005	308	100
	0.007	308	100
	0.009	308	100
BaS:Cu(with flux)	0.01	312	80
	0.015	312	80
	0.005	312	80
SrS:Cu(without flux)	0.001	302	100
	0.003	302	100
SrS:Cu(with flux)	0.001	312	80
	0.002	312	80
	0.003	312	80

It is evident from this table that the values of T_B and ΔT are very consistent for different phosphors. The span is good for BaS and SrS phosphors, whereas it is poor for CaS. Hence if the variation of lifetime of phosphorescence is to be used for measuring the temperature in this temperature range, BaS:Cu and SrS:Cu are good candidates. The variation of lifetime with temperature is also almost linear for these two systems of phosphors.

References

[1] P. Pringsheim: *Fluorescence and Phosphorescence*, Interscience Publishers Inc, New York (1949)

[2] G. J. Ferraudi: *Elements of Inorganic Photochemistry*, Wiley-Interscience, New York, (1988)

[3] S. Shionoya and W. M.Yen: *Phosphor handbook*. Boca Raton: CRC Press (1999)

[4] V. K. Rai, *IEEE Sensors Journal* **7**, 1110 (2007)

[5] M.D. Chambers et al., *Annual Review of Materials Research* **39**, 325 (2009)

[6] B G Koziol et al., *Journal of Optics* **12**, 015407 (2010)

[7] Marko G. Nikolić et al., *Applied Optics* **52**, 1716 (2013)

Chapter 6

Discussion and Conclusions

6.1 Introduction:

To recall, the aim of present investigation is to synthesize alkaline earth sulphide phosphors activated by copper and study their fluoro-optic behavior to assess their suitability for thermographic / thermometric applications.

This chapter is devoted to the discussion of all the results obtained through different studies of the synthesized materials. Some inferences have already been drawn and reported in the chapters dealing with specific investigations. Here an attempt has been made to summarize, correlate and discuss these results and judge the suitability of these materials for aimed applications.

6.2 Thermographic phosphors are better alternatives to common techniques for surface thermometry

Common techniques for surface thermometry are invasive thermocouples, non-invasive pyrometry as well as semi-invasive coatings of thermochromic liquid crystals, temperature sensitive paints, thermal paints or thermographic phosphors. The employment of thermocouples requires little effort. However, the presence of these invasive probes and their connections do often have a strong impact on the thermal state of the surface temperature and the entire device under test. The spatial and temporal resolution as well as the feasibilities of probe volume displacement or two-dimensional temperature imaging are strongly limited. Most often wiring is necessary, which is crucial regarding moving systems such as pistons in engines or rotors in gas turbines. Two-dimensional temperature maps can be visualized with very high temporal and spatial resolution using non-invasive pyrometry. However, accurate pyrometry requires exact knowledge about the emissivity of the surface. The emissivity, in turn depends on the wavelength, the detection angle and the surface properties of the device under test, which might even change during operation. Moreover, all interfering light e.g. from soot radiation or chemiluminescence is a further source of error, which is crucial particularly

in combustion environments. Therefore, in many cases pyrometry suffers from poor accuracy.

Semi-invasive diagnostics based on organic temperature-sensitive coatings such as thermochromic liquid crystals [1-2] or temperature sensitive paints [3] are generally limited to lower temperatures. In contrast to this, thermal paints (also termed as heat sensitive paints) are inappropriate for time-resolved measurements. They only allow an estimation of the peak temperature, which is indicated by an irreversible colour change of the paint [1,4].

Thermographic phosphors offer semi-invasive surface thermometry with high spatial and temporal [5] resolution over a broad temperature range from cryogenic temperatures [6,7] up to 1970 K [8]. The method is rather insensitive to the properties of the surface and robust against interferences from scattered light, chemiluminescence or soot radiation. Provided careful handling, its accuracy is better than 1%. Since phosphor thermometry needs to be calibrated against a temperature standard (most often a thermocouple), its accuracy is limited by this reference. However, phosphor thermometry overcomes many drawbacks of its temperature reference, since it is calibrated in a temporally and spatially homogeneous environment and then transfers its accuracy to a semi-invasive remote thermometry system with high spatial and temporal resolution.

In chapter 1, we have already discussed that there are several parameters of luminescence of some specific phosphors that have been used for remote as well as direct measurement of temperature of both static and moving objects. However, the number of such phosphors, which satisfy the requirement of linearity of response, stability and ease of synthesis, are very few. Therefore, there is a need to investigate more materials for this application. In this context, copper activated alkaline earth sulphides seem to be promising candidates as these phosphors can be easily synthesized, they are quite stable over long period of time (ten to fifteen years), if protected from moisture and their luminescence is sensitive to temperature. Therefore, the present system of phosphors was taken up for investigation.

6.3 Spectral characteristics of present system of phosphors at RT:

At room temperature (RT), the excitation spectra of CaS:Cu phosphors reveals that, in all the samples, the peak is around 310 nm and the emission spectra shows that its peak is around 480 nm. Addition of flux gives rise to two excitation peaks, one at 310 nm and second, at 345 nm. But the emission peak remains at 480 nm. The intensity, of course, changes with the concentration of Cu or flux.

In the case of BaS:Cu phosphors, two peaks around 340 nm and 410 nm are observed in the excitation spectra in all the samples. The emission spectra of all the samples consist of a single peak with a maximum around 560 nm.

In copper doped strontium sulphide phosphors, excitation spectra shows two prominent peaks around 310 and 345 nm and the emission peak is observed around 500 nm.

These results have been summarized in Table 6.1and have also been compared with that reported in the literature.

Table 6.1: Summary of excitation and emission spectra at RT of alkaline earth sulphide phosphors activated by Cu(with and without flux)

λ_{exc} and λ_{em} as obtained in the present investigation	λ_{em} (nm) as reported in the literature
<u>SrS:Cu without flux</u> λexc = 310 & 345 nm λem = 500 nm <u>SrS:Cu with flux</u> λexc = 350 & 410 nm λem = 500 nm	466, 515 [9] 471, 517, 548 [10] 478 [11] 459, 528 [12] 490 [13] 510 [14] 530 [15] 520 [16] 485 [17] 510 [18] 520 [19]

	475 [20]
BaS:Cu without flux λexc = 340 & 410 nm λem = 560 nm BaS:Cu with flux λexc = 367 & 408 nm λem = 560 nm	585 [21] 568, 589 [22] 518 [23] 588 [24]
CaS:Cu without flux λexc = 310 nm λem = 480 nm CaS:Cu with flux λexc = 310 & 345 nm λem = 480 nm	413 [12] 430 [25] 465 [26] 480 [15] 490 [27] 450 [28]

The emission bands in Cu- activated sulphides have been attributed to Cu^+ ions in the lattice and they have been thought to be due to a recombination process as is the case in the well known ZnS:Cu phosphors [29]. Such a model can easily explain two emission bands of SrS:Cu by two different acceptor levels within the SrS band gap due to the coexistence of Cu^+ and some co-activator such as halogenide ions or vacancies[17]. However, in the work done by Yamashita [11], the lightly doped SrS:Cu powder was found to have a broad band emission located at 513 nm at 80 K and it was attributed to the emission from isolated Cu^+ centre. Moreover there is a well established model for Cu^+ doped alkali halides [30] where the luminescence mechanism is based on $3d^{10} \rightarrow 3d^9 4s$ transition of Cu^+ ion. Most of the alkali halides also have same crystal structure as SrS. With such model, however, it is difficult to explain the thermal quenching of fluorescence. As discussed in the next section, all the series of phosphors in the present investigation exhibited strong thermal quenching. Therefore, Schon Klasens Model [31] for sulphide appears more applicable in our case. This has been discussed in the next section.

6.4 Temperature sensitive properties of present system of phosphors

We have already seen in chapter 4 that the fluorescence intensity at λ_{max} (the wavelength of maximum intensity at RT) decreases with increase in temperature for all the series of phosphors. This fall in intensity with temperature is related to the fluorescence efficiency η of the phosphors. The latter is given by

$$\eta = \frac{P_r}{P_r + P_{nr}} \qquad (4.1)$$

where P_r is the probability of radiative transitions and the P_{nr} is probability of non-radiative transitions. It is assumed that P_r is almost independent of temperature while P_{nr} rises rapidly with temperature.

The generally accepted Schon –Klasens Scheme [31] of Fig 6.1 furnishes a simple and interesting explanation of thermal quenching in these phosphors.

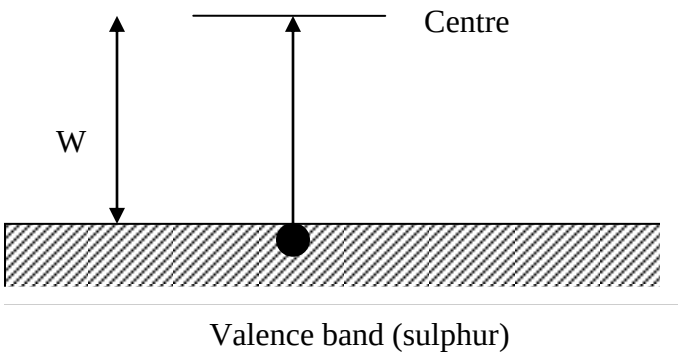

Fig 6.1: Schon –Klasens model for thermal quenching of luminescence in sulphide phosphors

An electron in the valence band can enter a luminescence center by a thermal activation of energy W. The electron previously removed from the center by optical excitation cannot now return and after diffusing in the conduction band for a while will finally recombine via some defect or other non-radiative transition.

It has been observed that in a specific range of temperatures (which we have termed span, ΔT), most of these phosphors show linear decrease in intensity. As we have discussed in

chapter 5, the lifetime of phosphorescence of these phosphors also show a similar behavior; that is the thermal quenching is almost linear in the range of span. Both these attributes are favorable for application of these phosphors in temperature sensing.

6.5 Conclusions:

Fiber optic luminescence thermography / thermometry normally utilize two properties of the phosphor; viz (i) variation of fluorescence intensity with temperature and (ii) variation of lifetime of fluorescence / phosphorescence with temperature. From this point of view, all the alkaline earth sulphide (Cu) phosphors, synthesized and studied in the present work seem to be the potential candidates for thermography / thermometry because (i) their fluorescence intensity varies markedly with temperature (at least in the range governed by the span) and (ii) their phosphorescence lifetimes also vary with temperature. In fact, these phosphors may be used in a variety of applications. **One of the applications for which these phosphors have been tested by Purohit and Khare is the measurement of temperature of hot surfaces [32]**. A self-explanatory diagram of this system is shown in Fig. 6.2 (shown in next page).

There are number of other applications for which these phosphors can be used. Some of these are summarized as follows:

6.5.1 Electrical Machinery:

The immunity of optical signals to electromagnetic interference makes phosphor thermometry very useful in diagnostic studies of electrical machinery. A thermographic phosphor based technique for monitoring the temperature of the rotor in a large turbogenerator may be developed. The motivation for doing this is to seek out any "hot spots" that might develop in the rotor of the generator as a result of several possible causes, including overheated insulation. A pulsed optical source may be used and the light conveyed along an all-silica optical fiber having a larger core diameter (Silica fibers are generally preferred over plastic-clad fibers because of their higher pulsed-power damage threshold and their superior transmission characteristics in the ultraviolet.)

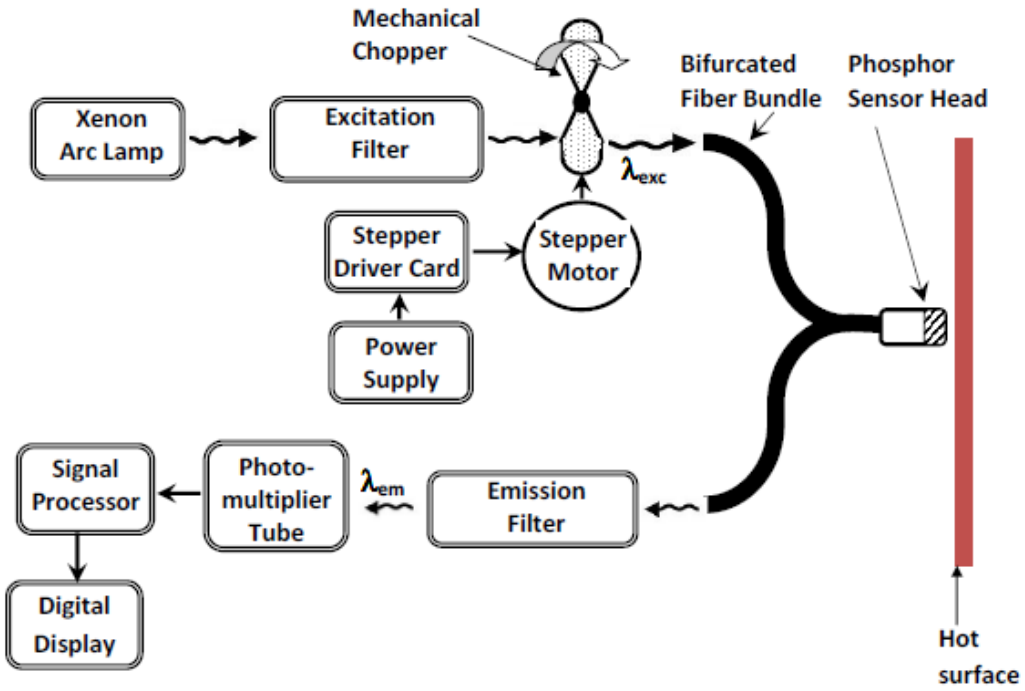

Fig. 6.2: *Fiber Optic Probe for Sensing Temperature of Hot Surfaces developed in the present investigation [32].*

A plastic-clad fiber can collect the fluorescence and convey it to a photomultiplier tube. A custom-designed data analysis system may be used to determine the phosphorescence decay times. A silicone binder, mixed 50% by weight with phosphor, may be painted in a 5- 10 cm wide stripe around the circumference of the rotor.

Hot spots are also developed in electrical transformers, and fluoro- optic thermometers have been used to determine the temperatures of the windings, the leads and the transformer tank. Other applications that call for the sensor to function in the presence of large electromagnetic fields include fiber optic thermometry-based measurements of microwave power and rf susceptibility.

6.5.2 Flow Tracing:

Phosphor particles may be used as tracer to aid in visualizing the flows of liquids. Both continuous ultraviolet lamps and the nitrogen laser may serve as sources of illumination for different configuration of this method. ZnS, CdS and CaS phosphors and their combinations have already been used in this technique. Longer phosphorescence

lifetimes of alkaline earth sulphide make them particularly well suited for measuring the flow of slowly moving liquids.

Very recently, such systems have also been used for temperature imaging in gas-phase flows [33].

6.5.3 Gas Centrifuges:

These phosphors may be used for making non-contact temperature measurement on the gas centrifuges. These devices are large right circular cylinders driven at very high speed. Their function is to separate U^{235} from the natural isotopic distribution in UF_6 gas to create enriched fuel for nuclear power reactors. The flow pattern inside the machine and, hence, the separation efficiency of the centrifuge is affected by thermal variations on the rotor surface. The goal of maximizing separation work performance provided the impetus for developing a remote thermometry system compatible with a high speed mechanism of this type.

6.5.4 Heat Flux:

The determination of heat flux through a surface is important in a variety of scientific and engineering applications. The method may consist of an array of discrete circular and triangular spots of phosphor on the surface to be mounted**.** The alkaline earth sulphide phosphor may be used for the development of several embodiments of the thermal phosphor- based heat flux gauges.

6.5.5 Particle Beam Characteristics:

Phosphors and other scintillating materials can be used to study the structure of high energy ion and electron beams, indicating the position, profile, and flux density of the beam as a function of phosphor brightness. Also, if the beam current is large enough to heat the material, then an appropriate method of phosphor- based thermometry can be used to diagnose the beam. Over time, as a significant dose accumulates the phosphors efficiency will deteriorate due to radiation damage. This process, which manifests itself as a decrease in brightness.

Such information may be of significance in assessing the use of phosphors in nuclear reactor as well as particle beam application. The present set of phosphors can also be used for such an application

6.5.6 Other applications:

Phosphor thermometry is extensively being used in monitoring combustion processes [34, 35] as well as many other applications [36, 37].

6.6 Suggestions for Further Research:

(i) As new applications for phosphor thermometry arise, there will be a concomitant need for target materials that have luminescence characteristics appropriate to the measurement being undertaken. For instance, although many of the phosphors that have been studied to date emit at the longer visible wavelengths, i.e., at the yellow to red end of the spectrum, some color- sensitive applications might call for a phosphor that emits at shorter wavelengths, near the blue- to- violet end of the spectrum.

(ii) At higher temperatures, the fluorescence lifetimes of virtually all phosphors are very short. Once the lifetime drops below about 100 μs, the speed, resolution, and accuracy requirements placed on the data acquisition system typically call for the use of sophisticated transient digitizers and fast pulse analyzers. Equipment of this type is used routinely in nuclear, particle, and laser physics laboratories. If more research is done on the temperature dependence of phosphorescence, it may be possible to adapt it for use in phosphor thermometry systems. Then the range over which temperature measurements could be made with this technique might be extended.

(iii) Improvement in the methods of phosphor bonding would also be welcome. A particularly valuable advance would arise from the development of a technique that would produce thin, durable, spray-on coatings like those created by flame and plasma deposition, but without the need for high temperature combusting gases and expensive apparatus.

(iv) Finally, the potential of thermogaphic phosphors to sense still other physical quantities should be explored.

References

[1] PRN Childs, JR Greeenwood, CA Long, *Rev Sci Instrum*, **71**, 2959 (2000).

[2] C Tropea, AL Yarin, JF Foss. *Springer handbook of experimental fluid mechanics*, Berlin: Springer; (2007).

[3] T Liu, BT Campbell, SP Burns, JP Sullivan. *Appl Mech Rev*, **50**, 227(1997).

[4] C Lempereur, R Andral, J Prudhomme. *Meas Sci Technol*, **19,** 105501(2008).

[5] N Fuhrmann, E Baum, J Brübach, A Dreizler: *Rev Sci Instrum*: **82**,104903, (2011).

[6] DL Beshears, GJ Capps, MR Cates, CM Simmons, SW Schwenterly. *SPIE Fiber Opt Smart Struct Skins*; III (1370), 365(1990).

[7] MR Cates, DL Beshears, SW Allison, CM Simmons: *Rev Sci Instrum* **68**, 2412, (1997).

[8] MR Cates, SW Allison, S Jaiswal, DL Beshears: *Proceedings of the ISA's 49th international instrumentation symposium*, **49**; 389 (2003).

[9] W. Lehmann, *J. Lumin.*, **5,** 87 (1972).

[10] B. B. Laud and V. W. Kulkarni, *J. Phys. Chem. Solids*, **39,** 555 (1978)

[11] N. Yamashita, *Jpn. J. Appl. Phys.*, **30,** 3335, (1991)

[12] F. Altukhova, K. Piir, F. Savikhin, , Trudy. Inst. Fiz, Akad. Nauk Est. *SSR* **54**, 188 (1983).

[13] *F. Urbach, D. Pearlman and H. Hemmendingr, J. Opt. Soc. Am.* **36**, 372 (1946).

[14] D. Sharma and A. Singh, *Ind. J. Pure &Appl. Phys.* **9**, 810 (1971).

[15] N. Singh, G. L. Marwaha and V.K. Mathur, *Phys. Status Solidi A*, **66,** 761 (1981).

[16] W. M. Li, M. Ritala M. Leskela, L. Niinisto, E. Soininen, S. S.Sun ,W. Tong and C.J.Summers, *J. Appl. Phys.*, **86**, 5017 (1999).

[17] J. Youngchore, S. M. Blomqno, D. C. Morton, *Appl. Phys. Lett.*, **80**, 4124 (2002).

[18] D. Wruck, R. Boyn, M. Wienecke, F. Henneberger, U. Troppenz, B.huttl, W.Bohne, B. Reinhold, and H.E. Mahnke, *J. Appl. Phys.* **91,** 2847, (2002).

[19] K. Ohmi, K. Yamable, H. Fukada, T. Fujiwara, S. Tanaka, and H. Kobayashi, *Appl. Phys. Lett.* **73,** 1889, (1998).

[20] W. Park, T. C. Jones and C. J. Summers, *Appl. Phys.Lett.,* **74**, 1785 (1999)

[21] B.B Laud and V.W Kulkarni; *Phys. Stat. Sol. (a),* **51**, 269 (1979).

[22] M. L. Yu Allsalu, E. P. Efanova, A. I. Lebedeva, V. V. Lebedeva, V. V. Mikhailin, E. Yu Pedak and A.A. Plachev, *J. Appl. Spectros,* **31**, 1441(1979).

[23] V. L. Rabotkin an, T. N. Stroganova, Bull, Acad. Sci. USSR, *Phys. Ser.* (USA), **30**, 1575 (1966).

[24] W. Lehmann, *J. Electrochem.Soc.*, **117,** 1389 (1970).

[25] A. Wachtel, *J. Electrochem. Soc.*, **107,** 199 (1960).

[26] M. Avinor, A. Carmi and Z. Weinberger, *J. Chem. Phys.*, **35,** 1978, (1961).

[27] A.K. Uppal, S.N. Chaturvedi, and N. Nath, *Ind. J. Pure. & Appl. Phys.*, **25,** 72, (1987).

[28] C.S. Gupta, *Ind. J.Pure Appl. Phys.*, **36,** 765 (1998).

[29] R.Pandey, and S. Sivaraman, *J. Phys.Chem. Solids*, **52,** 211 (1991).

[30] D. S. McClure and S.C. Weaver, *J. Phys. Chem. Solids*, **52,** 81 (1991).

[31] H. A. Klasens, *J. Phys. Chem. Solids,* **9,** 185 (1959).

[32] R. Purohit and R. P. Khare: *Journal of Instrumentation Technology & Innovation,* **2** (3), 9 (2012).

[33] Jonathan Jordan et al., *Applied Physics B*, **110**, 285 (2013).

[34] Jan Brübach et al., *Progress in Energy and Combustion Science*, **39**, 37 (2013)

[35] N. Fuhrmann et al., *Proceedings of the Combustion Institute*, **34**, 3611 (2013)

[36] M.D. Chambers et al., *Annual Review of Materials Research*, **39**, 325 (2009)

[37] K. T. V. Grattan et al., *MRS Bulletin*, **27**, 389 (2002)

List of Publications and Presentations

Related to present research

1. Temperature sensitive fluorescence of SrS:Cu phosphors for thermographic application, R. Purohit and R. P .Khare, Proceedings of National conference on Luminescence and its Applications, 7-9 February pp 214-216 (2006).
2. Thermographic Applications of Temperature Sensitive Fluorescence of SrS: Cu Phosphors, R. Purohit and R. P. Khare, Journal of Engineering Science and Technology, Vol. **5**, No. 4 pp 373 – 378 (2010).
3. Synthesis and Characterization of CaS:Cu Phosphors for Thermography, R. Purohit and R.P.Khare, Presented at National Symposium on Instrumentation (NSI-35), Visvesvaraya Technological University, Belgaum 7th to 9th January, (2011).
4. Fiber Optic Fluorescent Probe for Measurement of Temperature, R Purohit and R.P Khare, Journal of Instrumentation Technology & Innovations Volume **2**, Issue 3, December 2012, Pages 9-13.

Other Publications

1. R P Khare, R Purohit, Shweta Gaur, K Priya and Sudhir K, PC based fiber optic linear displacement sensor, Proc International Conference on Optics & Optoelectronics, IRDE, Dehradun (), Dec 9-12, 1998. Paper no IP972.
2. R Purohit, Aditya Goel, Deepika Juneja and Anupam Kumar, Development of Automated System for Water Supply in a Locality using Microcontroller, e-Proceeding IEEE International Advance Computing Conference-2009 (IEEE IACC-2009), March 6-7,2009, Thapar Univ., Patiala (Punjab).pp 972-974.
3. R P Khare, K Arvind, S Srirajkumar & R Purohit, A modified fiber optic reflective sensor, Sensors – 6 (Proc of 6th National Seminar on Physics and Technology of Sensors, held at TIET, Patiala) 4th to 6thMarch 1999. C23-1to4.

4. R P Khare; R Purohit; R V Aparna; Pragya Jain; & V Uma Maheshwari, BaS (Cu, Eu) phosphors for fluoro-optic temperature sensing, Proc National Seminar on Advanced Instrumentation (NSAI-2001), CSIO, Chandigarh, Jan 29-31, 2001.
5. R Purohit and R P Khare, Temperature Sensitive Fluorescence of SrS:Cu Phosphors for Thermographic Applications, Proc National Conference on Luminescence and Its Applications (NCLA 2006), Sant Gadge Baba Amravati University, Amravati, Feb 7-9, 2006. PP 214-216.
6. R Purohit; Shobha Prabhakar & Mahesh Kumar, Programmable Logic Controller Based Automation of Electro-Mechanical Devices, Proc National Conference on Information Technology: Emerging Engineering Perspectives and Practices, April 6-7, 2007 Thapar Univ., Patiala (Punjab). PP 323-325.
7. R Purohit, Jaideep A, Archana Varadarajan, Nitu, Industrial Applications of Microcontrollers– Development of a System for Automation of Wells on Campus, e-Proceeding IEEE International Advance Computing Conference-2009 (IEEE IACC-2009), March 6-7,2009, Thapar Univ., Patiala (Punjab). CSE 1-3.
8. R Purohit, Aditya Goel, Deepika Juneja and Anupam Kumar, Development of Automated System for Water Supply in a Locality using Microcontroller, e-Proceeding IEEE International Advance Computing Conference-2009 (IEEE IACC-2009), March 6-7,2009, Thapar Univ., Patiala (Punjab). PP 972-974.
9. Abhibrata Banerji, Kushagra Garg, Anuj Chandawalla and Rajesh Purohit, PLC based Automation of Electro-Mechanical System using PID Algorithm, e-Proceeding National Conference on Virtual and Intelligent Instrumentation-2009 (NCVII-09), BITS Pilani (Rajasthan). PP 1-24.
10. R. Purohit and Prince Kadyan, Microcontroller Based Design of A Soil Moisture Controller System for Drip Irrigation Related Applications, e-Proceeding National Conference on Virtual and Intelligent Instrumentation-2009 (NCVII-09), BITS Pilani (Rajasthan).PP 1-10.
11. Vaibhav Narayan Singh, Prince Kadyan, R.P. Pareek, Rajesh Purohit, Microcontroller Based Cardiac Monitoring System, e-Proceeding National

Conference on Virtual and Intelligent Instrumentation-2009 (NCVII-09), BITS Pilani (Rajasthan).PP 1-16.

12. R. Purohit and R. P. Khare, Thermographic Properties of Cu-Activated Calcium Sulphide Phosphors, e-Proceeding National Conference on Virtual and Intelligent Instrumentation-2009 (NCVII-09), BITS Pilani (Rajasthan).9B.7.
13. R. Purohit and R. P. Khare, Synthesis and Characterization of CaS:Cu Phosphors for Thermography, National Symposium on Instrumentation(NSI-35), Jan 7th to 9th,2011, Visvesvaraya Technological Univerisity, Belgaum.PP 99.

Books:

1. “Experiments in Instrumentation” by Rajesh Purohit and MMS Anand, Educational Development Division, BITS Pilani, 2003.It serves as a text book for the course INSTR C355 Electronic Instruments and Instrumentation Technology, a compulsory discipline course for students of B.E. (Hons.) Electronics & Instrumentation Programme of BITS, Pilani.
2. "Hand Book on Women and Computer Literacy" by Rajesh Purohit, Centre for Women Studies, BITS Pilani, 2010.It serves as a reference book for various training programmes conducted on computer literacy and various training programmes conducted by CWS BITS Pilani.

Brief Biography of the Candidate

I am presently Assistant Professor in Electronics and Communication Engineering at IET, JK Lakshmipat University, Jaipur (Rajasthan) India. Before joining JKLU I was lecturer at BITS Pilani, Pilani Campus and taught the courses of Electronics and Instrumentation for 19 years. I have done my undergraduate and postgraduate from BITS Pilani, Pilani Campus. I have published several research papers in National and International Journals and conferences.

Brief Biography of the Supervisor

Dr R. P. Khare is presently a Visiting Professor in the Department of Electrical & Electronics Engineering, Birla Institute of Technology & Science, Pilani (Rajasthan) India. A PhD in optical materials, he has published several research papers in Indian and International journals. He has also published two text books and four other books. His professional career (Teaching and Research) spans over 35 years. He is also a member of several professional organizations.